Spring 5-2011

Ruthenium-Based Olefin Metathesis Catalysts Bearing pH-Responsive Ligands: External Control of Catalyst Solubility and Activity

Shawna Lynn Balof
University of Southern Mississippi

The University of Southern Mississippi

RUTHENIUM-BASED OLEFIN METATHESIS CATALYSTS BEARING PH-RESPONSIVE LIGANDS: EXTERNAL CONTROL OF CATALYST SOLUBILITY AND ACTIVITY

by

Shawna Lynn Balof

Abstract of a Dissertation
Submitted to the Graduate School
of The University of Southern Mississippi
in Partial Fulfillment of the Requirements
for the Degree of Doctor of Philosophy

May 2011

ABSTRACT

RUTHENIUM-BASED OLEFIN METATHESIS CATALYSTS

BEARING PH-RESPONSIVE LIGANDS:

EXTERNAL CONTROL OF CATALYST SOLUBILITY AND ACTIVITY

by Shawna Lynn Balof

May 2011

Sixteen novel, Ru-based olefin metathesis catalysts bearing pH responsive ligands were synthesized. The pH-responsive groups employed with these catalysts included dimethylamino (NMe_2) modified NHC ligands as well as N-donor dimethylaminopyridine (DMAP) and 3-(*o*-pyridyl)propylidene ligands. These pH-responsive ligands provided the means by which the solubility and/or activity profiles of the catalysts produced could be controlled via acid addition. The main goal of this dissertation was to design catalyst systems capable of performing ring opening metathesis (ROMP) and ring closing metathesis (RCM) reactions in both organic and aqueous media.

In an effort to quickly gain access to new catalyst structures, a template synthesis for functionalized NHC ligand precursors was designed, in addition to other strategies, to obtain ligand precursors with ancillary NMe_2 groups. Kinetic studies for the catalysts produced from these precursors showed external control of catalyst solubility was afforded via protonation of the NMe_2 groups of their NHC ligands. Additionally, this protonation afforded external control of catalyst propagation rates for several catalysts. This is the first known independent external control for the propagation rates of ROMP catalysts. The incorporation of pH-responsive N-donor ligands into catalyst structures also provided the means for the external control of metathesis activity, as the protonation of these ligands resulted in an increased initiation rate based on their fast and

irreversible dissociation from the metal center. The enhanced external control makes these catalysts applicable to a wide range of applications, some of which have been explored by us and/or through collaboration.

Three of the catalysts designed showed remarkable metathesis activity in aqueous media. These catalysts displayed comparable RCM activity in aqueous media to a class of water-soluble catalysts reported by Grubbs *et al.*, considered to be the most active catalyst for aqueous olefin metathesis reactions. In ROMP reactions these particular catalysts dramatically outperformed the literature catalysts, accomplishing ROMP full conversion rates within 15 minutes compared to several hours observed with the literature catalyst. These catalysts were also able to accomplish these reactions at lower catalyst loadings than ever reported with the literature catalyst, making them the most active aqueous olefin metathesis catalysts to date.

The University of Southern Mississippi

RUTHENIUM-BASED OLEFIN METATHESIS CATALYSTS BEARING PH-RESPONSIVE LIGANDS: EXTERNAL CONTROL OF CATALYST SOLUBILITY AND ACTIVITY

by

Shawna Lynn Balof

A Dissertation
Submitted to the Graduate School
of The University of Southern Mississippi
in Partial Fulfillment of the Requirements
for the Degree of Doctor of Philosophy

Approved:

Hans Schanz
Director

Douglas Masterson

Wujian Miao

Sarah Morgan

Karl Wallace

Susan A. Siltanen
Dean of the Graduate School

May 2011

ACKNOWLEDGMENTS

I would like to thank my advisor and chair of my committee, Dr. Hans Schanz, as well as the other committee members, Dr. Douglas Masterson, Dr. Wujian Miao, Dr. Sarah Morgan, and Dr. Karl Wallace, for their advice and support throughout the duration of this project. I would especially like to thank Dr. Hans Schanz for his enormous patience and commitment to this project.

Special thanks go to the many collaborators of the Schanz research group, including Dr. Andrew Lowe, Dr. Edward Valente, Dr. Steven P'Pool, Dr. Allan Schiller, Dr. Bing Yu, Dr. Yan Ling, Dr. Yong Zhang, Dr. Kevin Müller, and Dr. Andrea Robinson. I want to express special thanks to the undergraduate students, including David Hudson, Adam Roberts, Miles Dunbar, Samantha Odom, and Allie Carpenter, who have contributed greatly to the synthesis of the compounds explored in this dissertation. Appreciation is also expressed to the Department of Chemistry and Biochemistry at The University of Southern Mississippi for giving me this great opportunity.

For funding I would like to thank the Trent Lott Center for Innovation, whose Innovation Award helped to fund my second year in graduate school. I would also like to thank BASF for providing the funding that has carried our research group for the past two years.

Finally, I would like to thank my friends and family. In particular my husband, our children, and my father, for the endless encouragement and many sacrifices they have made in order to allow me to study here.

TABLE OF CONTENTS

LIST OF TABLES

Table

LIST OF ILLUSTRATIONS

Figure

LIST OF SCHEMES

Scheme

CHAPTER I

INTRODUCTION, BACKGROUND, AND LITERATURE REVIEW FOR OLEFIN METATHESIS AND OLEFIN METATHESIS CATALYSTS

Introduction

Over the past five decades olefin metathesis has evolved into a powerful tool in the fields of organic[1] and polymer[2] chemistry. The 2005 Nobel Prize in Chemistry awarded to Yves Chauvin, Richard Schrock, and Robert Grubbs for their contributions to the field[3] clearly demonstrates the importance of olefin metathesis and acknowledges the impact of this technology on the sciences and society. Advantages of olefin metathesis for chemical synthesis include good product yields (often near quantitative) under mild reaction conditions, fewer synthetic steps to obtain the desired product, fewer side reactions when compared to many traditional methods of organic synthesis, and less generation of hazardous waste.[4] Since the mid 1990s, much of the research has been focused on Ru-based, single-site olefin metathesis catalysts due to their high activity and tolerance toward air, moisture, and many functional groups in comparison to catalytic systems based on other transition metals.[5]

Ru-based olefin metathesis catalyst designs have been investigated intensely over the last decade, and much progress has been made to optimize the activity and thermal stability of these complexes. The most prominent catalyst designs still feature several limitations including narrow-range solubility profiles, costly removal after use, and a lack of external activity controls. Currently no economically feasible solution exists for effective catalyst removal, and few external activity controls have been identified which can improve the applicability of these catalysts on a large, industrial scale. Also,

only a few catalyst designs are available for homogenous aqueous applications,[6] and those which were successfully developed are limited by their cumbersome syntheses.

The focus of this dissertation is the development of new Ru-based olefin metathesis catalysts bearing pH-responsive ligands. These ligands provide the means to externally control the solubility profile and activity of the catalyst. This allows for improved catalytic performance with respect to ring opening metathesis polymerization (ROMP) and ring closing metathesis (RCM) reactions. These ligands also provide the means to enhance the applicability of these catalysts in certain applications.

Background and Literature Review

Early Developments of Transition Metal-Mediated Polymerization and Olefin Metathesis

Karl Ziegler, a German scientist, is credited with discovering the first metal-catalyzed olefin polymerization in 1953 when he made use of an ill-defined catalyst system generated from trialkyl aluminum and titanium chloride which produced relatively linear polyethylene.[7] Similar catalysts were employed that same year by Giulio Natta for the production of mostly linear polymers from 1-alkenes, and the initial results led to the development of a wide variety of the so-called Ziegler-Natta catalysts.[8] For their work they were both awarded the Nobel Prize in Chemistry in 1963.[3]

Based on the initial research of Ziegler and Natta, the petrochemical industry investigated ill-defined transition metal catalysts for the production of polymers from olefins throughout the 1950s and 1960s.[9] During these investigations some researchers obtained unexpected products that could not be explained by any known olefin polymerization reaction. One example was observed by DuPont chemist Herbert S. Eleuterio in 1956.[10] While passing propylene feed over a molybdenum-on-aluminum catalyst in an attempt to synthesize a propylene polymer he instead obtained a

propylene-ethylene copolymer. Further analysis of the output gas showed that it was composed of a mixture of ethylene, propylene, and 2-butene. When he repeated this experiment with cyclopentene he obtained a linear, unsaturated polymer that appeared to be the opened ring joined end to end (Scheme 1) instead of a cyclopentane polymer composed of connected cyclic units.

Scheme 1. Results Obtained by Herbert S. Eleuterio in 1956[10]

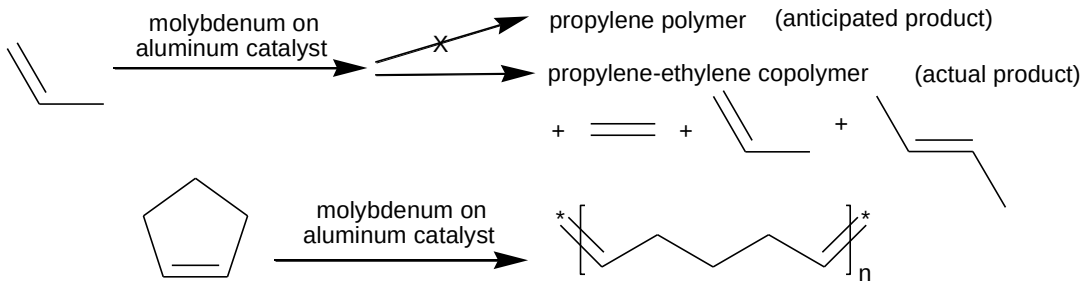

At first these reactions were not considered related to one another. It was not until four years later that it was recognized that these unexpected products were the result of a redistribution of C=C double bonds. In this redistribution one half of the C=C double bond of one olefin was exchanged for one half of the C=C double bond of a second olefin (Scheme 2). In 1967 Nissim Calderon, a chemist with Goodyear Tire Company, dubbed this reaction "olefin metathesis."[11]

Scheme 2. Olefin Metathesis

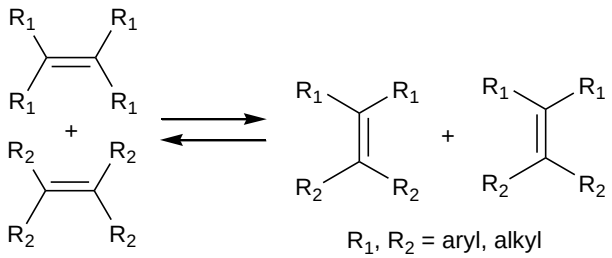

R_1, R_2 = aryl, alkyl

Mechanism of Olefin Metathesis

Even after scientists recognized the products of olefin metathesis were formed through a redistribution of C=C bonds, the actual mechanism for the transition-metal mediated olefin metathesis reaction remained elusive. Over several years many different mechanisms were proposed.[12] In 1971 Yves Chauvin and his student Jean-Louis Hérisson first introduced what is now the accepted mechanism of transition-metal mediated olefin metathesis (Scheme 3).[13] This mechanism involves the [2+2]cycloaddition of a C=C double bond to a transition metal alkylidene species to form a metallacyclobutane intermediate. This metallacyclobutane intermediate then undergoes a retro [2+2]cycloaddition to give either the starting materials or a new alkene and alkylidene. The alkene's interaction with the d_{xz} or d_{yz} orbitals on the metal catalyst lowers the activation energy, allowing for this reaction to proceed at moderate temperatures.[1a]

Scheme 3. The Chauvin Mechanism[13]

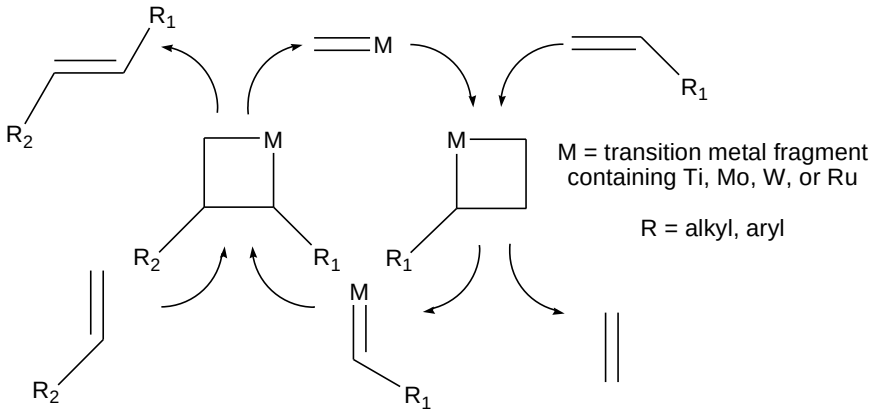

When Chauvin's mechanism for olefin metathesis was first published it was widely ignored. It remained that way until 1975 when Thomas Katz and his research group began publishing a series of papers that recognized and supported the Chauvin mechanism,[14] the first entitled "Mechanism of the Olefin Metathesis Reaction."[14a] In

these papers, Katz unambiguously showed that the metal-carbene was essential to the olefin metathesis mechanism and also provided further insight into the reasons this reaction produces such a variety of products from different starting materials. Later mechanistic work published by Robert Grubbs[15] and Richard Schrock[16] also supported the Chauvin mechanism. In his mechanistic studies, Grubbs used isotopically labeled olefins to track the exchange of groups. The products obtained could only be formed via the metal-carbene mechanism. Five years later, Schrock showed that metal-carbynes react with various acetylenes to give the expected alkyne metathesis products. The results of these studies resulted in an extension of, but also confirmed, the Chauvin mechanism, making it the accepted mechanism for olefin metathesis.

Types of Olefin Metathesis Reactions

Olefin metathesis is a versatile reaction that breaks and reforms C=C double bonds, making many different types of alkene products accessible. Variations of olefin metathesis include cross metathesis (CM), ring closing metathesis (RCM), acyclic diene metathesis (ADMET), ring opening metathesis (ROM), and ring opening metathesis polymerization (ROMP) as the most prominent examples. The type of metathesis reaction that takes place is mainly determined by thermodynamics of the reaction. For example, in the case of highly strained cyclic olefins, ROM or ROMP is usually favored due to the release of energy upon the opening of the ring. Likewise RCM is often preferred by certain dienes when the product formed is a cyclic molecule with low ring strain (Scheme 4). These reactions are often reversible, so factors such as temperature or substrate concentration can be used to drive the equilibrium in favor of the desired product.[17] Throughout this dissertation RCM and ROMP reactions were conducted to evaluate the activity for synthesized catalysts. The substrates for these reactions were selected to ensure that only one type of olefin metathesis reaction product was obtained.

Scheme 4. Thermodynamically-Driven Metathesis Reactions

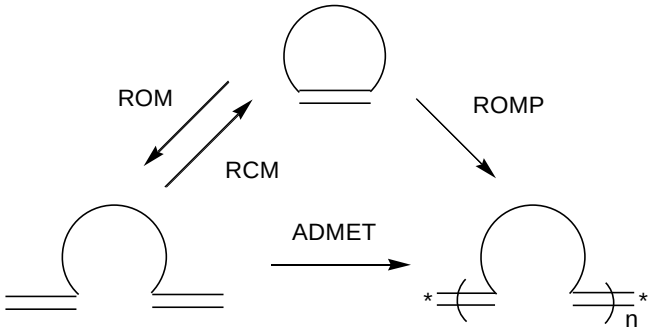

RCM is an intramolecular olefin metathesis reaction of a diene that forms a cycloalkene with low ring strain. Most commonly used are α,ω-diolefins. In the first step of an RCM reaction, one C=C double bond of the diene coordinates a metal-methylidene (which is formed from any catalyst after the first reaction with an α,ω-diolefin), followed by a [2+2]cycloaddition of the alkene and metal carbene to form the metallacyclobutane intermediate as proposed in the Chauvin mechanism. This metallacyclobutane intermediate then breaks apart through a retro [2+2]cycloaddition reaction, resulting in a new metal-alkylidene complex and ethylene. The second C=C double bond of the original diene then coordinates to the metal and is followed by another [2+2]cycloaddition to form a second metallacyclobutane intermediate that then reverses the cycloaddition to reform the metal-methylidene complex and the desired cycloalkene product (Scheme 5). The formation of volatile ethylene drives this reaction to completion as the gas is released from the reaction mixture.[18] RCM reactions are useful for the synthesis of cyclic alkenes, including macrocycles, or cyclic alkanes after hydrogenation, that are otherwise difficult to prepare by traditional synthetic methods. Hence, RCM is widely used by the pharmaceutical industry as a convenient synthetic step for the production of macrocyclic pharmaceutical products.[1c,19]

Scheme 5. Mechanism of RCM

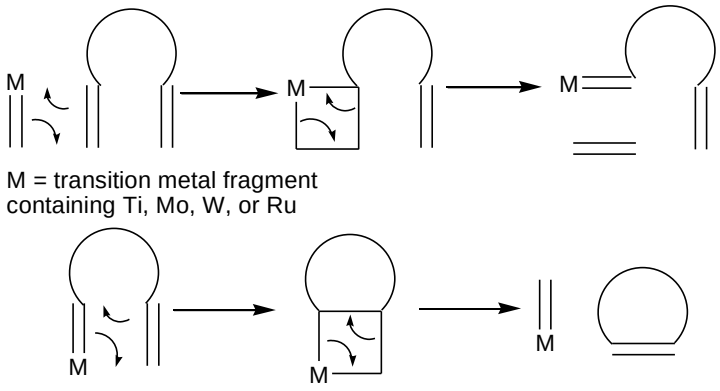

ROMP is a polymerization reaction that opens strained cycloalkenes. The main thermodynamic driving force behind ROMP reactions is the relief of ring strain; therefore, this reaction is usually not reversible for most ROMP substrates. Under optimal conditions, meaning very slow catalyst decomposition resulting in a low degree of termination, this reaction can propagate almost indefinitely, making ROMP one of the few living polymerization techniques.[1a]

ROMP propagates through coordination of the cyclic olefin to the metal-alkylidene with subsequent formation of the metallacyclobutane intermediate. This intermediate opens to yield a new linear metal-alkylidene, which relieves the ring strain of the original olefin. The new metal-alkylidene then continues to repeat the reaction with more substrate to produce a polymeric chain (Scheme 6). In the absence of termination reactions, propagation continues until all monomer substrate is consumed. Since the ROMP reaction is living under these conditions, the ROMP reaction will continue with the addition of more monomer. Termination often is induced externally, e.g., by chemical quenching with ethylvinyl ether.[20]

Scheme 6. Mechanism for ROMP

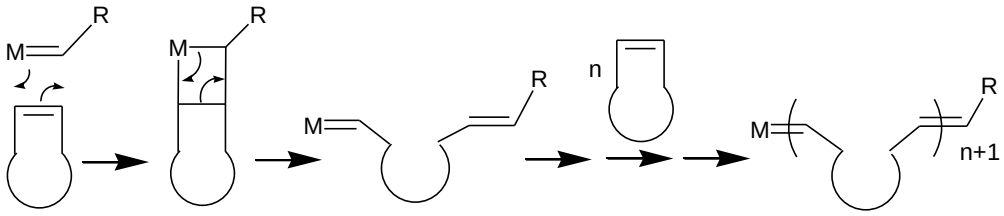

M = transition metal frgment containing Ti, Mo, W, or Ru
R = alkyl, aryl

ROMP is a useful synthetic tool for the production of specialized polymers, such as block copolymers.[21] These polymers are synthesized by sequential addition of different monomers. For catalysts which exhibit fast initiation but only moderate propagation rates, the polymerization becomes a controlled living polymerization, meaning the molecular weights of the polymers produced can be controlled by the monomer to catalyst ratio. Since all polymer chains start growing almost simultaneously and at the same rate, the polymers produced with these catalysts also have narrow molecular weight distributions. As a consequence, linear polymers produced via controlled ROMP have well-defined material properties.

Classes of Olefin Metathesis Catalysts

Over the past several decades, a variety of olefin metathesis catalysts have been developed. Catalytic systems have evolved from ill-defined, heterogeneous catalysts to well-defined, single site catalysts. There have been four distinct classes of olefin metathesis catalysts: (1) “black box” catalysts, (2) Titanocene-based (Tebbe-type) catalysts, (3) Mo- and W-based (Schrock-type) catalysts, and (4) Ru-based (Grubbs-type) catalysts.

The first metathesis catalysts are often referred to as “black box” catalysts because very little was known about their structure and the mechanism by which they operated. These heterogeneous, ill-defined catalysts were derived from elements of the early transition metal series and were usually either grafted onto silica or combined with

a main group alkylating agent.[22] They usually contain few active sites and therefore require high catalyst loadings. They are also often sensitive to air, moisture, and functional groups, which limits their applicability. Examples of “black box” catalysts still widely used today include $WCl_6/SnMe_4$ and WCl_6/Et_2AlCl, which are used to make a variety of plastics.[23]

The first well-defined olefin metathesis catalysts were the Titanocene-based, Tebbe-type catalysts. These were named after DuPont chemist Fred Tebbe who, in 1978, reported the results of his investigation into the structure and reactivity of a well-defined complex synthesized from titanocene dichloride and trimethylaluminum in a toluene solution[24] known today as the “Tebbe Complex” or “Tebbe’s Reagent” **1**. Once activated with a mild Lewis base, such as pyridine, it forms an active carbene species **2** (Scheme 7).[25] Since this catalyst was well-defined and slow to react, both the starting and propagating carbene species could be observed during a metathesis reaction, making it the first catalyst system used for mechanistic study of olefin metathesis.[26] However, drawbacks of these catalysts were their low reactivity, sensitivity to air and moisture, and low functional group tolerance, which prevented their use in commercial applications.[1a]

Scheme 7. Activation of Tebbe's Reagent[25]

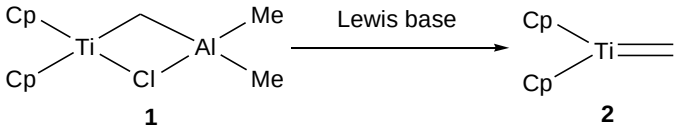

1 **2**

The catalyst activity was enormously improved with the development of the Schrock-type catalysts, which are tungsten-based[27] and molybdenum-based[28] carbene complexes originally developed by Richard Schrock in the mid-1980s. These catalysts even displayed a moderate functional group tolerance but still were sensitive to air and

moisture. The most successful Schrock-type catalysts used today are the Mo-based catalysts, such as **3** (Figure 1).[29] They preferentially coordinate olefins over several other functional groups such as ketones, esters, and amides.[30] This makes these catalysts applicable to a wider variety of substrates than the Tebbe reagents.

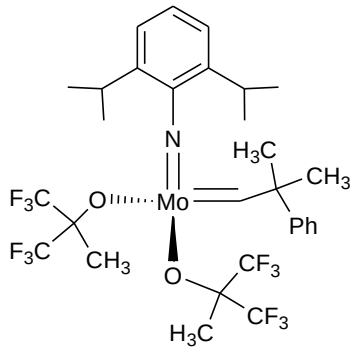

3

Figure 1. Mo-Based (Schrock-Type) Catalyst[29]

The most recent class of olefin metathesis catalysts based on Ru-carbene complexes. In the late 1980s, Robert Grubbs and Bruce Novak found that ruthenium chlorides and ruthenium tosylates could catalyze ROMP of 7-oxanobornene derivatives in water.[31] In these studies, it was observed that ruthenium was significantly more tolerant toward air, moisture, and functional groups than previous generations of catalysts. In 1992 Grubbs synthesized the first Ru-based carbene complex **4** (Figure 2), which exhibited very low metathesis activity and could only perform ROMP of a few select, highly strained cyclic systems.[5a] Since then, many modifications have been made to this original structure to produce a variety of functional, highly active catalysts that have revolutionized the field of olefin metathesis.

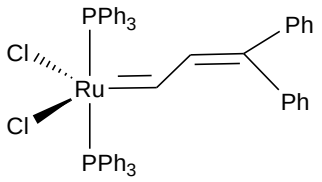

4

Figure 2. First Ru-Based Carbene Catalyst **4**[5a]

Varieties of Ru-Based Olefin Metathesis Catalysts

Over the past two decades, Ru-based olefin metathesis catalysts have been intensely studied. Most of these investigations have been centered on 16-electron, pentacoordinate Ru-alkylidene complexes, or Grubbs-type catalysts. Since the discovery of complex **4** many improvements have been made to the original catalyst design. The first of these improvements was replacing the PPh_3 in complex **4** with bulkier and more σ-donating tricyclohexylphosphine (PCy_3) to give complex **5** (Figure 3) with much higher olefin metathesis activity.[32] This success was followed by the synthesis of what would later be referred to as Grubbs' first generation catalyst **9**, the most active Ru-based catalyst at the time. This catalyst could be produced in a straightforward one-pot synthesis[5c] in which $RuCl_2(=CHR)(PPh_3)_2$ **8** was first generated from $RuCl_2(PPh_3)_3$ **6** via an alkylidene transfer from an aryl diazoalkane **7** then transformed into catalyst **9** through a simple phosphine exchange with excess PCy_3 (Scheme 8). Catalyst **9**, compared to all non-Ru-based olefin metathesis single-site catalysts at the time, exhibited superior tolerance towards air, moisture, and functional groups, though it did lack thermal stability at temperatures >60 ^{o}C. Yet, this catalyst triggered an explosion of research in the field that has transformed olefin metathesis into a very powerful technique in organic and polymer synthesis.

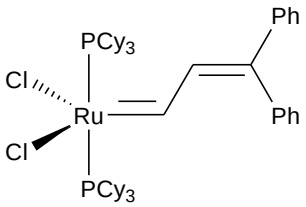

5

Figure 3. Improved Ru-Based Carbene Catalyst **5**[32]

Scheme 8. Synthesis of Grubbs' 1st Generation Catalyst **9**[34]

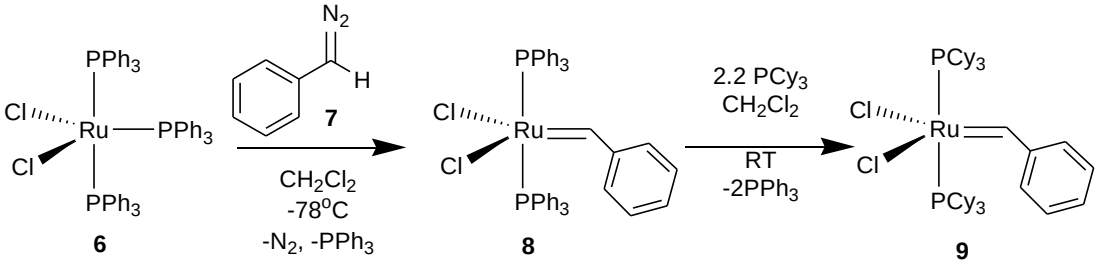

In 1998, Dixneuf *et al.* reported the synthesis of metathesis active, 18-electron Ru-allenylidene complexes.[33] These complexes were synthesized by adding a bulky phosphine-containing ligand precursor to [(*p*-cymene)$RuCl_2$]$_2$. The resulting intermediate was then reacted with propargyl alcohols, with subsequent reaction with $NaPF_6$ and PCy_3 in methanol to yield cationic allenylidene complexes, with complex **10** (Figure 4) as a prominent example. The advantage of these catalysts was that they could be synthesized without the use of the hazardous diazoalkanes employed in the synthesis of catalyst **9** and were thermally more stable than the Grubbs-type catalysts at the time. However, these complexes never gained the same popularity as the Grubbs-catalysts due to their much lower olefin metathesis activity.

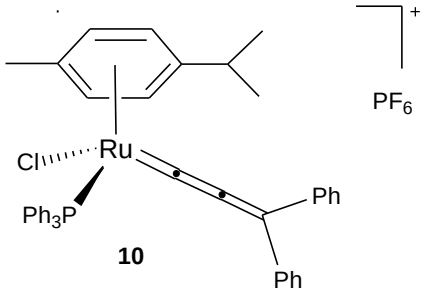

10

Figure 4. 18-Electron Allenylidene Complex **10**[33]

The limited thermal stability of catalyst **9** was improved upon by the development of catalysts coordinated by N-heterocyclic carbene (NHC) ligands, such as IMes[34] (IMes = 1,3-bis(2-,4-,6-trimethylphenyl)-imidazol-2-ylidene) and H_2IMes[35] ligands (H_2IMes = 1,3-bis(2-,4-,6-trimethylphenyl)-4,5-(dihydro)imidazol-2-ylidene). Herrmann *et al.* reported a stable Ru-based olefin metathesis catalyst bearing an NHC ligand **11** (Figure 5) in 1998, though the activity of their catalyst was considered poor due to its extremely slow metathesis initiation rate compared to catalyst **9**, requiring 12 hours to several days to initiate olefin metathesis reaction.[36] However, catalyst **11** did show the potential for NHC ligands to stabilize Ru-based catalysts.

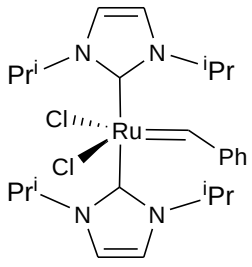

11

Figure 5. Catalyst **11** by Herrmann *et al.*[36]

Further research into the use of NHC ligands was independently pursued by the groups of Nolan,[37] Grubbs,[38] and Herrmann,[36,39] resulting in a variety Ru catalysts bearing NHC ligands, including Grubbs' second generation catalyst **12**, or (H_2ITap)(PCy_3)Cl_2Ru=CH-Ph.[38] This catalyst exhibited unseen high thermal stability

along with elevated activity compared to catalyst **9** as well as similar functional group tolerance. Complex **12** exhibited much slower initiation rates, typically requiring several minutes to initiate olefin metathesis reactions, but this was compensated by extraordinary propagation rates.[40] Hence, catalyst **12** was extremely efficient in RCM reactions. The fast propagation displayed by catalyst **12** is a consequence of the bulky and strongly σ-donating NHC ligand.[41] Catalyst **12** is synthesized through direct replacement of one PCy_3 ligand in catalyst **9** with an H_2IMes ligand which is obtained *in situ* from the dihydroimidazolium salt in the presence of a strong base (Scheme 9).[42]

Scheme 9. Synthesis of Grubbs' Second Generation Catalyst **12**[42]

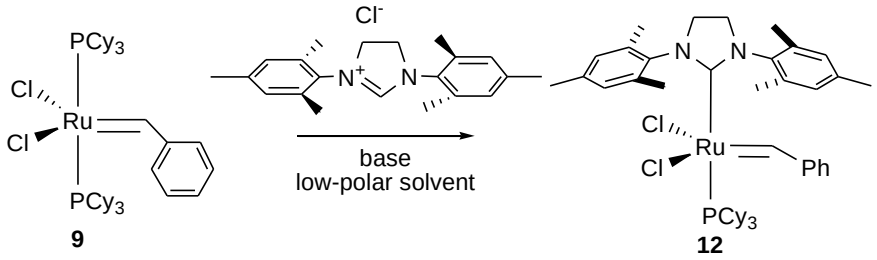

Another approach for modifying these Ru-based catalysts was first realized in 1997 when it was observed that *ortho*-styrenyl ethers could form stable cyclic ruthenacarbenes with these catalysts through bidentate coordination.[43] In 2000 this carbene modification was explored independently by the groups of both Hoveyda[44] and Blechert[45] who simultaneously reported a phosphine-free catalyst bearing the H_2IMes ligand. This catalyst eventually became known as the Hoveyda-Grubbs catalyst **13**. It was synthesized from Grubbs' second generation catalyst **12** and *i*-propoxystyrene in the presence of copper chloride (Scheme 10). This catalyst had certain advantages over catalyst **12**, most importantly it displayed enhanced stability in air, which is attributed to its bidentate coordination which protects the Ru-metal center from oxidation. For this reason, catalysts bearing the bidentate benzylidene ligand were developed for catalyst immobilization and recycling.[46] Otherwise, catalyst **13** exhibited a similar activity profile

to catalyst **12**, including slow initiation and fast propagation rates in comparison to first generation catalyst **9**. Modifications of complex **13** at the benzylidene moiety have also been explored, such as *p*-substitution of the phenyl ring, which sometimes afforded increased initiation rates in comparison to catalyst **13**.[5d]

Scheme 10. Synthesis of Hoveyda-Grubbs Catalyst **13**[44,45]

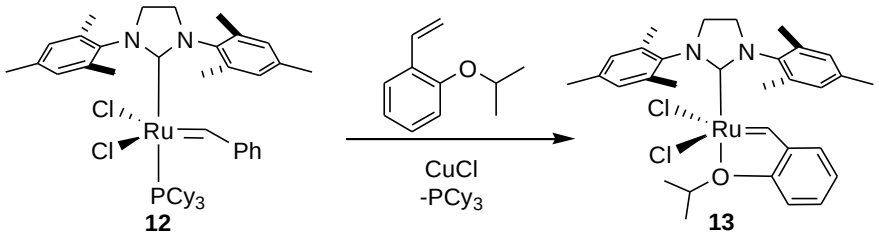

Another modified Grubbs-type catalyst bearing an NHC ligand is Grubbs' third generation catalyst **14** (Figure 6).[38] For this catalyst, which was also derived from catalyst **12**, the phosphine ligand was replaced by two weakly donating 3-bromopyridine ligands. Because these ligands dissociated quickly to free up the necessary coordination site for metathesis, this catalyst exhibited a fast rate of initiation, fast propagation, and therefore extremely high overall catalytic activity. In fact, it is considered the most active olefin metathesis catalyst to date. This catalyst was ideal for specialized ROMP reactions but was not as widely used as catalysts **12** and **13** due to its much decreased thermal stability and its tendency to produce undesired side products as a result of several different types of simultaneous olefin metathesis and hydride shift reactions, both attributed to its extremely high activity.[30]

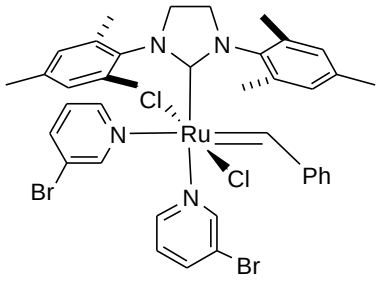

14

Figure 6. Grubbs' Third Generation Catalyst **14**[38]

Modifications of the Ru-carbene moiety were also intensely investigated, leading to a multitude of active Ru-catalyst structures. In 1996, Grubbs *et. al.* explored several different complexes with modified carbene structures, including *para*-substituted benzylidene complexes, such as complex **15**, methylidene complex **16**, alkylidene complexes, such as complex **17**, and vinylidene complex **18** (Figure 7).[5d,h] This study showed that *para* substitution of the benzyilidene ligand did not have a strong effect on the overall activity of the catalyst, though faster initiation rate was observed with Grubbs' first generation catalyst **9**, which did not possess this modification. Complexes **16** and **18** were low-active in metathesis reactions when compared to catalyst **9**, which was attributed to their poor catalyst initiation. As a result of this decreased activity, catalysts with these carbene modifications have not been as widely explored as the traditional benzylidene motif. Alkyl methylidene complexes **17** exhibited higher activity than catalyst **9**. They were synthesized via carbene exchange from catalyst **9** using an excess of the respective alkene gas. However, complexes **17** were the only kinetic product and further converted into complex **16**, which made their isolation cumbersome.[5h]

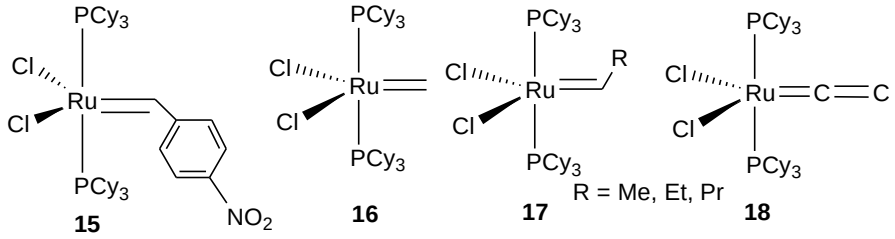

Figure 7. Catalysts **15**-**17** With Modified Carbene Ligands[5d]

In 1999 Schanz and coworkers reported the first coordinately unsaturated 16-electron allenylidene structures **19** and **20**.[37c] As with some of the previous catalysts, these structures utilized strongly donating, bulky PCy_3 ligands, which provided the ruthenium center with a high electron density. The use of the PCy_3 ligands also allowed for straighforward phosphine-ligand exchange reactions, thereby giving access to NHC-ligand bearing allenylidene structures (Scheme 11). Though this class of catalysts displayed significantly lower activity than aforementioned benzylidene catalysts, as they often required several hours to several days to complete a metathesis reaction under similar reaction conditions), allenylidene catalysts were attractive because they tend to exhibit high thermal stability.[37c] These catalysts were also attractive because they can be made from inexpensive, non hazardous starting materials in a straight-forward, one-step synthesis reaction[33a,b,37c] and, last by not least, because the intellectual property for this class of catalyst is not protected.

Scheme 11. 16-Electron Allenylidene Complexes **19** and **20**[37c]

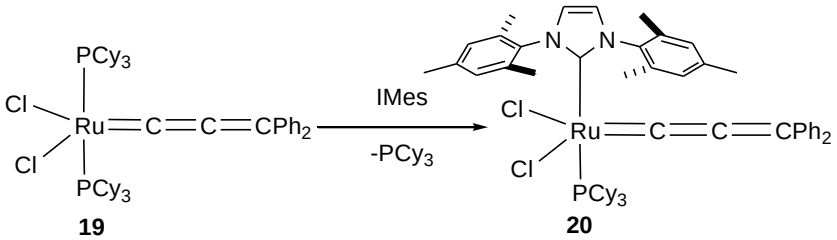

Simple rearrangement of allenylidene structures also granted access to indenylidene catalysts. An early example of this class of catalyst was structure **21**

(Figure 8), which was originally synthesized by Hill and co-workers.[47] This complex was mistakenly first reported as a 16-electron allenylidene complex, but further studies by Jafarpour *et al.*[37b] determined it had an indenylidene structure, a result of an acid-catalyzed rearrangement of the C=C=C spine.[37] NHC-ligated 16-electron indenylidene complexes **22** and **23** were also reported in the same publication (Figure 8).[37b] In general, these indenylidene complexes exhibited better metathesis activity than their allenylidene counterparts combined with very high thermal stability. Today, Ru-indenylidene complexes have become the most popular alternative to the Grubbs-type benzylidene complexes. Several generations of these catalysts are commercially available and are used in a large variety of applications.[48]

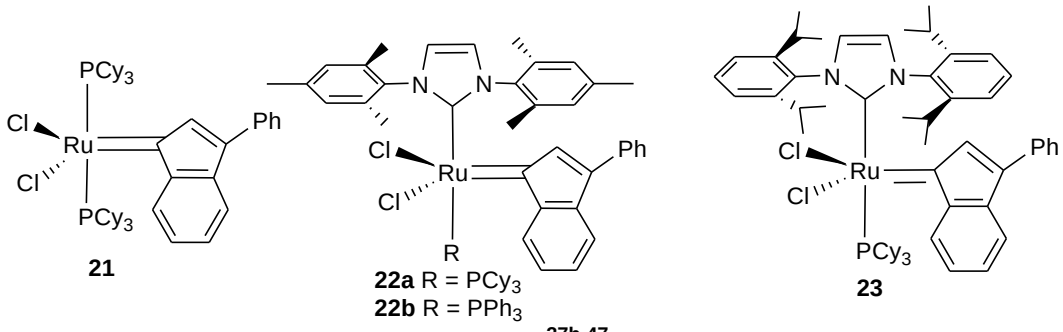

Figure 8. Early Indenylidene Complexes **21**-**23**[37b,47]

Another modification to the Ru-carbene moiety were the Fisher-type carbene complexes, such as those reported by Louie and Grubbs in 2002.[38a] In this study, a series of Fisher-type complexes with the structure $(PCy_3)_2Cl_2Ru=C(H)ER$ or $(IMes)(PCy_3)Cl_2Ru=C(H)ER$ were synthesized with a π-electron donating group directly attached to the carbene carbon. The general activity for these complexes followed the trend E = C > N > S > O. Many of these Fisher-type complexes were metathesis active, but displayed much lower reactivity than catalyst **9**, which was not surprising considering that the generation of Fisher-type carbene complexes, such as those formed upon the addition of excess ethyl vinyl ether, are often used to quench metathesis reaction.

Further studies of Fisher carbene complexes conducted by Ozawa and company found that catalyst structures **24** and **25** (Figure 9) could perform highly selective ring opening / cross metathesis (ROCM) of certain norbornene derivatives with select vinyl chalcogenides, despite their low activity.[49]

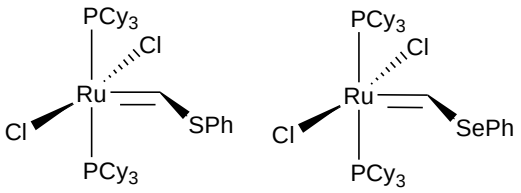

Figure 9. Fischer-Type Carbene Complexes **24**and **25**[49]

Importance of Ru-Based Olefin Metathesis Catalysts

Ru-based Grubbs-type olefin metathesis catalysts have had an enormous impact on organic synthesis. These catalysts have a high preference for carbon-carbon double bonds and often tolerate the presence of alcohols, amides, aldehydes, and carboxylic acids, making them applicable to a wide variety of substrates.[1] More importantly, their use often does not require severe reaction conditions, making them an attractive technology for large-scale industrial applications. These catalysts are also useful to synthetic organic chemists for the production of unique olefins that difficult to synthesize through more traditional organic synthesis methods.

Ru-based Grubbs-type catalysts are currently used to produce a wide variety of products, including highly specialized polymeric materials such as polydicyclopentadiene (poly-DCPD) which is a high-performance, lightweight, corrosion resistant material used to make many products, including unbreakable baseball bats, corrosion resistant piping, lightweight vehicle parts, and bathroom fixtures.[50] These catalysts are also used by the pharmaceutical industry to make macrocyclic compounds which are processed to

generate pharmaceuticals, such as HCV protease inhibitor BILN 2061, which is used to treat hepatitis C,[19a] as well as antitumor macrolides Pladienolide B and D.[19b] The uses for these catalysts continues to grow quickly as more application-specific improvements are made to catalyst designs.

Current Limitations of Ru-Based Olefin Metathesis Catalyst Systems

Even though Ru-based olefin metathesis catalysts have emerged as the preferred catalysts for ROMP and RCM reactions, many problems still exist with their large-scale use. One drawback to most Ru-based catalyst systems is that they are sensitive to air when in solution. While a few Ru-based olefin metathesis catalysts, such as the Hoveyda-Grubbs catalyst **13**, can still perform somewhat effectively under non-inert conditions,[44,45] most Ru-based catalysts are commonly used under inert gas conditions to guarantee optimal performance. Some catalyst designs, such as catalyst **13**, utilize bidentate coordination ligands, which greatly improves the stability of the catalyst by protecting both the carbene ligand and the Ru-metal center.[51] The main drawback to most of these catalyst designs is that upon initiation, metathesis and metal oxidation with molecular oxygen become competing reactions. Hence, activity loss in reactions in air is often significant.

Another limitation for most Ru-based catalysts is a lack stereoselectivity control. There are very few efficient Ru-based olefin metathesis catalysts which exhibit a high degree of *cis* / *trans* selectivity, especially in ROMP and CM reactions. Recently several groups have explored a number of structural modifications, such as bidentate, bulky, and asymmetric ligands, but high *cis / trans* (E/Z) control is still elusive for Ru-based systems in ROMP and CM reactions.[51] While some catalyst designs have afforded improved enantioselectivity in certain applications, particularly for asymmetric ring-closing

metathesis (ARCM),[52,53] these catalyst designs lack high enantioselectivity for a range of different substrates and applications. Though Ru-catalyst stability and stereoselectivity are important limitations being studied, this will be the extent that these are discussed as improving these limitations are not a focus in this dissertation.

One drawback that is important for this dissertation and which is displayed by most Ru-based olefin metathesis catalyst systems is their limited solubility profiles. The majority of these catalysts can only be used in organic solvents of a small polarity range. Only a few designs exist which can be used homogenously in aqueous media.[6] Water is an attractive solvent for many applications due to its low toxicity, relative abundance, and cost-effectiveness.[51,54] Reactions in aqueous media have been carried out with water-insoluble Ru-based olefin metathesis catalysts by the means of sonication,[55] or in the presence of an organic co-solvent[56] or surfactant,[57] however none of these methods were very efficient or environmentally advantageous.

Several water-soluble Ru-based olefin metathesis catalysts have been synthesized that promote metathesis reactions homogeneously in aqueous media.[6,58] Some of these catalysts bear NHC ligands modified with hydrophilic groups, such polyethylene glycol (PEG) along the NHC backbone. Hong and Grubbs published one notable example in 2006.[6a] This Hoveyda-Grubbs type catalyst **26** (Figure 10) displayed higher ROMP, RCM, and CM activity than most previous water-soluble catalysts. Other ligand modifications have incorporated charged ionic functionalities for enhanced solubility in aqueous media. This has typically been accomplished through ionic ammonium groups added to the backbone of the NHC ligand such as those present on complex **27** or through ammonium groups attached to the chelating benzylidene moiety in complexes **27** and **28** (Figure 10).[6c,58] Catalyst **27** is very attractive due to its relatively straightforward synthesis, but it is not highly soluble in purely aqueous media, requiring

an alcohol co-solvent for homogenous conditions. Catalysts **26** and **28**, on the other hand, are highly water-soluble but require an intense synthetic effort, with up to eight additional synthetic steps. Additionally, these catalysts are limited as they do not perform well-controlled aqueous ROMP. Hence, these designs are not attractive beyond conceptual studies.

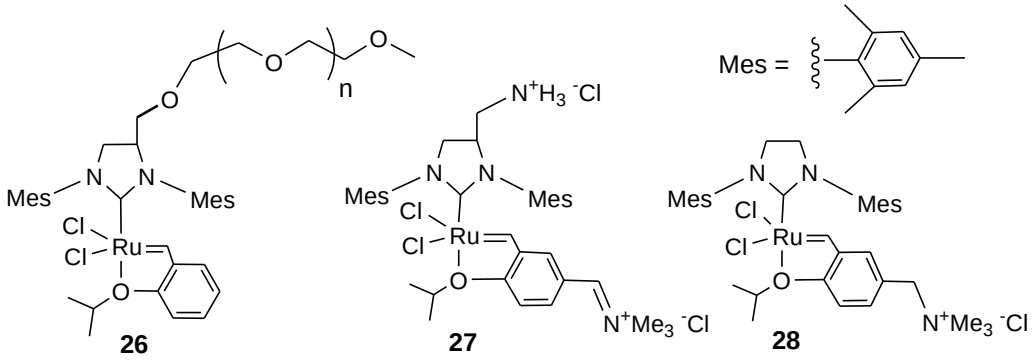

Figure 10. Examples of Water-Soluble Ru-Based Olefin Metathesis Catalysts **26**-**28**[6,58b]

Another limitation or Ru-based olefin metathesis catalyst systems is the removal of the Ru-metal catalysts from the product stream. Because Ru-based olefin metathesis catalysts are used homogenously, catalyst removal is often difficult and costly. This is particularly problematic for the pharmaceutical industry. Currently the pharmaceutical industry performs column chromatography over silica gel for effective Ru removal. This method is very costly and time consuming, often requiring several repetitive column cycles (typically 5-10) to reduce the Ru-contamination levels below 10 ppm, the upper limit for Ru contamination in pharmaceutical products.[6b,59] Alternative methods for catalyst removal do exist, such as chemical scavenging[60] and physical absorbtion,[61] but to date these methods are generally not used due factors such as cost, toxicity, and long processing times. Additionally, none of these methods on their own successfully reduce the Ru-metal contamination <50 ppm, still far above the required pharmaceutical standard.

In recent years some advancements have been made with catalysts designed specifically for enhanced removal after metathesis reactions from the product stream.[22] Several catalysts were designed for improved separation via column chromatography, though most of these designs do not sufficiently reduce the level of Ru-metal contamination below the pharmaceutical standard through just one cycle.[51] Other catalysts have been designed with modified solubility profiles that allow for extraction of the catalyst with water or ionic liquids, but to date only a few, such as catalyst complex **29** (Figure 11), reduce the level of Ru below the required pharmaceutical standard.[62] Using another approach, some catalysts have been immobilized on solid support. Complex **30** (Figure 11) is the most successful example, which leaves less than 20 ppb Ru-metal contamination in its products.[63] Though these catalyst designs were very successful at reducing Ru-metal contamination in metathesis products and could be reused several times, they still require high catalyst loadings (>2%) and an enormous synthetic effort to produce, which again makes them very little attractive for large-scale, industrial use.

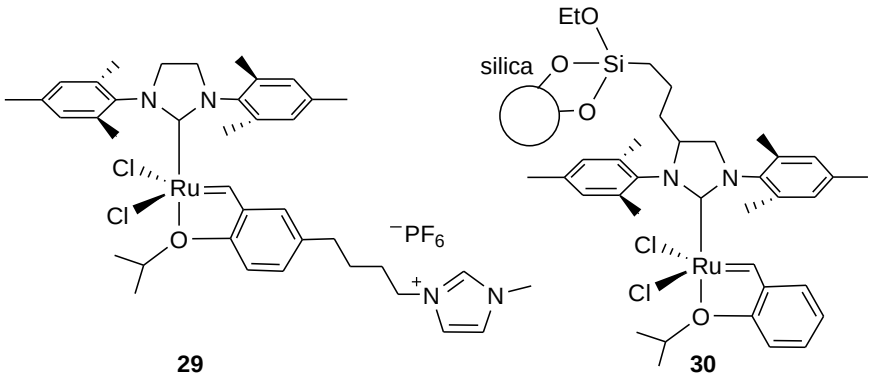

Figure 11. Catalyst Complexes **29**[62] and **30**[63] With Improved Removability

The lack of external activity controls is another issue that is problematic in several applications. Typically, when a catalyst is added to substrate, the metathesis reaction proceeds until all substrate is consumed or the catalyst decomposes. This is

particularly problematic for the production of specialized polymers and poly-DCPD, whose physical properties and production safety suffer from this uncontrolled activity. These could be improved by externally triggering a latent catalyst, which would allow for safe mixing of substrate and catalyst.

In 2007, Schanz *et al.* published a method that chemically enabled the independent reversible inhibition and subsequent reactivation of a catalyst system.[64] This was accomplished through the addition of N-donor ligands to catalyst **9**, resulting in the formation of an inhibited species with very little ROMP activity. The method allowed for mixing of a monomer substrate and inhibited catalyst without any catalytic activity until an acid was applied to reactivate the catalyst. This was the first reversible "off/on" switch for the olefin metathesis reaction. The two ligands utilized in this inhibition with subsequent reactivation protocol were 1-methyl imidazole (MIM) and 4-dimethylaminopyridine (DMAP). The inhibition was based on the formation of low-active complex **31** additionally inhibited by free PCy_3 ligand until the addition of acid generates complex catalyst **32**, thereby restoring the catalyst's activity (Scheme 12). Other catalysts bearing acid-responsive donor ligands have been developed. Many of these catalysts are coordinated by pentane-2,4-dione and salicyaldimine ligands, which dissociate from the Ru-metal center upon addition of a Lewis acid or Brönsted acid, such as HCl.[64,65]

Scheme 12. Inhibition and Subsequent Reactivation of Catalyst **31**[64]

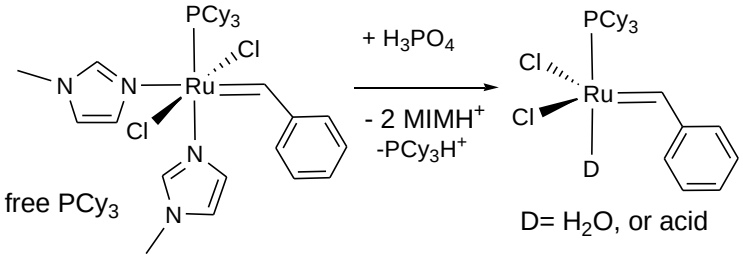

31
Catalyst is Inhibited
No ROMP Activity

32
Catalyst is Activated
High ROMP activity

Heat is another straightforward stimulus that has previously been used to trigger ROMP reactions. The catalysts used in these methods often contained a back-biting N[66] or S-donor ligand.[67] ROMP reactions with these catalysts start by thermally triggering the dissociation of the bidentate ligand. Although these catalysts were easily and safely handled, their application suffered from very low catalyst efficiencies due to the fact that they have to exhibit zero-activity at ambient temperature, as a result of extremely low rates of olefin metathesis initiation. Since only a very low fraction (far below 5%) of the catalyst is typically activated during the reaction, high catalyst loadings (usually ≥2%) were required, which is not very economical.

In a few studies, light has been used as external stimulus for activation of Ru-based olefin metathesis catalysts. An early study of catalyst **9** found that photolysis with light (λ = 546 nm) triggered the dissociation of one phosphine ligand,[68] however, no further studies for catalyst **9** were conducted with respect to enhanced metathesis initiation under these conditions. Few Ru-based light-activated metathesis reactions have been described in the literature,[69] but until quite recently the pre-catalysts used in these studies lacked the presence of an active alkylidene moiety. For these catalysts, the alkylidene was generated *in situ* from the substrate. The advantage of these light activated catalyst systems was that they do not rely on sophisticated and expensive Ru-

alkylidene complexes as starting materials, but their drawback was the ill-defined nature of the reactive species, which made performance optimization difficult. Additionally, these catalysts only were successfully used with substrates of extremely high ROMP activity, namely norbornene. Because thermally and light triggered catalyst systems only worked at elevated temperatures and/or require long reaction times (up to 24 hours) for catalyst initiation, they generally did not demonstrate well-control ROMP reactions or low catalyst/substrate ratios. In 2009, Grubbs *et al*. reported the first successful photo-activated metathesis reaction protocol for a Ru-alkylidene complex in combination with a photoacid generator, however a high catalyst/substrate ratio was required and many reactions did not go to completion.[70]

Controlled Polymerizations (ROMP)

In 1956 Szwarc defined a "living polymerization" as one that proceeds "without chain transfer or termination".[71] When no noticeable catalyst decomposition occurs, ROMP is as a living polymerization (LROMP).[1a] One of the earliest examples of LROMP using Ru-based olefin metathesis catalysts was published by Kanaoka and Grubbs in 1995.[72] In this study, catalysts **4** (Figure 2) and **5** (Figure 3) produced homogenous polymers as well as block copolymers from silicon-containing norbornene derivatives, and several of these reactions proceeded in a somewhat controlled fashion. This method was applied in organic media, but to date only one Ru-based olefin metathesis catalysts has been reported to perform controlled ROMP homogenously in aqueous media. [6a]

Key to controlled ROMP is a high ratio between the rates of initiation and propagation. A controlled polymerization must be living and additionally requires fast and complete initiation. When these conditions are met, the polymers produced have a polydispersity index (PDI) <1.5.[1b,73] A few methods have been identified that enhance the initiation rate of Ru-based catalysts using Brønsted or Lewis acids.[64,65] However, no

methods have been identified for external control of the rate of propagation in the LROMP reaction. The moderation of the rate of propagation could be a complementary approach to controlled LROMP, particularly considering the low thermal stability exhibited by fast ROMP initiators and the higher degree of secondary metathesis reactions exhibited by fast ROMP propagators.

Dissertation Goals

The main purpose of this dissertation research was to develop Ru-based olefin metathesis catalysts with pH-responsive ligands. These pH-responsive ligands provided the means to externally control the solubility profile and, in many cases, the activity of the catalyst via acid addition. External control of the catalyst's solubility allowed for use of these catalysts with a wider range of solvents and substrates, including olefin metathesis reactions in aqueous media. Some of these catalysts exhibited a reversible solubility profile, which made them useful for applications such as efficient catalyst removal after RCM reactions. External control of catalyst activity was used to alter the rate of initiation and/or propagation of the catalyst, thereby changing the overall activity of the catalyst. The overall goal of this research is to develop catalysts capable of performing RCM and ROMP reactions in both aqueous and organic media with extreme efficiency and high activity.

CHAPTER II

NHC LIGAND PRECURSOR SYNTHESIS

NHC Ligand Precursors Modified With pH-Responsive Dimethylamino Groups

Several modifications to the NHC ligands of Ru-based olefin metathesis catalysts have been made in an effort to improve several attributes of the catalyst, including solubility, activity, and selectivity.[22,51] The modification of NHC ligand precursors is synthetically more straightforward than for phosphine ligands, and therefore is a more feasible approach to the synthesis of novel, Ru-based olefin metathesis catalysts.[74] Typically, NHC ligands are generated *in situ* via deprotonation of the NHC ligand precursor salt (**A**) with a strong base, such as potassium hexamethyldisilazane (KHMDS) or potassium *tert*-butoxide (KO*t*-Bu) (Scheme 13). This yields the singlet carbene species **B**, which is in equilibrium with the imidazoline structure **C**. Structure **B** is the free ligand species needed for the phosphine-NHC ligand exchange reaction described in Chapter I. For imidazole-2-ylidenes, such as the IMes ligand, the free carbene **B** is preferred, as this configuration affords 4n+2 Hückel aromaticity resulting from the four-electron three-center π system of the N-C-N in combination with the two π-electrons of the NHC ligand backbone.[75,76] For dihydroimidazol-2-ylidenes, such as the H_2IMes ligand, which lack Hückel aromaticity in configuration **B**, imidazoline **C** is dominant in the equilibrium as the thermodynamically more favored structure.[75,76] When neutrally charged, the NHC free carbene readily undergoes ligand exchange with the phosphine in commercially available Grubbs' first generation catalyst **9** when low-polar solvent conditions are applied. These low-polar solvent conditions are a requirement for complete ligand exchange.[41,77] This phosphine-ligand exchange provides the means to generate new olefin metathesis catalysts.

Scheme 13. Deprotonation of NHC Ligand Precursor Salt

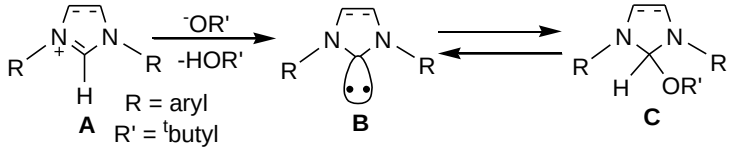

For this dissertation, several functionalized, pH-responsive NHC ligand precursors were synthesized. This was accomplished by incorporating pH-responsive dimethylamino (NMe_2) groups into the NHC ligand precursors. NMe_2 groups were ideal for this study because they are compatible with Ru-based systems[78] and are neutrally charged, therefore they do not negatively impact the phosphine-NHC ligand exchange at the Ru-center in low-polar solvents, allowing for straightforward access to new catalyst structures. The resulting catalysts are pH-responsive, which opens up the possibility for external control of catalyst properties via acid addition. Once protonated, these NMe_2 groups become charged ionic species, which will alter catalysts' solubility profiles. Protonation of these groups may also change the electronic environment of the ligand, depending on the position of the NMe_2 group of the ligand, hence modifying the donating ability of the ligand, thereby impacting the overall activity profile of the catalyst.

Synthesis of the H_2ITap·HCl and ITap·HCl Ligand Precursors

The first NHC ligand precursor salt synthesized for this project was H_2ITap·HCl **37** (H_2ITap = 1,3-bis(2',6'-dimethyl-4'-dimethylaminophenyl)-4,5-dihydroimidazol-2-ylidene) containing two NMe_2 groups bound directly to the aromatic NHC ligand substituents.[79] Precursor **37** was synthesized from commercially available starting material *N*,*N*-3,5-tetramethylaniline **33**. Compound **33** was converted into phenylenediamine derivative **34** according to literature procedures[80] with 45% overall yield. Following the literature procedure for the production of the H_2IMes ligand[41] with a few modifications, **34** was then converted into the respective NHC ligand precursor salt

37 in three steps (65% overall yield) via intermediates **35** and **36** (Scheme 14). In this process, an improved hydrogenation procedure was developed for diimine **35** utilizing $NaBH_4$ and H_3BO_3 to afford the diamine **36** in high yield and purity.[79]

Scheme 14. Synthesis of Ligand Precursor **37** : (i) (1) $NaNO_2$/conc. HCl_{aq}, 60 min, -5 ^oC, (2) Sn/HCl, 70 ^oC (45%); (ii) $(CHO)_2$/MeOH [HCl], 24 h, RT (85%); (iii) $NaBH_4$/ H_3BO_3/thf, 60 min, 30 ^oC (88%); (iv) $HC(OEt)_3/NH_4Cl$, 12 h, 130 ^oC (87%).

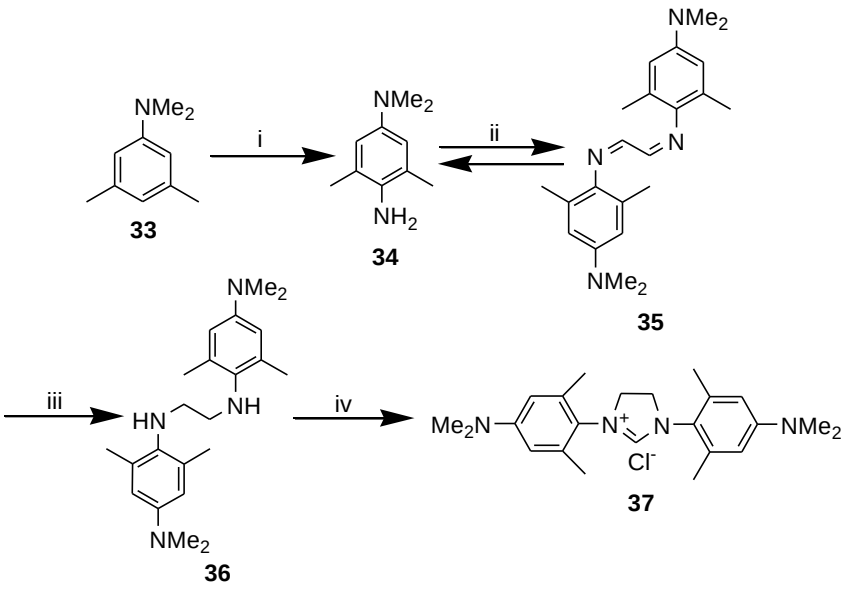

As a complimentary motif, NHC ligand precursor ITap·HCl **38** (ITap = 1,3-bis(2',6'-dimethyl-4'-dimethylaminophenyl)imidazol-2-ylidene) was synthesized with an unsaturated backbone. ITap•HCl **38** is the unsaturated analogue to H_2ITap•HCl **37**. In general, NHC ligands with unsaturated backbones (imidazole-2-ylidenes) typically have lower activity than catalysts bearing dihydroimidazol-2-ylidenes, their saturated counterparts.[51] The synthesis of this ligand precursor was accomplished with a 78% yield by reacting diimine **35** with paraformaldehyde and Me_3SiCl in ethyl acetate at 70 °C using a modified literature procedure (Scheme 15).[81]

Scheme 15. Synthesis of ITap·HCl **38**

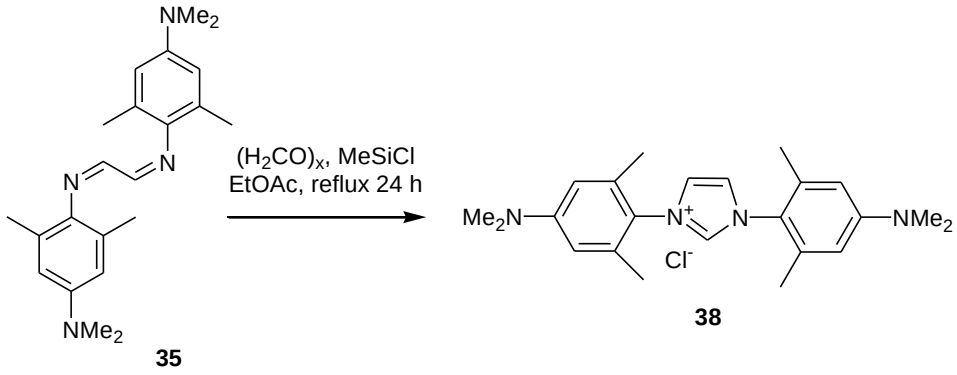

35 **38**

Ligand Precursors Using a Template Synthesis

In an effort to quickly gain access to a library of additional unique NHC ligand precursors, a template synthesis for a variety of ligand precursor salts was developed. These, like ligand precursor salts **37** and **38**, also contained two ancillary NMe_2 groups. The key synthetic step to this template synthesis was the functionalization of diiodinated diamine intermediates **48**-**50** via Cu-mediated C-heteroatom coupling reactions,[82] allowing for simplified access to several unique ligand precursors. In the first part of this template synthesis method, iododiamine intermediates were synthesized from commercially available anilines. The anilines chosen were 2,6-dimethylaniline **39**, 2,6-diisopropylaniline **40**, and 2,4-dimethyl aniline **41** (Figure 12). These anilines were first iodinated at their unsubstituted ortho or para positions.[83] The resulting iodoaniline derivatives **42**-**44** were then converted into their corresponding double Schiff bases **45**-**47** using glyoxal.[78] These double Schiff bases were then reduced, resulting in the desired diamine intermediates **48**-**50** (Scheme 16). Using this strategy, three new di(iodophenyl)diamine intermediates were generated (Figure 13).

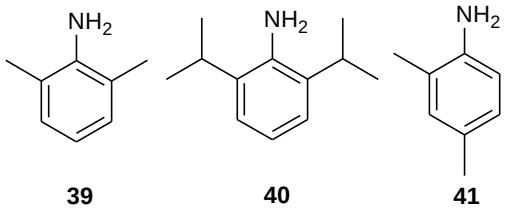

Figure 12. Commercially Available Anilines

Scheme 16. Synthesis of Diamine Intermediates **48**-**50**

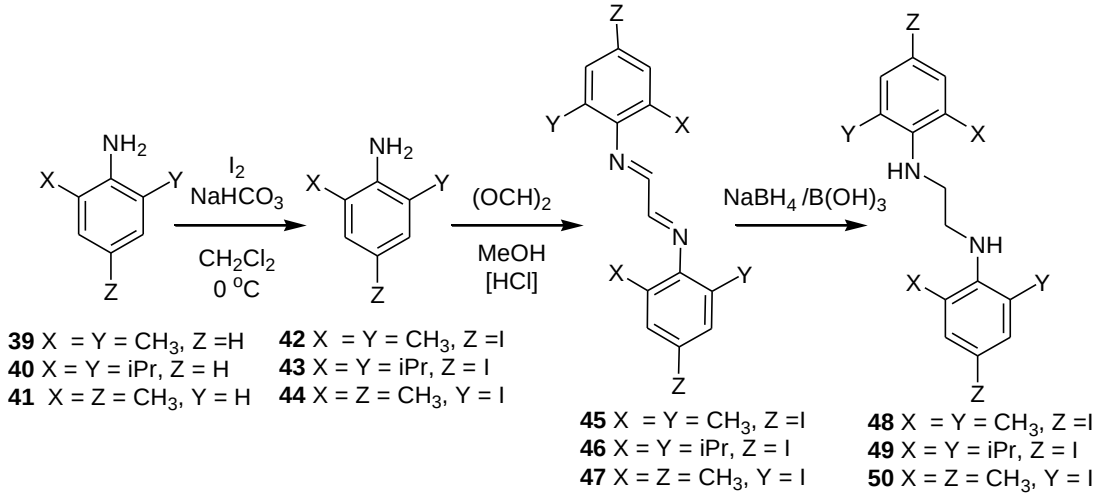

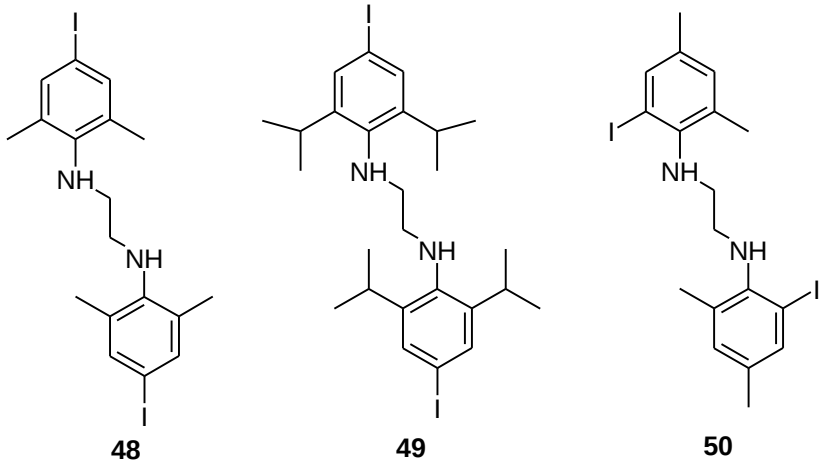

Figure 13. Iododiamine Intermediates **48**-**50**

More ligand diversity was introduced starting from the iododiamine intermediates, which were functionalized through Cu-mediated coupling reactions to obtain functionalized diamines **51**-**54** and **59**, **60** with the aryl substituents E-CH_2-CH_2-NMe_2 (E

= S or O). These ether and thioether groups possessed the pH-responsive NMe_2 groups that allowed for external control of a catalyst via acid addition. Since these NMe_2 groups were separated from the aryl groups of the NHC ligand substituents by an E-CH_2-CH_2 spacer, the electronic effect on the donor ability of the NHC ligand by protonating these groups were significantly reduced (*vide infra*). Four of these functionalized diamines (**51**-**54**) were successfully converted into NMe_2 functionalized NHC ligand precursor salts **55**-**58** by performing a ring closing reaction[78] with triethyl orthoformate (Scheme 17). For functionalized diamines **59** and **60** no pure NHC ligand precursor salt could be isolated due to extensive formation of unknown side products (Scheme 18). Therefore, the ortho functionalized ligand precursors were not further pursued in this project. Overall, four new NHC ligand precursors **55**-**58** (Figure 14) were prepared using the template synthesis. Throughout this dissertation, the ligands generated from these precursors will be referred to as IXyONMe_2 (IXyONMe_2 = 1,3-bis(4'-[2''-dimethylaminoethoxy]-2',6'-dimethylphenyl)-4,5-dihydroimidazol-2-ylidene), IXySNMe_2 (IXySNMe_2 =1,3-bis(4'-[2''-dimethylaminoethanethio]--2',6'-dimethylphenyl)-4,5-dihydroimidazol-2-ylidene), IDippONMe_2 (IDippONMe_2 =1,3-bis(2',6'-diisopropyl-4'-oxo-N,N-dimethylethanaminophenyl)-4,5-dihydroimidazol-2-ylidene), and IDippSNMe_2 (IDippONMe_2 =1,3-bis(2',6'-diisopropyl-4'-thio-N,N-dimethylethanaminophenyl)-4,5-dihydroimidazol-2-ylidene), respectively.

Scheme 17. Synthesis of Ligand Precursors **55**-**58**

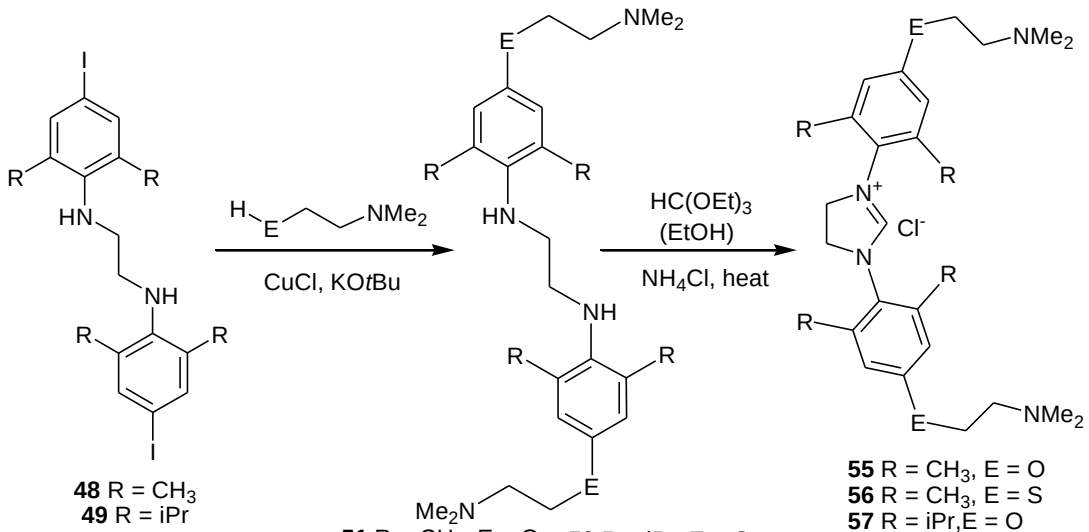

Scheme 18. Reaction Products Obtained from Iododiamine Intermediate **50**

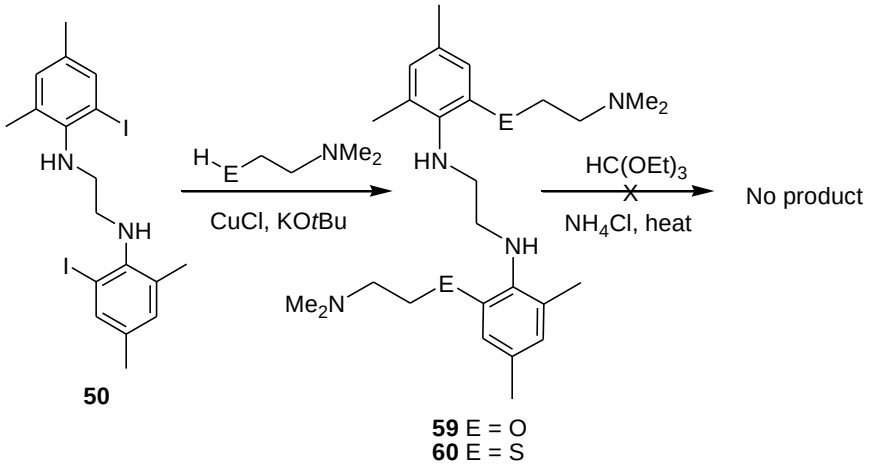

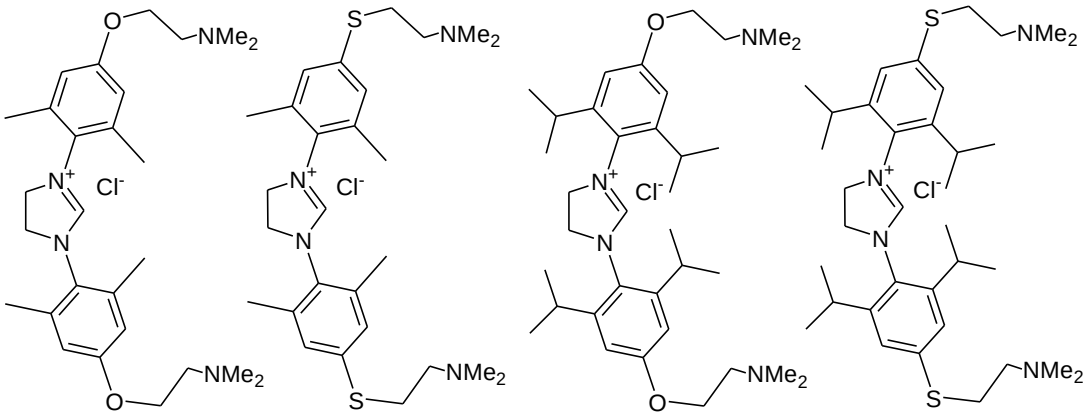

55 **56** **57** **58**

Figure 14. NHC Ligand Precurors **55**-**58**

CHAPTER III

CATALYST SYNTHESIS

Ru-Based Olefin Metathesis Catalysts Bearing pH-Responsive Ligands

The purpose of this dissertation was to synthesize Ru-based olefin metathesis catalysts bearing pH-responsive ligands. The catalysts that were generated for this project bear NHC ligands modified with NMe_2 groups, as described in Chapter II. Once protonated, these groups are converted from neutral amino groups into cationic ammonium groups, allowing for external control of catalyst solubility profiles and via acid addition. For some of these catalysts, the functionalized NHC ligand also permits the external control of catalyst activity, particularly for those bearing an H_2ITap or ITap ligand, due to a change in the electronic environment and therefore overall donating ability of the NHC ligand.

Several of the catalysts generated for this study also bear basic, pH-responsive N-donor ligands. As described in Chapter I, the Schanz research group has pioneered a method that uses N-donor ligands for the inhibition of catalyst systems with subsequent reactivation via acid addition.[73] Kinetic studies for these complexes showed that the overall reaction times for all reactivated ROMP reactions were faster than the same reactions with the precursor catalyst **9** due to the near-instant formation of a very fast-initiating species. The N-donor ligands chosen for this work were DMAP and the bidentate 3-(*o*-pyridyl)propylidene moiety. The use of these ligands in conjunction with NMe_2 modified NHC ligands should yield unprecedented catalyst systems that exhibit simultaneous external control of catalyst solubility and activity in metathesis reactions via the degree of protonation of the pH-responsive functionalities.

Synthesis of Catalysts Bearing pH-Responsive Ligands

Grubbs-Type Benzylidene Catalyst Synthesis

The first pH-responsive NHC ligand precursor used to generate the catalyst for this study was the H_2ITap ligand precursor salt **37**. This was reacted *in situ* with Grubbs' first generation catalyst **9** in the presence of a strong base to produce the second generation-type catalyst (H_2ITap)(PCy_3)Cl_2Ru=CH-Ph **61** in 70% yield via phosphine ligand exchange in accordance with literature procedure.[38,78] It should be noted that a similar catalyst, with two NEt_2 instead of NMe_2 groups, was simultaneously synthesized by Plenio *et al.*, though external control of the catalyst via acid addition was not initially explored by this group.[84] Catalyst **61** was then converted into Hoveyda-Grubbs-type catalyst (H_2ITap)Cl_2Ru=CH-(C_6H_4-O-*i*Pr) **62**, also in 70% yield, using 2-*i*-propoxystrene in the presence of CuCl (Scheme 19), also in accordance with literature procedures.[44,45] The bidentate coordination of this catalyst's modified benzylidene ligand has previously been shown to enhance the overall stability of the catalyst without causing a significant loss of activity compared to its PCy_3-coordinated benzylidene counterpart.[44,45] Suitable crystals of complexes **61** and **62** were then grown, and their structures in solid state were solved via X-ray crystallography (Figures 15 and 16).[79]

Scheme 19. Synthesis of Catalyst Complexes **61** and **62**: (i) **9**/KOtBu/heptane, 24 h, 60 ^{o}C (70%); (ii) 2-i-propoxystyrene/CuCl, 2 h, 35^{o}C (70%).

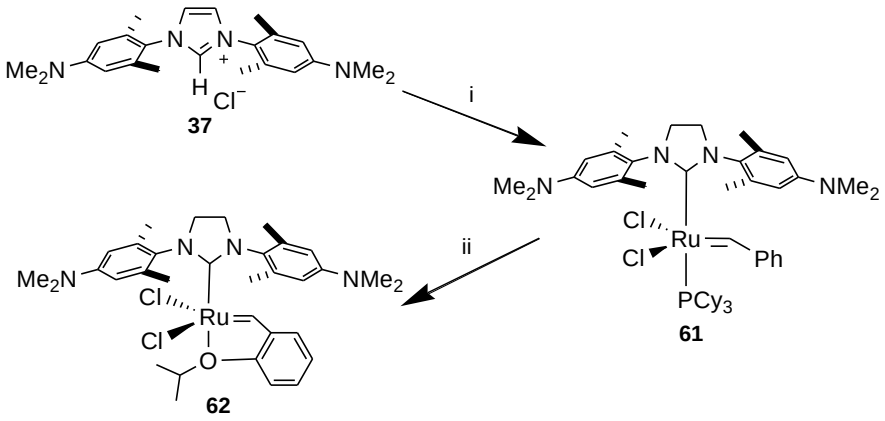

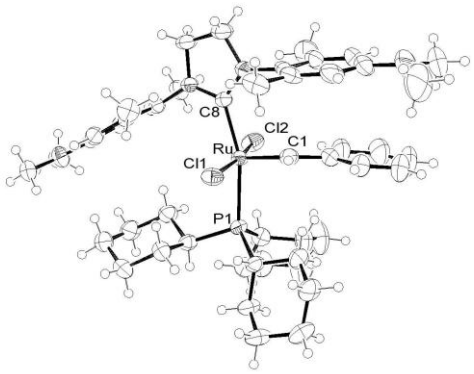

Figure 15. Oak Ridge Thermal-Ellipsoid Plot Program (ORTEP) Diagram of Catalyst **61**

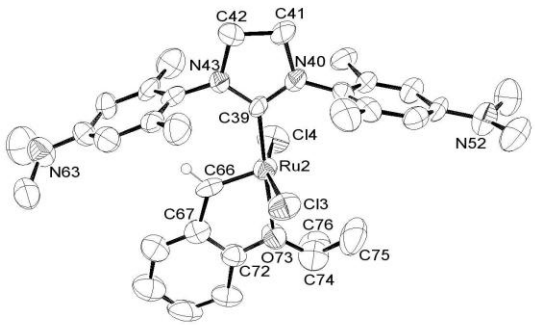

Figure 16. ORTEP Diagram of Catalyst **62**

Analysis of the crystal structures showed that complexes **61** and **62** exhibit a distorted square pyramidal ligand environment, which is typical for pentacoordinate Ru–carbene complexes. The base is formed by the donor ligands and the chlorides, and the benzylidene moiety is in the apex. In catalyst **61**, all bond distances and bond angles involving the ruthenium center were in the same range as for catalyst complex **63** (Figure 17) bearing a 1,3-dimesityl-1,4,5,6-tetrahydropyrimidin-2-ylidene ligand, the only other crystal structure published for a Grubbs second generation-type complex bearing an unsaturated NHC ligand backbone, within a margin of 0.01 Å and 0.6^{o}.[85] The only exception was the Ru-C_{NHC} distance of 2.075 Å, which was actually shorter in complex

61 by more than 0.03 Å (2.106 Å) than observed for complex **63**. This bond distance was more similar to the Ru–C_{NHC} distance of the corresponding (IMes)(PCy_3)Cl_2Ru=CHPh complex **64** (Figure 17) with a Ru-C_{NHC} distance of 2.069 Å.[37a] This was not surprising as the mesityl substituents are less angled towards the metal center in catalyst **61** than in the tetrahydropyrimidin-2-ylidene complex **63** due to its shortened NHC ligand backbone. As a result, the steric interference with the benzylidene moiety was less pronounced. This was also reflected in the longer distance between the mesityl *ipso*-carbon atom to the benzylidene carbon atom in catalyst **61** compared with complex **63** (3.01 Å *vs.* 2.9 Å). The long distance between the aromatic ring and the carbene moiety was speculated to be responsible for lowered metathesis activity of the tetrahydropyrimidin-2-ylidene complex **64** in comparison to Grubbs' second generation catalyst **12**.[85]

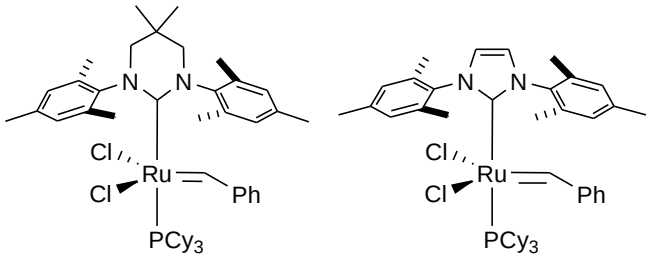

63 **64**

Figure 17. Catalyst Complexes **63**[85] and **64**[37a]

The unit cell of the crystal structure of catalyst **62** contained two discrete complex molecules and one molecule of CH_2Cl_2 in solvation. The averaged bond distances of both molecules were similar to those of the H_2IMes analogue **13**[44] (deviations <0.01 Å) with one exception. The distance between the Ru-center and the benzylidene carbon atom was extremely short in catalyst **62** (1.735 Å), shorter by almost 0.1 Å than in catalyst Hoveyda-Grubbs catalyst **13**. As the only structural difference between the two catalyst complexes was the presence of the remote *p*-NMe_2 groups in catalyst **62** instead of the *p*-methyl groups in catalyst **13**, it is likely that this shortening of the metal–

carbene bond was less due to steric reasons than electronic differences. In comparison to catalyst **13**, the *trans* bond angles at the metal center and the C–Ru–C *cis* angle were slightly larger in catalyst **62** by approx. 2–3°. However, the C–Ru–O *cis* angle for catalyst **62** (78.1°) is smaller by 1.3° than in catalyst **13**. This was unexpected due to the shorter Ru–carbene bond, which should have caused a widening of this angle assuming comparable bond angles in the relatively rigid benzylidene chelate. The small C–Ru–C *cis* angle also caused a large distance between the mesityl *ipso*-carbon atom to the benzylidene carbon atom in catalyst **62** (3.08 Å) in comparison to PCy_3 coordinated complex **61**.

Table 1. Selected Bond Angles [°] and Distances [Å] for Catalysts 61 and 62[79]

	61	**62**
Ru=C(H)	1.826(2)	1.735(9)
Ru-C(NHC)	2.0746(19)	1.966(7)
Ru-O	-	2.260(5)
Ru-P	2.4419(6)	-
Ru-Cl	2.4080(6) 2.3809(6)	2.330(2) 2.339(2)
P-Ru=C(H)	91.45(9)	-
O-Ru=C(H)	-	78.1(3)
C(H)=Ru-C(NHC)	99.49(9)	103.2(3)
P-Ru-C(NHC)	179.41(9)	-
O-Ru-C(NHC)	-	178.5(3)
Cl-Ru-Cl	169.64(4)	159.69(8)

Catalyst **61** was also used to synthesize two catalysts with pH-responsive N-donor ligands. The first was $(H_2ITap)(DMAP)_2Cl_2Ru$=CH-Ph **65** (Figure 18), which was synthesized by reacting catalyst **61** in the presence of excess DMAP in *t*-butyl methyl ether, in accordance with the procedure developed in our laboratories.[64] Since this catalyst was virtually insoluble in the reaction solvent it was isolated through vacuum filtration of the green precipitate, giving complex **65** in very high yield (90%) and purity (>99%, ^{1}H NMR spectroscopy). The incorporation of the pH-responsive DMAP ligands allows for the control of catalyst activity via acid addition. Thus, protonation with excess

non-nucleophillic acid would cause the DMAP ligands of this catalyst to dissociate, freeing up the necessary ROMP coordination site, thereby accelerating the initiation rate of the catalyst.

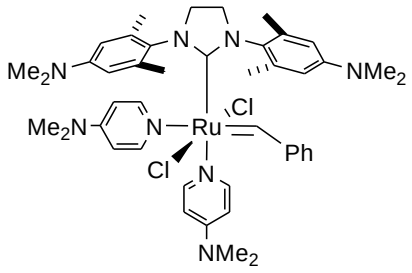

65

Figure 18. DMAP Catalyst Complex **65**

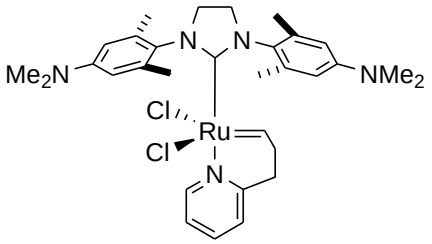

66

Figure 19. Catalyst Complex **66**

(H_2ITap)Cl_2Ru(=CH-CH_2-CH_2-C_5H_4N) **66** (Figure 19) is another complex synthesized from catalyst **61** that bears a pH-responsive N-donor ligand. In this structure, the PCy_3 and carbene ligands of catalyst **61** were replaced by a backbiting N-donor ligand. This ligand was incorporated into the catalyst structure by reacting complex **61** in the presence of excess 2-(3-butenyl)pyridine, generating complex **66** via simple carbene exchange. This product complex **66**, like DMAP complex **65**, was not soluble in the reaction solvent and was isolated as a green precipitate with an 88% yield. This backbiting ligand affords much slower initiation than observed with precatalysts **9** and **61**, but upon protonation the nitrogen of this ligand dissociates from the metal center, thereby accelerating the rate of catalyst activity.

The next pH-responsive ligand precursor examined for the synthesis of Grubbs-type benzylidene catalysts was ITap·HCl salt **38**. This salt was first used to synthesize (ITap)(PCy_3)Cl_2Ru=CH-Ph **67**, followed by complexes (ITap)Cl_2Ru=CH-(C_6H_4-O-*i*Pr) **68**, and (ITap)$(DMAP)_2Cl_2$Ru=CH-Ph **69** (Figure 20) following the procedures described for their unsaturated analogues, catalysts **61**, **62**, and **65**. They were obtained in yields between 67-95%. Attempts to synthesize the ITap analogue to catalyst **66** were not

successful, which might be attributed to the decreased activity of its precursor complex **67**.

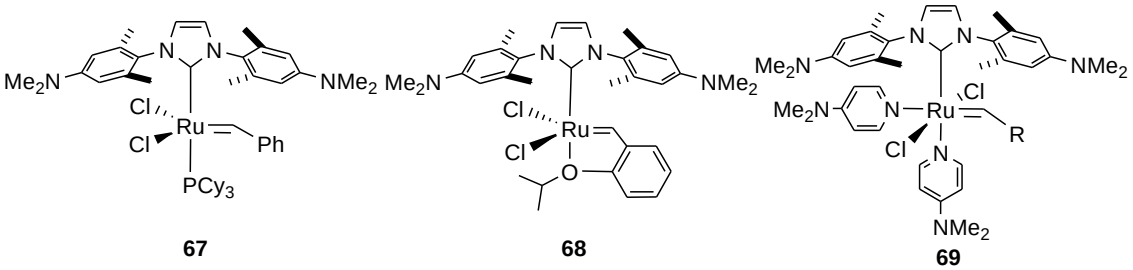

67 **68** **69**

Figure 20. Catalyst Complexes **67**-**69** With Unsaturated NHC Ligand Backbones

Previous studies with complexes bearing IMes and H_2IMes ligands demonstrated that catalysts possessing an unsaturated NHC backbone generally have lower activity than their counterparts with a saturated backbone. On the other hand, such catalysts frequently exhibit enhanced thermal stability, making them the preferred catalyst motif for certain applications.[51] As such, we expected that complexes **67**-**69** would exhibit significantly lower activity than seen with complexes **61**, **62**, and **65**.

The syntheses of Grubbs-type catalysts bearing the NHC ligand precursors **55**-**58** (Figure 21), which were produced via the template synthesis described in Chapter II, have proven much more difficult. To date, the only Grubbs second generation-type catalyst successfully isolated from any of these ligand precursors is ($IXyONMe_2$)(PCy_3)Cl_2Ru=CH-Ph **70** (Figure 22). This complex was obtained via a ligand exchange reaction with catalyst **9** using the $IXyONMe_2$ precursor salt **55**, as was used to synthesize complex **61**.[79] This ligand exchange reaction required prolonged reaction time (48 hours) compared to that required for catalyst complex **61**. Since catalyst **61** precipitated from solution in heptanes, isolation of the pink product proceeded via vacuum filtration. The isolated yield (40%) was lower than for catalysts **61** and **67**. Though similar in structure to ligand precursor salt **55**, attempts to synthesize analogous

complex **71** (Figure 22) using IXySNMe$_2$ precursor salt **56** did not afford any noticeable ligand exchange from catalyst **9**, even after running the reaction for ten days. As such, other target complexes bearing the IXySNMe$_2$ ligand were not pursued.

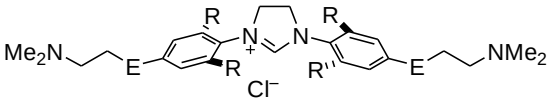

55 E = O, R = CH_3
56 E = S, R = CH_3
57 E = O, R = ^{i}Pr
58 E = S, R = ^{i}Pr

Figure 21. NHC Ligand Precursor Salts **55**-**58**

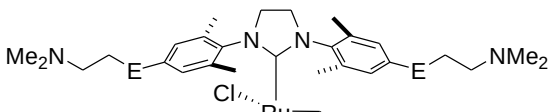

70 E = O
71 E = S

Figure 22. Catalyst Complexes **70** and **71**

Two other second generation Grubbs-type complexes, **72** and **73** (Figure 23), have been generated *in situ* from reactions with catalyst **9** and ligand precursor salts **57** and **58**, respectively, but to date neither complex has been successfully isolated and purified. The presence of these complexes was indicated by both ^{1}H and ^{31}P NMR spectra obtained after solvent removal. For example, when the ^{1}H NMR spectra for complex **73** was examined, the Ru=C*H* signal present at 19.7 ppm was indicative of the formation of a second generation-type catalyst, as was the ^{31}P signal present at 29.0 ppm (Figures 24 and 25, obtained before completion of the reaction). However, these catalysts exhibited appreciable solubility in heptane as well as in a 1:1 mixture of 2-propanol/water, the solvents or solvent mixture which are usually used for precipitation. Attempted precipitation of complexes **72** and **73** with other solvents and solvent mixtures were not successful. Product isolation via column chromatography was also not successful as the complexes adhered to acidic, neutral, and basic stationary phases regardless of what solvent conditions were applied. It is likely that this was a result of catalyst degradation on the column.

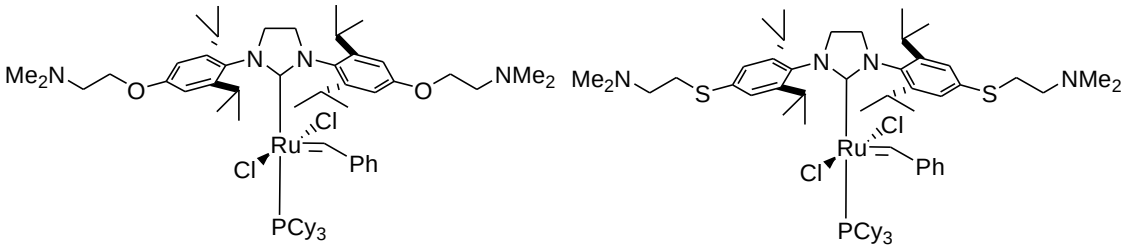

72 **73**

Figure 23. Catalyst Complexes **72** and **73** Generated *in situ*

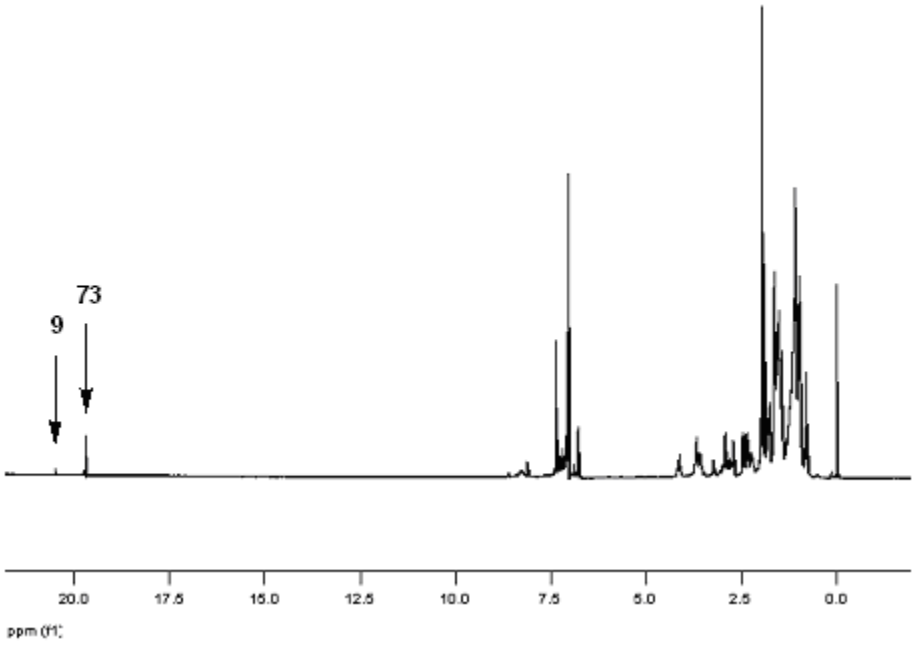

Figure 24. ^{1}H NMR Spectrum of Complex **73** Generated *in situ* (300.1 MHz, 20 ^{o}C, C_6D_6)

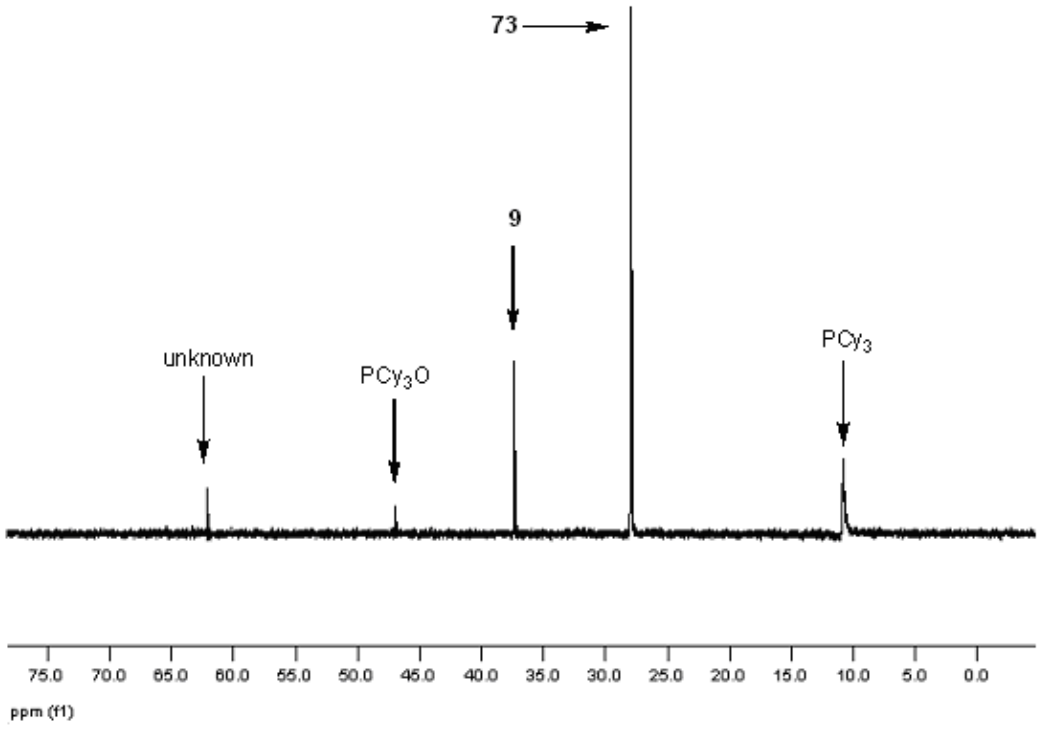

Figure 25. ^{31}P NMR Spectrum of Complex **73** Generated *in situ* (300.1 MHz, 20 ^{o}C, C_6D_6)

Though complexes **72** and **73** could not be isolated, attempts were made to generate Hoveyda-Grubbs-type complexes **75** and **76** (Scheme 20). One strategy was to filter the reaction solutions containing the parent complexes and to react them *in situ* with 2-*i*-propoxystrene and CuCl. Once again, ^{1}H NMR indicated the presence of the desired complexes, however attempts to isolate these complexes by removing the CuCl and other impurities via column chromatography or recrystallization proved fruitless. It should be noted that removal of the Cu-based byproduct in the exchange reaction has only been accomplished via flash column chromatography to date. Hence, complexes **75** and **76**, which contain very basic NMe_2 groups, very likely decomposed on a basic column, as OH^- ions are known to decompose Grubbs-type catalysts.[40c] The catalysts also could not be separated from neutral or acidic column media due to protonation of the NMe_2 groups, which made the catalysts adhere very strongly to the stationary phase.

An alternate synthetic route based on a literature procedure developed by Grela *et al*. was also attempted.[86] In this procedure, first generation Hoveda-Grubbs complex **74** was first synthesized, isolated, and purified. Then this complex was reacted with ligand precursor salts **57** or **58** in an attempt to form catalyst complexes **75** and **76** (Scheme 20). Though fewer impurities were present in this reaction solution, attempts to isolate the product complexes via flash column chromatography were once again unsuccessful.

Scheme 20. Synthesis of Complexes **75** and **76** via an Alternate Syntetic Route

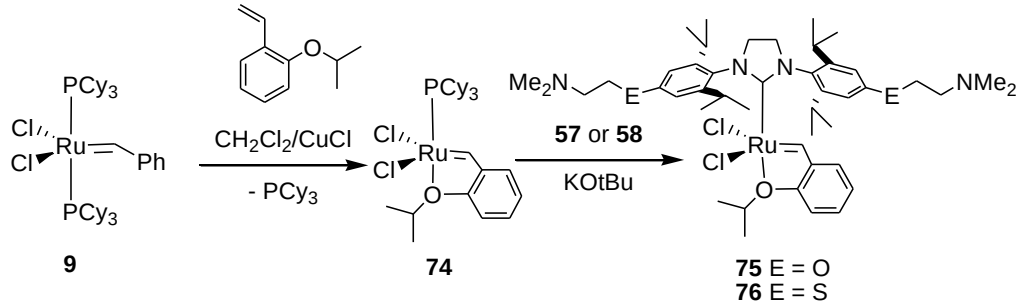

Synthesis and isolation of DMAP derivatives (IDippONMe$_2$)(DMAP)Cl$_2$Ru=CHPh **77** and (IDippSNMe$_2$)(DMAP)Cl$_2$Ru=CH-Ph **78** (Figure 26) from complexes **72** and **73** proved much more fruitful. As with the initial attempts to synthesize Hoveyda-Grubbs-type catalysts, derivative complexes **77** and **78** were obtained via direct filtration of the reaction solutions of the parent complexes **72** and **73**, followed by subsequent reaction *in situ* with excess DMAP. The new solutions were then either sonicated or stirred for periods of 2-24 hours. Complexes **77** and **78** then precipitated from solution, allowing for their isolation via filtration. As with catalyst complexes **65** and **69**, complexes **77** and **78** contain a DMAP ligand and a pH-responsive NMe$_2$, allowing for external control of solubility and activity. However, complexes **77** and **78** only bear one DMAP ligand, very likely as a result of the larger steric bulk provided by the NHC ligands. Pentacoordinate Ru-alkylidene complexes bearing only one N-donor ligand have been islated before,[51]

and the DMAP ligand is always coordinated *trans* to the NHC donor ligand in these complexes.

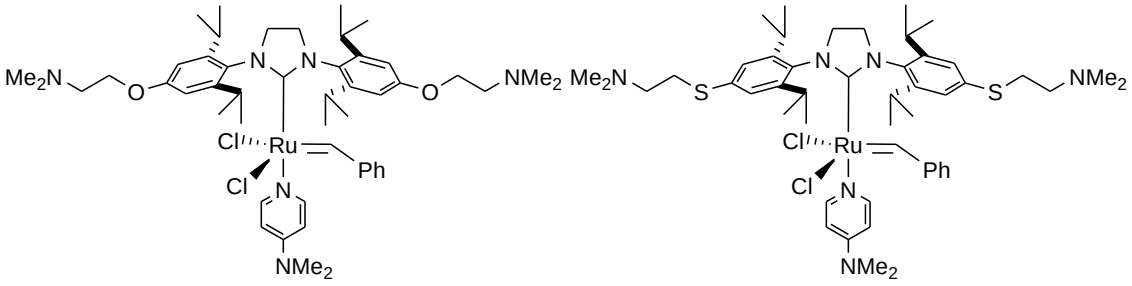

77 **78**

Figure 26. DMAP Catalyst Complexes **77** and **78**

Because catalyst complexes **70**, **77**, and **78** possess an unsaturated NHC ligand backbone, they were expected to have similar activity to their H_2ITap ligand bearing analogues **61** and **65** under non-acidic conditions. Under acidic conditions, however, the NHC ligation of these catalysts were anticipated to exhibit less influence on the activity due to the proximity of their NMe_2 groups from the aryl substituents of their NHC ligands by an E-CH_2-CH_2 spacer, where E = O or S. This spacer minimizes the interference of the protonated N^+HMe_2 with the electron donating properties of the NHC ligands. This allows for the external control of catalyst solubility with pH-responsive N-donor ligands being the only influence on the catalyst activity upon protonation where present (*vide infra*). The alkyl NMe_2 groups of these NHC ligands are also much more basic than the aryl NMe_2 groups of the H_2IMes ligand, so gradual protonation of complexes **77** and **78** should afford protonation of these NMe_2 groups before significant protonation at the N-donors occurs.

Synthesis of Catalysts With a SPh Modification to the Carbene Ligand

Previous studies have shown that catalysts containing Ru-carbenes modified with SPh groups are capable of some degree of substrate selectivity under certain conditions.[49] These catalysts have also shown decreased activity when compared to their traditional benzylidene counterparts,[38a] though this decreased activity could be an advantage when applied to substrates that exhibit very high metathesis activity since reduced catalyst activity also means a lower degree of side reactions.[51] These properties make the SPh modified Ru-carbene catalysts an interesting alternative to the benzylidene Ru-carbene catalysts which were the main focus of this dissertation for the use in specialty applications. By incorporating NMe_2 modified NHC ligand precursors H_2ITap or ITap, these phenylthiomethylidene catalysts should also exhibit externally controllable activity and solubility profiles.

Hence, catalyst complexes (H_2ITap)(PCy_3)Cl_2Ru=CH-SPh **79**, and (ITap)(PCy_3)Cl_2Ru=CH-SPh **80** (Figure 27) were synthesized from catalyst precursor **24** (Figure 9) using ligand precursor salts **37** and **38** respectively, employing protocols very similar to those employed to generate corresponding benzylidene catalysts. Because SPh precatalysts are much slower initiators than their benzylidene counterparts, complete phosphine-ligand exchange required much more time (4-6 days) to obtain complete conversion to obtain second generation products when compared to the synthesis of catalyst **61**. The isolated yields obtained were also lower, with 68% for complex **79** and 78% for complex **80**. By reacting these products with excess DMAP, structures **81**, (H_2ITap)$(DMAP)_2Cl_2$Ru=CH-SPh, and **82**, (ITap)$(DMAP)_2Cl_2$Ru=CH-SPh, were also synthesized (Figure 27) in very high yields (>90%). Dissociation of these DMAP ligands via acid addition was expected to improve catalyst initiation, thereby improving the overall activity of these catalysts.

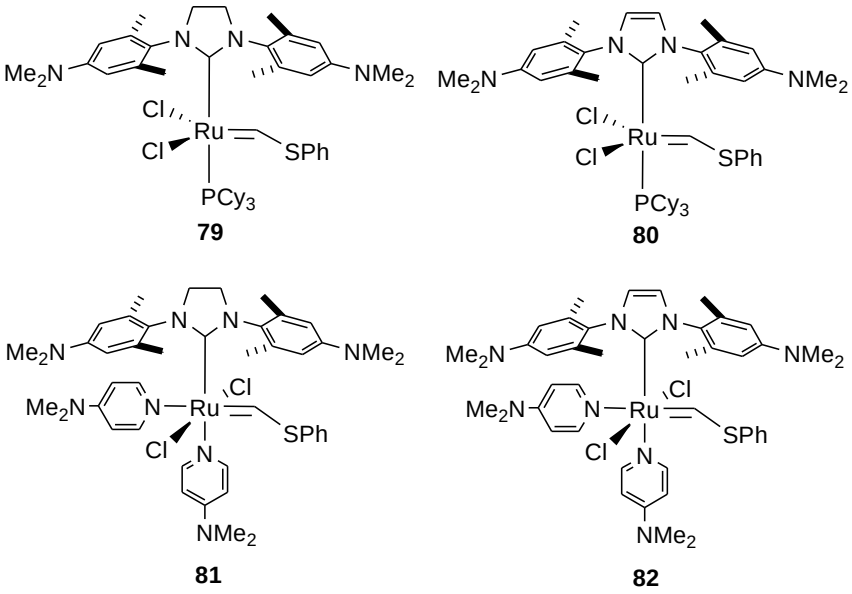

Figure 27. Catalyst Complexes **79**-**82** with SPh Modified Carbenes

Suitable crystals were obtained for catalyst complex **81**, and its structure in solid state was solved via X-ray crystallography (Figure 28). As expected, analysis of the crystal structure showed that this hexacoordinate complex exhibits a slightly distorted octahedral geometry. When compared with $(H_2IMes)(DMAP)_2Cl_2Ru$=CH-Ph **83** (Figure 29), a similar NHC-ligand bearing DMAP catalyst complex previously published by the Schanz research group,[87] the results showed that all bond distances in **81** are slightly shorter (0.01-0.06 Å) than in catalyst **83** with the exception of one of the Ru-Cl bonds. The Ru-N distance to the DMAP *trans* to the alkylidene was shorter by 0.06 Å in complex **81** than **83**, suggesting that this DMAP ligand should be more labile in complex **83** (Table 2). The bond angles also showed a few more significant differences between the structures. First was the *trans* bond angle between the same DMAP and the Ru-carbene, which was nearly 180^o in complex **83** but bent more by 13^o in complex **81**. The second noticeable difference was the *trans* angle between NHC ligands and the other DMAP ligand, which was nearly linear in complex **81** but smaller by 15^o in complex **83**. The differences suggested that less internal geometric strain exists in complex **81**

between the alkylidene and the NHC ligand, very likely due to the presence of the sulfur, which increases the distance between the phenyl group and the metal center, allowing for a tighter arrangement (shorter distances) of the ligands around the Ru-metal center without significantly distorting the octahedral arrangement. This was also reflected by the *trans* chloride ligands of complex **81**, which had nearly identical bond lengths and more linearity to their *trans* bond angle when compared to those of complex **83**.

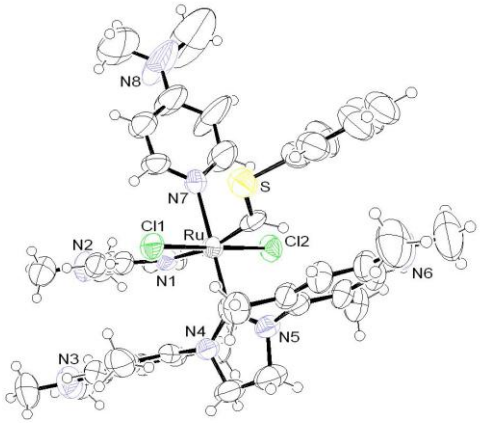

Figure 28. ORTEP Diagram of Catalyst **81**

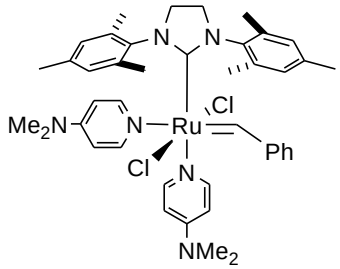

83

Figure 29. DMAP Catalyst Complex **83**

Table 2. Selected Bond Angles [°] and Distances [Å] for Catalysts 81 and 83

	81	**83**
Ru=C(H)	1.849 (3)	1.873 (2)
Ru-C(NHC)	2.031 (3)	2.051 (2)
Ru-N	2.184 (3)	2.1933 (16)
	2.272 (3)	2.3309 (17)
Ru-Cl	2.4132 (9) 2.4255 (9)	2.3847 (5) 2.4372 (5)
(NHC)C-Ru=C(H)	96.05 (13)	95.00 (9)
N-Ru=C(H)	163.82 (10)	176.64 (7)
	86.23 (12)	101.27 (7)
N-Ru-C(NHC)	99.26 (11)	97.01 (7)
	177.73 (13)	162.41 (8)
Cl-Ru-Cl	179.25 (4)	177.54 (2)

Attempts were also made to generate complexes **84**, **85**, and **86** (Figure 30) using ligand precursor salts **55**, **57**, and **58**, respectively. Though these catalysts would also be low active catalysts, they were expected to exhibit enhanced stability. This quality would have been advantageous for applications in aqueous media upon protonation of the NMe_2 groups of their NHC ligands. Unfortunately, none of these ligand precursors afforded complete ligand exchange with catalyst precursor **24**, with only 30-70% conversion to product obtained. Attempts to isolate these products from the starting complex were unsuccessful.

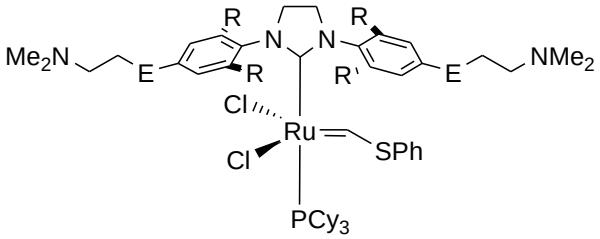

84 E = O, R = CH_3
85 E = O, R = ^{i}Pr
86 E = S, R = ^{i}Pr

Figure 30. Target Complexes **84**, **85**, and **86**

Synthesis of Indenylidene Catalyst Complexes

Indenylidene Ru-catalyst complexes are also an attractive alternative to the traditional benzylidene (Grubbs-type) catalysts. These catalysts are easily obtained via acid-catalyzed rearrangement of the C=C=C spine of allenylidene catalysts structures,[37b] which makes them as commercially attractive as their allenylidene counterparts. Many of these complexes display high activity, though they are often not quite as active as benzylidene catalysts. Their main advantage over most of their benzylidene counterparts is their high thermal stability, which makes them the preferred catalysts for many applications, in particular at elevated temperatures.[51]

Another advantage is the stability of the $(PPh_3)_2Cl_2$Ru-3-phenylindenylidene precursor catalyst **21**. Hence, catalyst modifications may avoid the use of the expensive PCy_3 ligand, which usually is sacrificed in later catalyst modifications. So far, the only indenylidene complexes that could be generated in the project were made using ITap ligand precursor salt **38**. To synthesize these complexes, phenylindenylidene parent complex **21** was first synthesized according to literature procedure.[37b,47] Complex **21** was then used to generate (ITap)$(PPh_3)Cl_2$Ru-3-phenylindenylidene **87** in moderate yield (67%) via phosphine ligand exchange. An excess of DMAP was then added to this complex to generate (ITap)$(DMAP)_2Cl_2$Ru-3-phenylindenylidene **88**, which was afforded in 87% yield (Scheme 21). For complexes **87** and **88** the protonation of their pH-responsive groups was expected to change their solubility and activity. They were also expected to exhibit higher thermal stability than benzylidene counterparts **67** and **69**.

Scheme 21. Synthesis of Phenyl Indenylidene Catalyst Complexes **87** and **88**

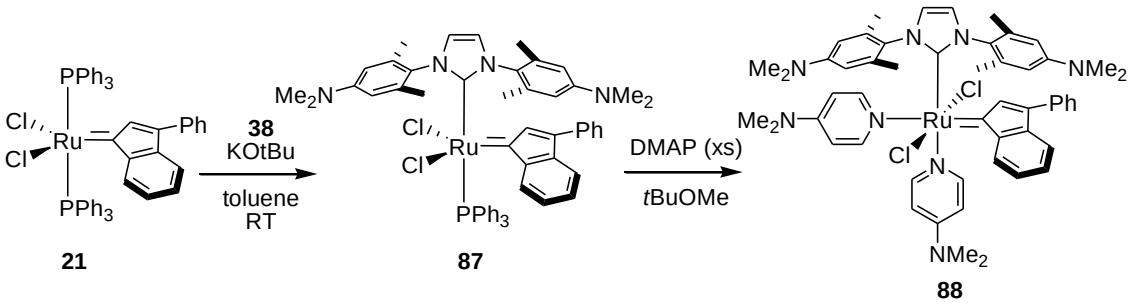

Summary

For this dissertation, many different catalyst structures were attempted. Most of these were benzylidene-carbene (Grubbs-type) catalysts, though other alkylidene motifs were also explored. All of the catalysts generated bear pH-responsive NMe_2 modified NHC ligands, though some also possess pH-responsive DMAP or 3-(*o*-pyridyl)propylidene N-donor ligands. In all, a total of 16 new catalyst complexes were synthesized, isolated, and characterized. Most of these were generated using H_2ITap or ITap ligands precursor salts **37** and **38**. Catalysts made with ligand precursor salts **55**-**58** proved much more difficult to synthesize and isolate, and hence, they are only found in three of the new catalyst structures.

CHAPTER IV

KINETIC STUDIES IN ORGANIC MEDIA

Substrates and Methods for Relative Kinetic Studies in Organic Media

To assess the basic olefin metathesis activity for each of the new catalysts described in Chapter III, ROMP and RCM reactions were conducted in organic media. The substrates selected for these studies were chosen in order to avoid competing secondary metathesis reactions. The activity of the new catalysts was compared to commercially available catalysts under the same reaction conditions. Relative kinetic studies for some of these catalysts were also conducted in the presence of acid to assess the change in catalyst solubility and activity afforded by their pH-responsive ligands upon protonation.

The substrates selected for ROMP reactions in organic media included cyclooctene (COE) and *exo*-7-oxanorbornene derivative **89** (Scheme 22). Experiments with COE were conducted small scale in an NMR tube, and the progress of the reaction was directly monitored via ^{1}H NMR.[79] To monitor conversion of norbornene substrate **89** to poly-**89**, kinetic studies were conducted by quenching aliquots of a reaction solution collected over specific time intervals with ethyl vinyl ether,[20] which were then individually analyzed via ^{1}H NMR spectroscopy after solvent removal. The relative amounts of monomer and polymer present were determined by integration of the sufficiently separated monomer and polymer signals for select hydrogen atoms of each substrate at specific time intervals. Unless otherwise stated, all ROMP reactions were conducted in benzene with [Ru] = 0.5 mM and 0.5% catalyst loadings. In a few reactions, polymers were produced on a larger scale and isolated according to literature procedures.[64] The isolated polymers were then analyzed via gel permeation chromatography (GPC) to determine the average molecular weights and polydispersity indices (PDIs) of the

polymers produced in order to establish the degree of control and initiation efficiency provided under specific conditions.

Scheme 22. ROMP Substrates

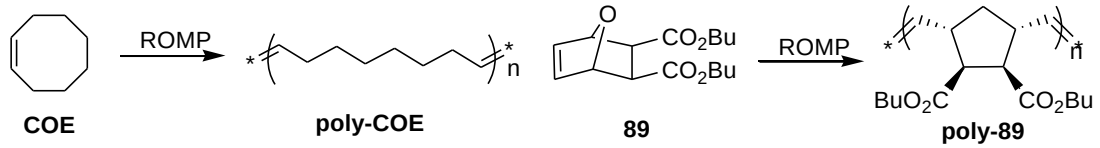

COE **poly-COE** **89** **poly-89**

For RCM reactions, diethyldiallylmalonate (DEDAM) and 3,3-diallylpentane-2,4-dione (DAP) were the substrates chosen for kinetic studies in organic media (Scheme 23). These two substrates dramatically favor their cyclopentene RCM products **90** and **91** over all other olefin metathesis products under most reaction conditions. For these substrates, as with COE, small-scale reactions were monitored directly in an NMR tube,[78] and conversion to product was determined via ^{1}H NMR by integration of sufficiently separated substrate and product signals for their allylic hydrogens. Unless otherwise stated, these reactions were conducted in benzene with [Ru] = 1.0 mM and 1.0% catalyst loadings. It has been established that terminal olefins, such as those found in DEDAM and DAP, are generally more reactive substrates for olefin metathesis than the 1,2-disubstituted olefins used in ROMP, therefore initiation is faster in RCM than in ROMP.[1g] This increase in activity, however, does come at a price, as many RCM reactions never reach full conversion to product due to the formation of unstable Ru-methylidene intermediate complexes that degrade noticeably in the reaction solution, in particular when the RCM activity is low.[64] According to our observations, DMAP ligated catalysts generally exhibit faster decomposition in RCM reactions than other pyridine complexes.[64] The reason for this is not known for certain, but the elevated nucleophilicity of the DMAP in comparison to far less basic pyridines is likely the most important factor. The result is a very low stability for the corresponding Ru-methylidene complex generated during the RCM reaction.

Scheme 23. RCM Substrates

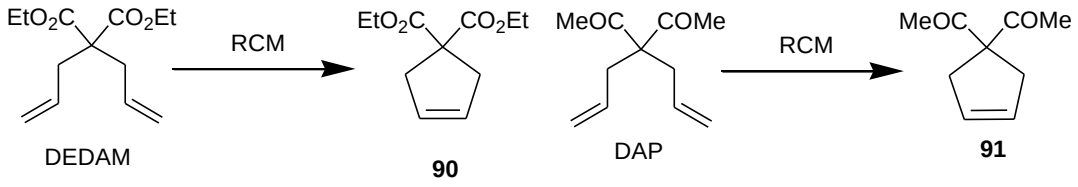

Once ROMP and RCM kinetic profiles were obtained for each of the new catalysts, they were then compared to those obtained for commercially available catalysts under similar reaction conditions. The commercially available catalysts selected were Grubbs second generation catalyst **12** and Hoveyda-Grubbs catalyst **13** (Figure 31). These catalysts were chosen not only for their structural similarity to many of the catalysts that were examined, but also because they are widely used for commercial applications. Therefore, catalysts **12** and **13** provide a standard for comparing the relative profiles of the new catalysts, based on their modified NHC ligands.

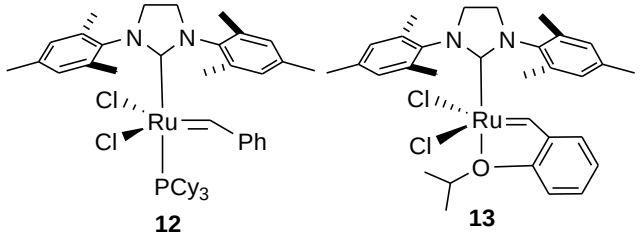

Figure 31. Commercially Available Catalysts **12** and **13**

After obtaining kinetic profiles under standard, non-acidic conditions, many of these studies were repeated in the presence of various equivalents of acid. The two acids that were chosen include H_3PO_4 and *p*-toluenesulfonic acid (TsOH). Non-nucleophillic acids were chosen because they do not significantly affect the coordination at the Ru-center, which is sometimes observed in the presence of nucleophillic acids. These studies were conducted to determine the degree of external control on the solubility and activity profiles for these catalysts afforded via protonation of their pH-responsive ligands. Specific emphasis was placed on the study of ROMP kinetic profiles,

particularly on the rates of initiation and propagation relative to those acquired under standard conditions, to evaluate the change in activity upon protonation of the pH-responsive groups.

Kinetic Studies

Kinetic Studies of Benzylidene Catalysts Bearing an H_2ITap Ligand

The first two catalysts evaluated using ROMP and RCM reactions were (H_2ITap)(PCy_3)Cl_2Ru=CH-Ph **61** and (H_2ITap)Cl_2Ru=CH-(C_6H_4-O-*i*Pr) **62** (Figure 32). Their catalytic activity was then compared to that of commercially available catalysts **12** and **13** under similar reaction conditions. Since the overall structure of catalysts **61** and **62** were very similar to their commercially available counterparts, they were expected to exhibit similar activity profiles under standard conditions. Any differences in activity were attributed to the electronic effects afforded by the NMe_2 groups of their H_2ITap ligands.

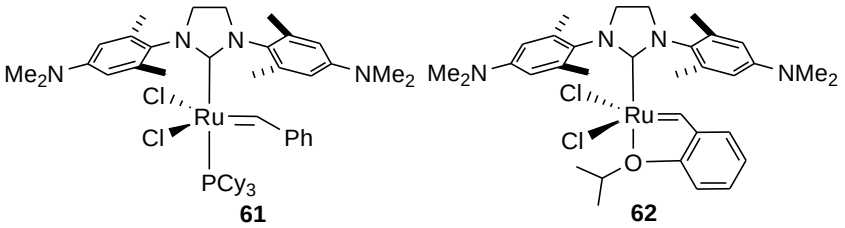

Figure 32. Complexes **61** and **62**

Relative kinetic results showed that both H_2ITap catalysts **61** and **62** were very active in olefin metathesis and performed ROMP of COE with similar activity to their commercially available counterparts (Figure 33). Evaluation of the kinetic profiles suggested that catalyst **62** had a faster rate of initiation, as catalyst **13** exhibited a significantly longer induction period before the dramatic rate increase was observed. Such long induction times are typical for slow-initiating but fast-propagating olefin metathesis catalysts and thus strongly affect the overall reaction rates.[3] The kinetic results also showed that both PCy_3 ligated complexes **12** and **61** initiated at significantly faster rates than Hoveyda-Grubbs-type catalysts **13** and **62**.

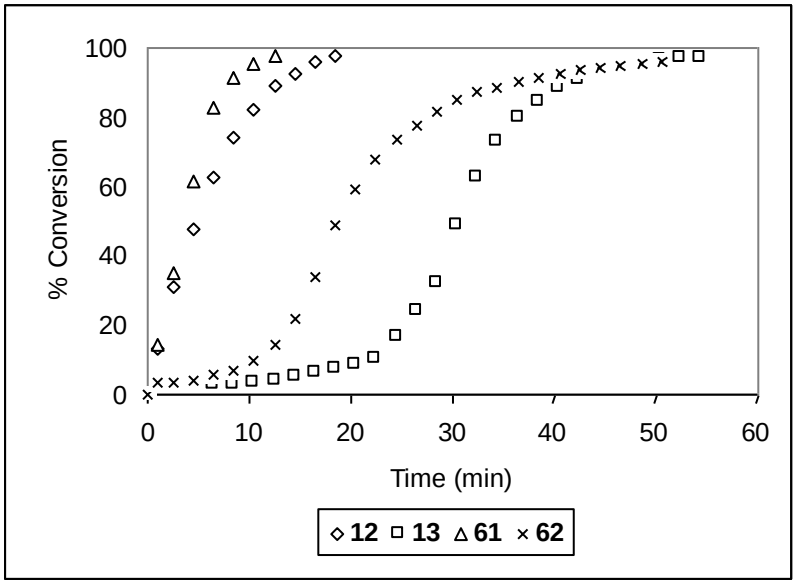

Figure 33. ROMP of COE With Catalysts **12**, **13**, **61**, and **62** ([Ru] = 0.5mM, 0.5% Catalyst Loading, Room Temperature)

RCM reactions of DEDAM were then conducted in benzene (Figure 34). Examination of these kinetic profiles showed catalysts **12** and **61** performed at nearly identical rates. As with the ROMP reactions, both of these catalysts exhibited a much faster rate of initiation, as shown by the faster initial conversion, compared to catalysts **13** and **62**. Interestingly, commercially available catalyst **13** was slightly more active than catalyst **62** in the RCM reaction, which is in contrast to the performances observed for the ROMP reaction. It should be noted that catalysts **12** and **13** are considered highly active olefin metathesis catalysts,[22,51] therefore the kinetic results from both the ROMP and RCM reactions mean that catalysts **61** and **62** also belong in the same category.

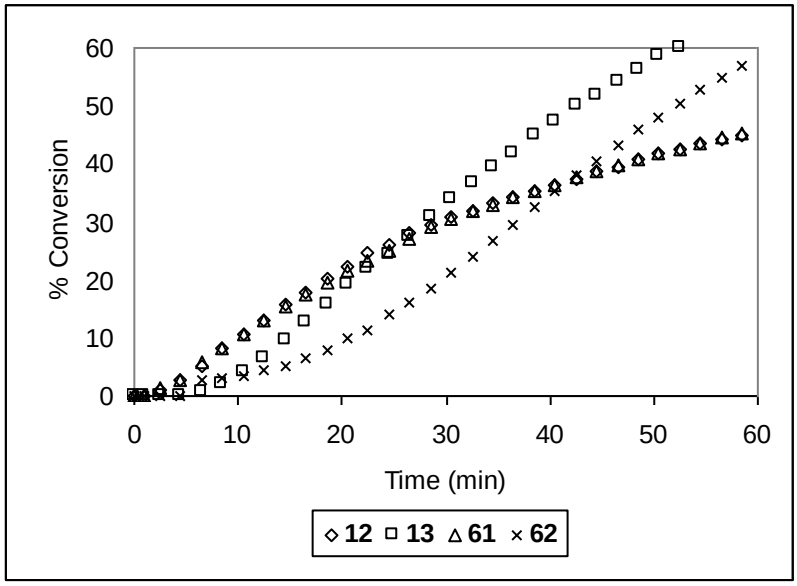

Figure 34. RCM of DEDAM With Catalysts **12**, **13**, **61**, and **62**
([Ru] = 1.0 mM, 1.0% Catalyst Loading, Room Temperature)

To evaluate the effect of protonation of the NMe_2 groups of the H_2ITap ligand on the activity profile of catalysts **61** and **62**, additional ROMP reactions using *exo*-7-oxanorbornene derivative **89** were conducted in the presence of variable amounts of *p*-toluenesulfonic acid (TsOH).[88] TsOH was chosen for this study because it is a non-nucleophilic acid that does not cause precipitation of the catalysts from the organic reaction medium via formation of an insoluble salt. These reactions were conducted in 1.0 mM catalyst solutions with 1.0 % catalyst loadings in polar organic solvents (CD_2Cl_2 and $CDCl_3$) to maintain solubility of the protonated species. The results (Figures 35 and 36) showed that the rate of ROMP conversion for both catalysts slowed dramatically with increasing equivalents of acid. This was counterintuitive to all previous reports, where addition of acid to a Ru-based olefin metathesis catalyst accelerated the overall rate.[58a,64,77,89]

The effect of different substitution in the 4-position of the phenyl rings on the NHC ligand properties has been studied by Plenio *et al.* by generating a small library of symmetric and unsymmetric ligands.[84,90] Through these studies, it was found that the

change from electron-withdrawing to donating groups in the phenyl-*para* position had a significant impact on the redox potentials of Ir and Ru complexes. NHC-Ir complexes bearing σ-donating NEt_2 groups had the lowest cathodic redox potential in the series indicating significantly enhanced donating properties of this ligand.[89b] This effect also translated into elevated RCM and CM activities of the corresponding NHC-Ru carbene complexes.[84] In light of this information, we hypothesized that transformation of the π-donating NMe_2 group into a σ-withdrawing NMe_2H^+ moiety must have caused significant electronic changes in the H_2ITap ligand that also impacted the overall catalyst's electronic environment and thus caused reduced metathesis activity. This allowed for a novel and unique external activity control for the ROMP reaction via degree of protonation.

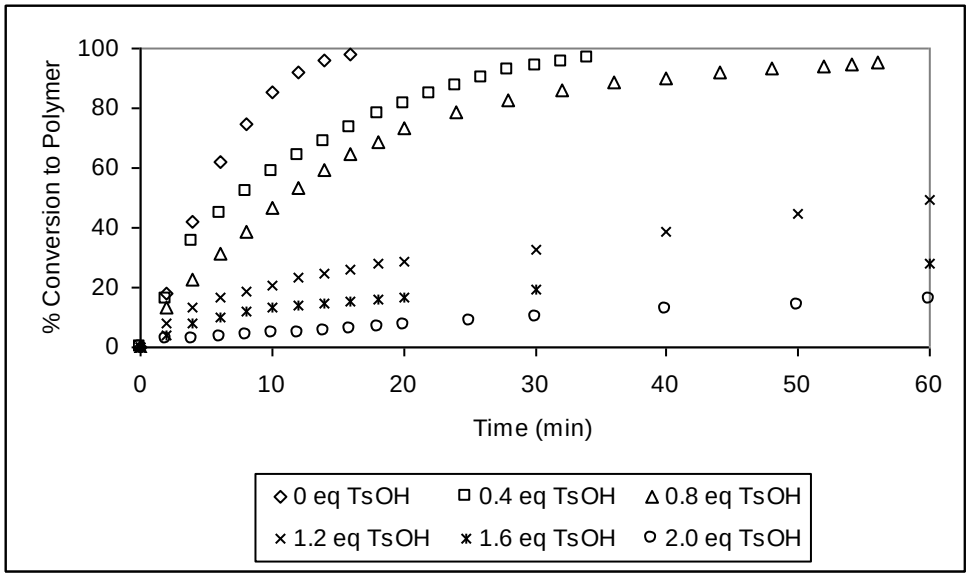

Figure 35. ROMP of **88** With Catalyst **61** in CD_2Cl_2
([Ru] = 1.0 mM, 1.0% Catalyst Loading, Room Temperature)

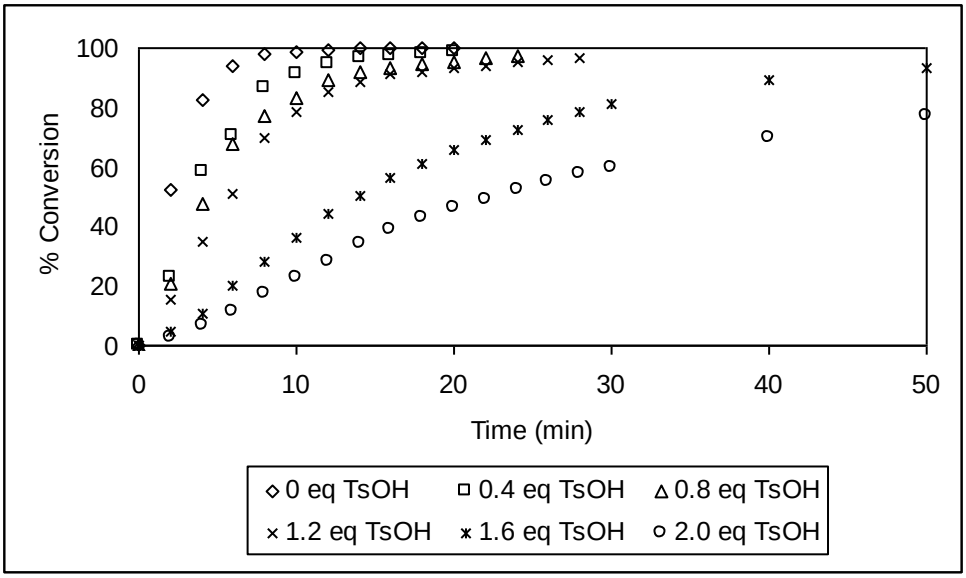

Figure 36. ROMP of **88** With Catalyst **62** in $CDCl_3$
([Ru] = 1.0 mM, 1.0% Catalyst Loading)

To determine whether the observed deceleration of the ROMP reaction with complexes **61** and **62** upon acid addition was mostly due to a change initiation rate or propagation rate, poly-**89** was also produced on a larger scale under identical reaction conditions as the kinetic investigations and analyzed by GPC analysis (Table 3). Due to the unfavorable ratio of the rates of initiation and propagation, the H_2IMes ligated catalysts **12** and **13** do not promote controlled ROMP, meaning that the polymer molecular weights obtained with these catalysts are substantially higher than the theory.[51] Since catalysts **61** and **62** exhibit a similar reactivity profile, the measured average molecular weights (M_P) of poly-**89** (Table 3) in the absence of acid were likewise significantly larger (> 150,000 for catalyst **61**, 80,000 for catalyst **62**) than the theory (27,600), indicating incomplete initiation under these reaction conditions (Table 3). However, with increased TsOH amounts present in the ROMP reaction, the average molecular weights of the polymers produced grew progressively smaller. For catalyst **61**, the M_p was reduced to 55,500 (approx. one third of the M_P obtained for the acid-free ROMP) when two equivalents of TsOH was added. For catalyst **62**, the addition of 1.6

equiv. of TsOH produced poly-**89** with an M_P of 34,600, which is very close to the theoretical value. Further addition of TsOH reduced the molecular weights far below the theoretical value, which was partially due to incomplete polymerizations attributed to catalyst decomposition. The improved molecular weight control indicates that the acid addition mostly affected the rates of propagation, which resulted in more favorable $k_{initiation} / k_{propagation}$.

Table 3. GPC Results for ROMP Polymers (Poly-89) From TsOH Studies
[Ru] = 1.0 mM, 1.0% Catalyst Loading, Room Temperature

Catalyst	TsOH (equiv.)	Time [min] (>95% conv.)	M_p (theory)	M_P (GPC)	*PDI*
61[a]	0	14	27,600	> 150,000	1.23
	0.4	32		138,700	1.34
	0.8	56		141,000	1.31
	1.2	210		119,200	1.33
	1.6	600		95,900	1.6
	2.0	-		55,500	1.73
62[b]	0	8		80,000	1.64
	0.4	14		75,300	1.57
	0.8	20		68,200	1.52
	1.2	24		66,800	1.46
	1.6	60		34,700	1.63
	2.0	100		9,000[c]	1.8

[a] with CH_2Cl_2 as solvent; [b] with $CHCl_3$ as solvent; [c] incomplete polymerization attributed to catalyst decomposition

Slowing the propagation in olefin metathesis usually is not desired for most applications since it reduces the activity and also the potential turnover numbers, making the reaction less efficient. However, decreased propagation rates can be advantageous for controlled ROMP reactions, where a low propagation/initiation ratio is desired to ensure a simultaneous start of all growing polymer chains. Unfortunately the PDIs for the polymers produced in these reactions did not give a consistent picture of the improved ROMP control that was expected with the improved propagation control of catalysts **61** and **62** upon the addition of TsOH. Catalyst **62** exhibited the expected development of the PDIs for the better controlled ROMP reactions with increasing acid amounts present

during the polymerization up to 1.2 equivalents of TsOH were added, reducing the values from 1.64 to 1.46. Further increase of the TsOH amount then led to a higher PDI's again (1.8 for 2.0 equiv. of acid). For catalyst **61**, the increased ROMP propagation control was not reflected in lower PDIs. However, the "uncontrolled" ROMP with the acid-free catalyst produces a polymer with an amazingly low PDI of 1.23, which is in stark contrast to the high experimental M_p. The PDIs then gradually increased to 1.73 with increased TsOH amounts present during the reaction. Very likely, despite the lowered propagation rates, the ROMP reaction with catalysts **61** and **62** was not sufficiently controlled to give well-defined polymeric materials.

To confirm these findings of the external propagation control with acid, DFT calculations performed by Dr. Yong Zhang (The University of Southern Mississippi) were used to determine the Mulliken atomic charges for model complexes **93**, **93a** and **93b** (Figure 37) which bear a PMe_3 ligand instead of the PCy_3 ligand and differ in the degree of protonation at the H_2ITap ligand (Table 4). The charges were calculated using a B3LYP method with a large basis (6-311++G(2d.2p)) for first coordination shell atoms on geometries optimized by using the mPW1PW91/sdd method (details in Chapter VIII), which were found to give good predictions of geometric and electronic properties for late transition metal complexes.[91] A recent report described a correlation between the Mulliken atomic charges at the metal center in Ru-carbene complexes and the rate of metathesis initiation.[92] In this report it was demonstrated that the Ru-center in slow-initiating Grubbs' second generation catalyst **12** in fact is more positively charged than in fast-initiating Grubbs' first generation catalyst **9**. This was used as a rational to explain the influence of the remaining donor ligand (NHC versus PCy_3) on the dissociation rates of the other PCy_3 ligand which determines the initiation rate. For this reason, the calculations also included catalysts **91** and **92** (Figure 37), the PMe_3-ligated counterparts

of complexes **9** and **12**, for comparison. Similar to the reported calculations,[92] the Ru-center was found to be more positively charged in the NHC ligated complex **92** than in complex **91**. The Mulliken atomic charges for the Ru-center in complex **93** were nearly identical to complex **92** which was not surprising with respect to the similar activities for catalysts **12** and **61** in the ROMP and RCM reactions. More interestingly, the charges became less positive with increasing protonation to complexes **93a** and **93b**, however, these charges were still more positively charged than complex **91**. This was somewhat surprising since the H_2ITap ligand became positively charged and thus an increase in the charge at the metal center was expected. Following the rational of the previous calculations,[92] it can only mean that the π-acceptor capability of the H_2ITap ligand was reduced upon protonation. These results also meant that the initiation rates of model complexes **93a** and **93b** should not be lower in comparison to complex **93**. Therefore, these calculations confirmed that the reduced overall activity exhibited by gradual protonation of catalysts **61** and **62** was a result of slower ROMP propagation.

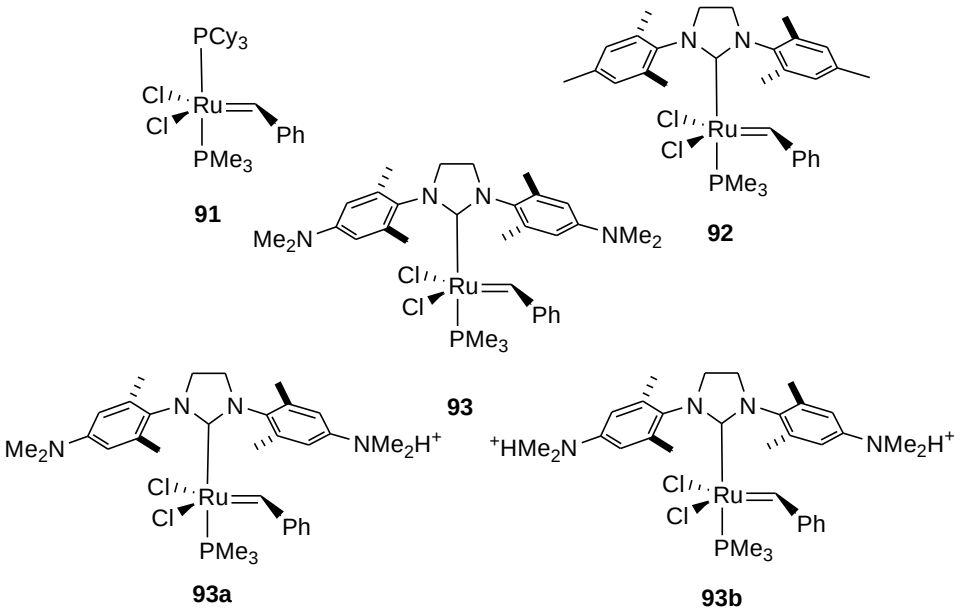

Figure 37. Complexes Used for DFT Calculations

Table 4. DFT-Calculated Mulliken Atomic Charges at the Ru-Center for Model Complexes

complex	q^{Mlk}	Δq^{Mlk} (90)	Δq^{Mlk} (91)
91	0.313	-	- 0.621
92	0.834	+ 0.621	-
93	0.851	+ 0.638	+ 0.017
93a	0.831	+ 0.618	- 0.003
93b	0.712	+ 0.499	- 0.122

As further proof, the relative initiation rates for complexes **61** and **62** were determined experimentally without and in the presence of TsOH. This was accomplished by monitoring the conversion of the Ru-species with ethylvinyl ether (EVE). [40b] The reaction affords only one turnover to form the metathesis-inactive Fischer-carbene complexes **93** (Scheme 24) and hence is only dependent on the metathesis initiation. We monitored the changes for the ^{1}H NMR signal for the benzylidene-H atom (δ = 19.02 ppm for **61**; δ = 16.80 ppm for **62**). PCy_3-containing complex **61** was converted into the respective ethoxymethylidene species **94** which was observed via the methylidene-H signal at δ = 13.73 ppm. Reactions with TsOH did not afford a stable ethoxymethylidene complex containing a ^{1}H NMR signal which could be reliably integrated. With TsOH, a species at δ = 13.73 ppm was observed with complex **61**, however, over time the signal disappeared, very likely due to degradation. Complex **62** solutions generated multiple broad signals in the range between 9 and 16 ppm in the presence of EVE. Hence, the conversion was monitored by the reduction of the benzylidene-H signal versus an internal standard in these reactions.

Scheme 24. Conversion of Catalysts **61** and **62** with EVE into Ethoxymethylidene Complexes **94**

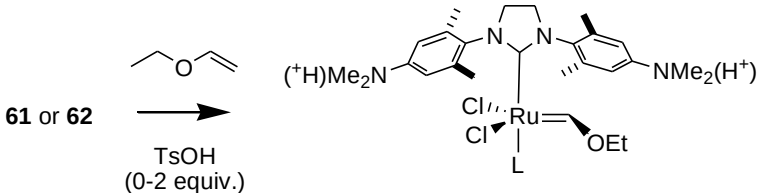

94

L = PCy_3 or vacant site

As expected, the catalyst conversion increased slightly with increased acid amounts. Only 24 % of catalyst **61** initiated in 60 min without TsOH, but the presence of 1 equivalent of TsOH afforded 52.7% conversion. With 2 equiv. of TsOH, > 50% conversion was reached after 5 min, but after 30 min a plateau at 67% conversion was observed (Figure 38), most likely a result of catalyst decomposition. Catalyst **62** generally exhibited faster initiation than catalyst **61**, though the differences in the conversion of EVE in the presence of TsOH were much less pronounced (Figure 38). However, the overall trend showed that the EVE conversion proceeded marginally faster at higher acid concentrations. For example, after 6 min complex **62** was converted by 52.0% (acid-free), 58.2% (1 equiv. TsOH) and 63.3% (2 equiv. TsOH). All conversions with complex **62** went > 95%. These results, when combined with the results from the ROMP reactions and DFT calculations, unambiguously show the decreased activity observed for catalysts **61** and **62** was exclusively due to a decrease in propagation rate. To the best of our knowledge, this is the first example of external control of the ROMP propagation rates, almost independent from the initiation values.

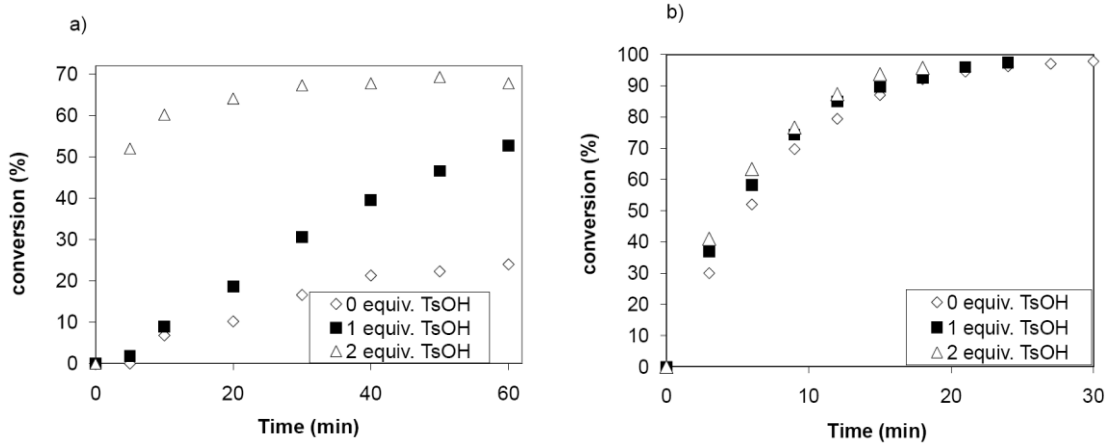

Figure 38. Conversion of Catalysts With 100 Equivalents EVE
a) Catalyst **61** [Ru] = 4 mM, CD_2Cl_2, 20 ^oC, b) Catalyst **62** [Ru] = 2 mM, $CDCl_3$, 20 ^oC

The next benzylidene catalyst bearing a pH-responsive H_2ITap ligand examined was DMAP catalyst **65**, or (H_2ITap)(DMAP)$_2$Cl$_2$Ru=CH-Ph. Because this catalyst had multiple protonation sites, we expected gradual protonation with non-nucleophillic acid would produce several complexes (**65**, **65a**, and **65b**), each with a different ROMP reaction activity profile (Scheme 25), allowing for external control of catalyst activity via acid addition. The order of anticipated protonation was based on the approximate pKa values of the conjugate acids for the pH responsive ligands, with the more basic DMAP ligands (DMAPH$^+$ pKa = 9.2) dissociating before protonation of the aryl amines (aryl ammonium pKa ~ 4-6). In contrast to catalysts **61** and **62**, this catalyst was expected to exhibit lower olefin metathesis activity than commercially available catalyst **12** under standard, non-acidic conditions due to the presence of the inhibiting DMAP ligands. Upon dissociation of these DMAP ligands via addition of two equivalents of non-nucleophillic acid, highly active, fast initiating complex **65b** would then be formed. Acid addition beyond two equivalents would then protonate the NMe$_2$ groups, thereby slowing catalyst propagation, as seen with catalyst **61** and **62**.

Scheme 25. Gradual Protonation of Catalyst Complex **65**

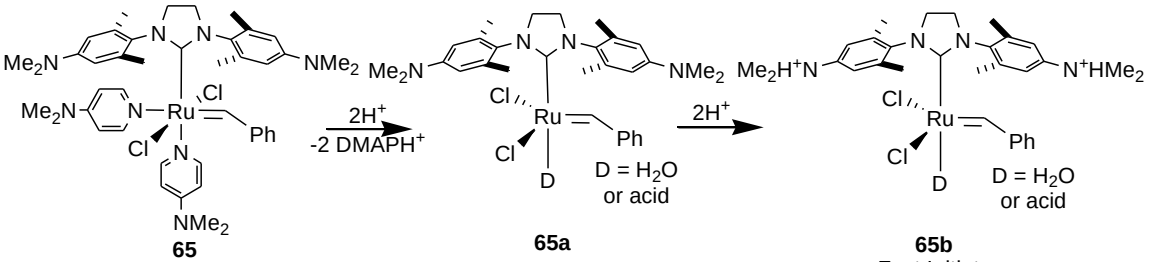

65
Moderate Initiator
Moderate Propagator

65a
Fast Initiator
Fast Propagator

65b
Fast Initiator
Slow Propagator

The anticipated activity profile for catalyst complex **65** was confirmed by performing ROMP reactions of COE with zero, two, and four equivalents of H_3PO_4 (Figure 39). Catalyst complex **65** displayed slightly lower activity than commercially

available catalyst complex **12** under similar reaction conditions. Based on previous studies by the Schanz research group, the high ROMP activity of hexacoordinate NHC(DMAP)$_2$Ru alkylidene complexes is caused by relatively fast initiation rates compared to catalysts **12** but slower propagation.[64] As expected, upon the addition of two equivalents of H_3PO_4, catalyst activity for complex **65** was greatly enhanced, dramatically exceeding the activity for catalyst **12**, with 96.8% conversion to ROMP polymer achieved within 15 minutes. Upon protonation of the DMAP ligand, the predicted effect was observed, generating species **65a** with significantly faster initiation and propagation. When four equivalents of H_3PO_4 were added, the initial activity observed for catalyst **65b** were very similar to those seen with catalyst **12**, however the conversion quickly reached a plateau and precipitation of the catalyst complex was observed, resulting in only 41.3% conversion to polymer after 30 minutes. It is likely that the precipitation was a result of rapid degradation of the fast initiating species **65b**.

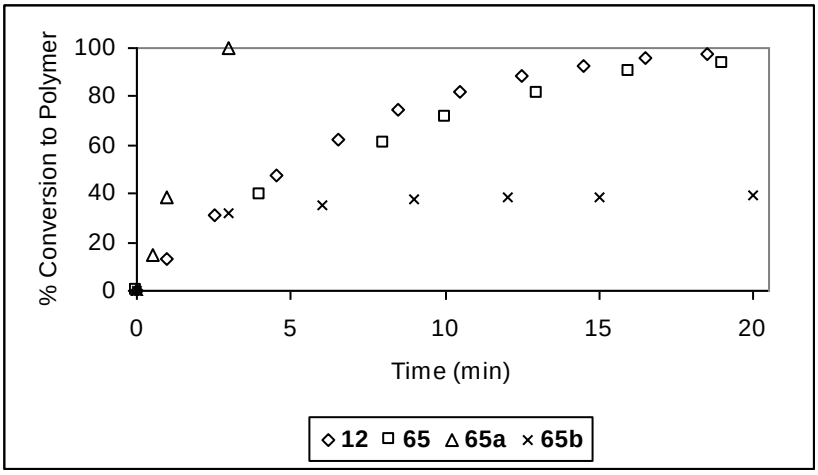

Figure 39. ROMP of COE With Complexes **12**, **65**, **65a**, **65b**
[Ru] = 0.5 mM, 0.5% Catalyst Loading, 20 ^{o}C

Table 5. RCM of DEDAM With Catalysts 12 and 65
[Ru] = 1.0 mM, 1.0% Catalyst Loading

Catalyst	Equivalents of H_3PO_4	Time (min)	% Conversion to Product
12	0	3	1.2
12	0	15	15.8
12	0	30	30.2
65	0	3	1.9
65	0	30	7.2
65a	2	3	31.5
65a	2	15	43.5
65a	2	30	46.7
65b	4	3	10.2
64b	4	15	13.3
64b	4	30	14.4

RCM reactions of DEDAM with catalyst **65** (Table 5) confirmed the change in the activity and solubility tends observed in the ROMP reactions. For the RCM reactions, catalyst **65** displayed noticeably lower RCM activity than catalyst **12** in the absence of acid, rather than the comparable activity seen in the ROMP reactions. Once again, upon addition of two equivalents of H_3PO_4 the activity rate of catalyst **65** initially increased beyond catalyst **12**, however, this was soon followed by significant catalyst degradation which was observed as a plateau in conversion within 15 minutes, as well as significant precipitation of the catalyst. With four equivalents of H_3PO_4, decreased activity and significant catalyst precipitation was observed, similar to the ROMP reaction. This once again implies that the fast-initiating catalyst species most likely degraded quickly in solution.

Catalyst **66**, or $(H_2ITap)Cl_2Ru(=CH\text{-}CH_2\text{-}CH_2\text{-}C_5H_4N)$, was the final benzylidene catalyst bearing an H_2ITap ligand that was evaluated. This catalyst contained a pH-responsive, backbiting 3-(*o*-pyridyl)propylidene N-donor ligand in addition to the NMe_2 groups of its NHC ligand. We hypothesized that this back-biting ligand would cause very low catalyst activity until protonation via addition of excess non-nucleophillic acid caused dissociation of the coordinated nitrogen from the metal center, thereby forming activated

catalyst complex **66a** (Scheme 26). The anticipated degree of inhibition afforded by the 3-(*o*-pyridyl)propylidene in catalyst **66** was expected to be much greater than the inhibition observed with the DMAP ligands of catalyst **65**. Unlike catalyst **66**, gradual protonation studies were not conducted with catalyst **66** because the aryl NMe_2 groups and the N-donor ligand were expected to exhibit similar pKa values, therefore gradual protonation would most likely have produced a mixture of complexes, each with a different kinetic profile.

Scheme 26. Activation of Catalyst Complex **66**

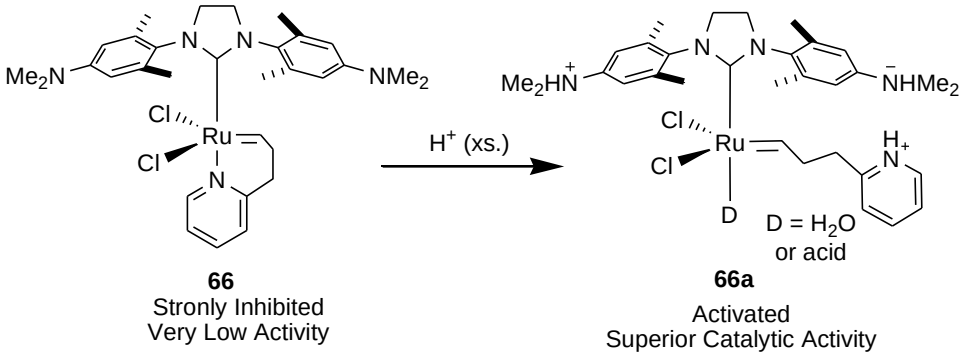

66
Stronly Inhibited
Very Low Activity

66a
Activated
Superior Catalytic Activity

Kinetic profiles obtained for ROMP of COE (Figure 40) with catalyst **66** confirmed that stronger inhibition of catalyst activity was observed for catalyst **66** than seen for DMAP catalyst **65**. As expected, with the addition of four equivalents of H_3PO_4 an increase in activity was observed. This was most likely due to an increase in initiation, but because protonation of the NMe_2 groups also reduce the catalyst's propagation rates, complex **66a** still performs at lower rates than those seen for catalysts **12** and **61**. Catalyst **66** also displayed lower activity than catalyst **62**, but upon acidification complex **66a** displayed significantly increased rates initiation compared to catalyst **62**, as indicated by the sudden increase in ROMP activity, which is present from the very beginning of the reaction with complex **66a**. Also, as with complex **65b**, significant precipitation of the catalyst complex was observed, which implies that fast-initiating complex degrades quickly.

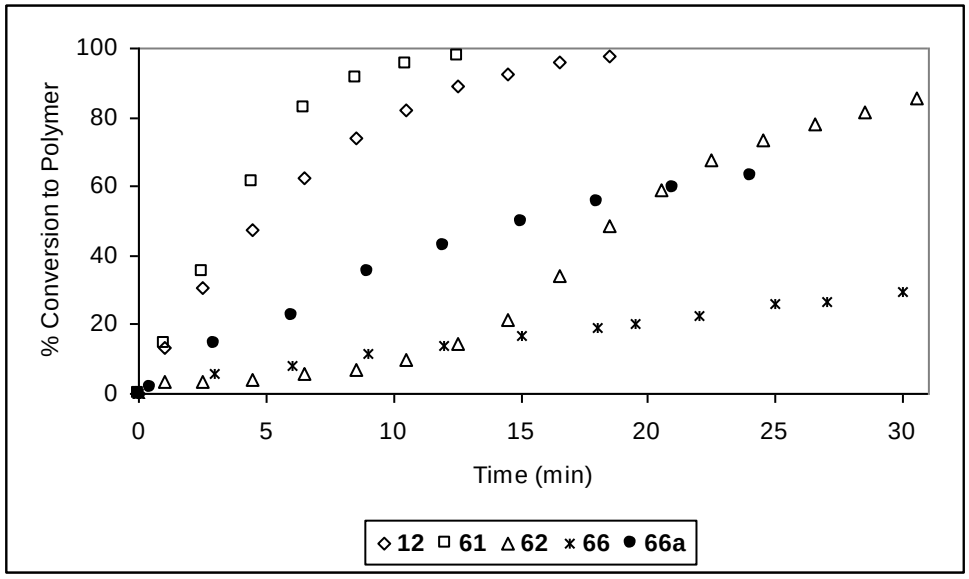

Figure 40. ROMP of COE With Complexes **12**, **61**, **62**, **66**, and **66a**
[Ru] = 0.5 mM, 0.5% Catalyst Loading, 20^{o}C

RCM of DEDAM was also conducted with catalyst **66**. Conversion rates with DEDAM in the absence of H_3PO_4 of complex **66** were very low, with only 6.2 % conversion to product observed after 30 minutes. The addition of excess H_3PO_4, afforded only a slight improvement, with 12.9% conversion after 30 minutes. Once again, precipitation of the catalyst was observed, which likely accounted for the extremely low rate of RCM conversion observed with complex **66a**.

Kinetic Studies of Benzylidene Catalysts Bearing ITap Ligands

The next catalysts studied in the standard ROMP and RCM reactions in organic media were benzylidene catalysts **67**-**69** bearing ITap ligands (Figure 41). Since catalysts with unsaturated NHC ligand backbones are generally less active than their counterparts with saturated backbones,[51] (ITap)(PCy_3)Cl_2Ru=CH-Ph **67**, (ITap)Cl_2Ru=CH-(C_6H_4-O-*i*Pr) **68**, and (ITap)(DMAP)$_2Cl_2$Ru=CH-Ph **69** were expected to perform ROMP of COE and RCM of DEDAM at much slower rates than observed with unsaturated analogues **61**, **62**, and **65**. ROMP and RCM kinetic results at room temperature confirmed this hypothesis (Tables 6 and 7). Because catalysts with

unsaturated backbones tend to exhibit enhanced thermal stability, kinetic studies were also conducted at elevated temperature (60 ^{o}C) with catalyst **67** and **69**. This elevated temperature provided an extraordinary improvement in the conversion rates for ROMP of COE with both of these catalysts, as well as a superior RCM reaction for phosphine-ligated catalyst **67**. Acceleration of kinetic rates at elevated temperature was expected and has been demonstrated before with other catalyst systems.[51,67,68] However, the activity was improved by at least two orders of magnitude, and the overall activity is significantly higher than the activity of catalysts **12** and **13** at ambient temperature. This is without precedence for this moderate temperature increase. Very likely, most of this activity jump is caused by much elevated initiation rates, thus generating a larger number of active species.

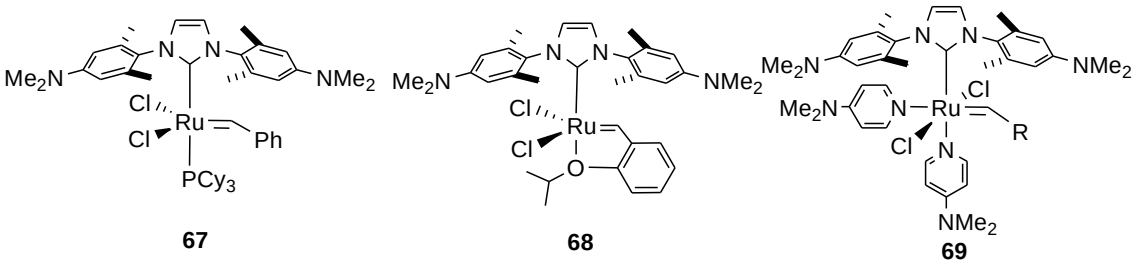

Figure 41. Catalyst Complexes **67**-**69**

Table 6. ROMP of COE With Catalysts 67-69
[Ru] = 0.5 mM, 0.5% Catalyst Loading

Catalyst	Time (min)	Temperature (˚C)	% Conversion to Polymer
67	60	20	8.5
67	120	20	22.3
67	790	20	76.5
67	6	60	>99
68	60	20	54.1
68	120	20	93.3
69	60	20	72.3
69	120	20	90.4
69	5	60	95.5

Table 7. RCM of DEDAM With Catalysts 67-69
[Ru] = 1.0 mM, 1.0% Catalyst Loading

Catalyst	Time (min)	Temperature (˚C)	% Conversion to Product
67	60	20	23.2
67	240	20	77.2
67	6	60	>99
68	60	20	64.7
68	120	20	87.4
68	180	20	96.0
69	60	20	8.9
69	120	20	12.6
69	180	20	13.5
69	10	60	20.9
69	60	60	30.6

Kinetic Studies of Benzylidene Catalysts Bearing Other pH-Responsive Ligands

Kinetic studies in organic media were also conducted with ($IXyONMe_2$)(PCy_3)Cl_2Ru=CH-Ph **70**, ($IDippONMe_2$)(DMAP)Cl_2Ru=CHPh **77**, and ($IDippSNMe_2$)$(DMAP)_2Cl_2$Ru=CH-Ph **78** (Figure 42) to establish their metathesis activity under standard conditions. Though the electronic influence of the NMe_2 groups of these catalysts was considered minimal with these catalysts, it was unknown how the sterics of these bulky NHC ligand precursors would affect the metathesis activity of the catalyst. DMAP catalysts **77** and **78** were expected to have lower metathesis activity than Grubbs second generation catalyst **12**, since this has been previously observed for analogous IMes ligated DMAP complex **83**. This catalyst exhibited a reduced rate for ROMP od COE by a factor of 0.57 from those observed for homologous catalyst **12**.[87]

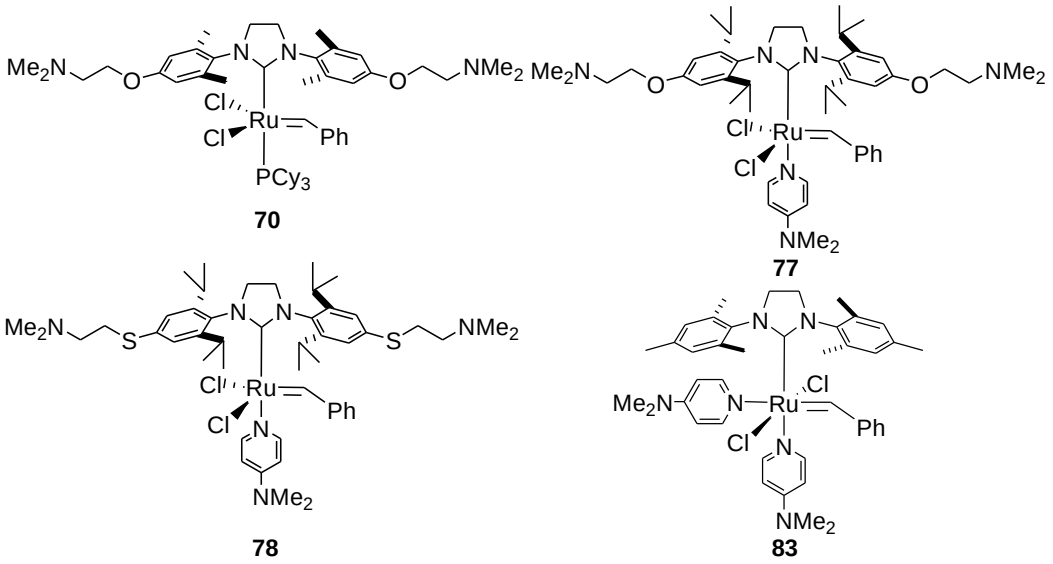

Figure 42. Catalyst Complexes **69**, **76**, **77**, and **82**

A study of the relative kinetic profiles obtained through ROMP of COE showed catalysts **70**, **77**, and **78** each have lower ROMP metathesis activity than catalyst **12** (Figure 43). Compared to the other catalysts, complex **70** exhibited a much lower rate of initiation, as seen by the delay in initial conversion, as well as an unexpectedly low ROMP activity compared to complex **12**. Catalysts **77** and **78** exhibited nearly identical activities, as was expected by their very similar structure. They were faster in the ROMP reaction than complex **70**, and showed only slightly lower activity than seen with catalyst **12**, though this decrease in activity was much less than what was previously reported for complex **83**. However, the activities of **77** and **78** were not quite unexpected. Although DMAP Ru-alkylidene complexes are generally slower than their second generation counterparts,[87] the bulky *o*-iPr groups in the NHC ligand have been shown to accelerate both the rates of initiation and propagation compared to their *o*-CH_3 substituted counterparts.[93] Furthermore, the pentacoordinate structure containing only one DMAP ligand is also expected to generate a lower amount of free DMAP in the reaction mixture, and it was shown that increased amounts of N-donor ligand reduced the conversion rates in ROMP reactions with Ru-alkylidene complexes. Hence, the reduced reactivity

due to the presence of the DMAP ligand in these catalysts was more than compensated by the bulkier NHC ligand and the low DMAP content of the catalyst. Therefore, these catalysts exhibited a higher activity than catalyst **70**.

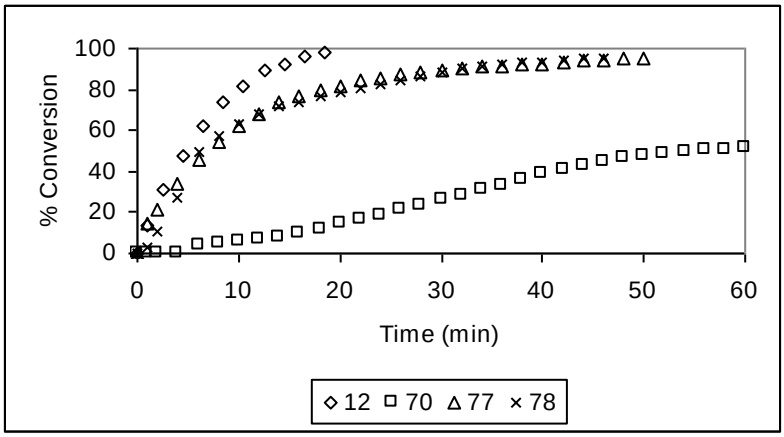

Figure 43. ROMP of COE With Catalysts **12**, **70**, **77**, and **78**
([Ru] = 0.5 mM, 0.5% Catalyst Loading)

The RCM reactions with DEDAM exhibited a markedly different activity trend for this group of catalysts (Table 8). Catalyst **78** dramatically outperformed catalyst **12**, with >95% conversion within one hour. Catalyst **77** accomplished only 36.5% conversion observed at one hour, which was slightly less than standard setting catalyst **12**. This difference in activity between catalysts **77** and **78** was unexpected due to their structural similarities as well as the nearly identical activity seen in their ROMP reactions. Catalyst **70** displayed very little RCM metathesis activity, with only 2.1% conversion observed within the same time frame, indicating the very slow initiation also observed in the ROMP reaction.

Table 8. RCM Reactions of DEDAM With Catalysts 12, 70, 77, and 78
[Ru] = 1.0 mM, 1% Catalyst Loading

Catalyst	Time (min)	% Conversion to Product
12	60	46.1
70	60	2.1
77	60	36.5
78	56	95.2

Kinetic Studies of Phenylthiomethylidene (Ru=CH-SPh) Catalysts

Previous studies of phenylthiomethylidene (Ru=C-SPh) catalysts have shown that these catalysts perform at much slower rates than their benzylidene counterparts in ROMP and RCM metathesis reactions. As such, the activity profiles for $(H_2ITap)(PCy_3)Cl_2Ru$=CH-SPh **79**, $(ITap)(PCy_3)Cl_2Ru$=CH-SPh **80**, $(H_2ITap)(DMAP)_2Cl_2Ru$=CH-SPh **81**, and $(ITap)(DMAP)_2Cl_2Ru$=CH-SPh **82** were expected to show much lower activity in ROMP and RCM reactions than observed with their benzylidene counterparts, complexes **61**, **65**, **67**, and **69**, respectively. The experimental data supports this prediction, with very little activity observed for most of these complexes at room temperature (Tables 9 and 10). When these reactions were repeated at elevated temperatures, all of these catalysts displayed dramatically improved metathesis activity, which should be attributed mostly to an increase of catalyst initiation rates. It should be mentioned that the nature of the alkylidene group only influences the initiation, since the first metathesis turnover generates the same propagating species from different Ru-alkylidene catalysts. Hence, once initiated, these catalysts should exhibit the same activity as their otherwise equally ligated counterparts which display much faster metathesis reactions at ambient temperature as seen throughout this chapter. For catalyst **81**, two and four equivalents of H_3PO_4 were added, and the ROMP and RCM reactions were monitored at both 20˚C and 60˚C. This was implemented in an effort to improve catalyst activity by means of dissociation of the DMAP ligands, however no metathesis activity was observed in any of these reactions with acid, likely due to catalyst degradation in the presence of acid. Since no metathesis activity was observed for these reactions, it is likely that complex **81a**, formed upon dissociation of the DAMP ligand, rapidly decomposed following the known dimerization pathway,[40c] in particular if this process for this pathway is faster than the first catalyst turnover (Scheme 27).

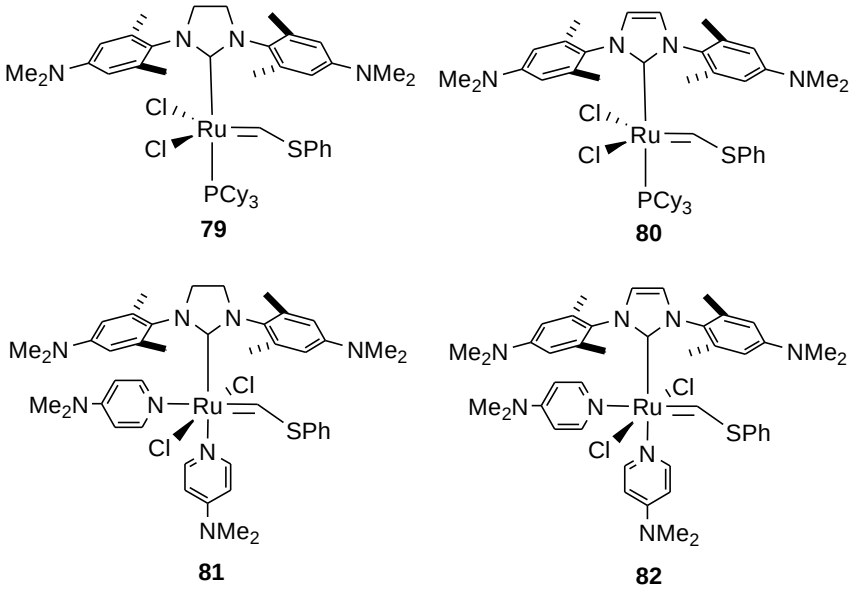

Figure 44. Catalyst Complexes **79**-**82**

Table 9. ROMP Reactions of COE With Catalysts 79-82
[Ru] = 0.5 mM, 0.5% Catalyst Loading

Catalyst	Time (min)	Temperature (˚C)	% Conversion to Polymer
79	60	20	<1
79	24	60	96.1
80	60	20	20.5
80	120	20	39.6
80	790	20	99.1
80	60	60	77.0
80	108	60	95.2
81	60	20	3.9
81	30	60	32.4
81	60	60	36.3
81	120	60	37.8
82	180	20	<2
82	30	60	52.2
82	60	60	77.0
82	90	60	91.6

Table 10. RCM Reactions of DEDAM With Catalysts 79-82
[Ru] = 1.0 mM, 1.0% Catalyst Loading

Catalyst	Time (min)	Temperature (˚C)	% Conversion to Product
79	60	20	2.2
79	60	60	89.4
80	720	20	19.9
80	50	60	85.4
81	60	20	1.2
81	60	60	67.2
82	300	20	3.6
82	60	60	16.7

Scheme 27. Failed Initiation of Catalyst **81** With H_3PO_4

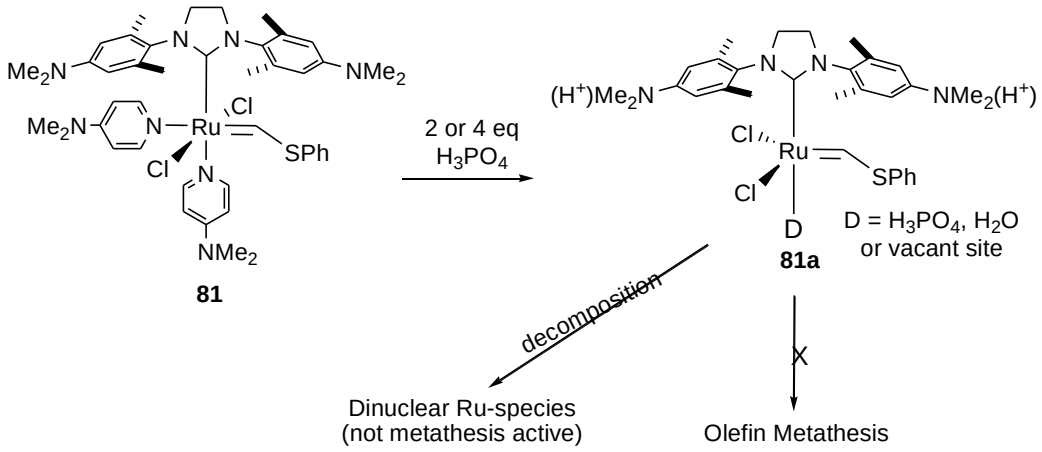

Kinetic Studies of Indenylidene Catalyst Complexes

The final catalysts tested in organic media were (ITap)(PPh_3)Cl_2Ru-3-phenylindenylidene **87** and (ITap)$(DMAP)_2Cl_2$Ru-3-phenylindenylidene **88** (Figure 45). Because indenylidene catalyst structures typically exhibit enhanced thermal stability when compared to their benzylidene counterparts, we hypothesized that these catalysts would remain stable under acidic conditions as well as at elevated temperatures. As such, ROMP and RCM reactions were conducted with catalyst under acidic conditions and at elevated temperature (60 ^{o}C) in addition to the standard kinetic studies. For catalyst complex **87**, results showed this complex exhibited very low activity in both ROMP and RCM reactions (Tables 12 and 13). Additionally, reactions conducted at elevated temperatures did not afford any metathesis products, most likely due to an

advanced rate of decomposition. This was in very stark contrast to results observed for benzylidene counterpart **67**, which showed a dramatic increase ion activity at elevated temperature. The addition of H_3PO_4 did improve the metathesis activity for complex **87**, though faster rates of catalyst degradation were also observed, which resulted in a lower overall yield in the ROMP reaction.

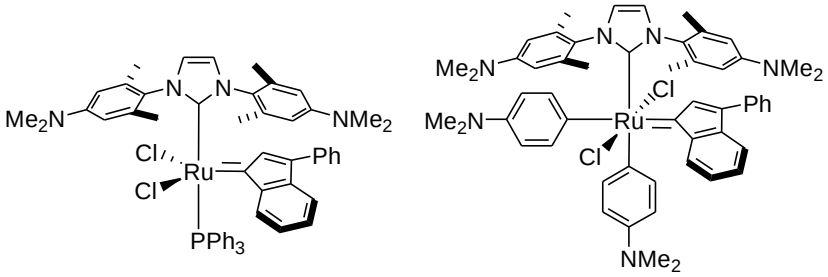

87 **88**

Figure 45. Phenylindenylidene Catalyst Complexes **87** and **88**

Table 11. ROMP Reactions of COE With Catalyst Complex 87
[Ru] = 0.5 mM, 0.5% Catalyst Loading

Temperature (˚C)	Equivalents of H_3PO_4	Time (h)	% Conversion to Polymer
20	0	1	<1
20	0	24	12.1
20	0	48	20.9
60	0	1	<1
20	2	1	<1
20	2	5	10.6

Table 12. RCM Reactions of DEDAM With Catalyst Complex 87
[Ru] = 1.0 mM, 1.0% Catalyst Loading

Temperature (˚C)	Equivalents of H_3PO_4	Time (h)	% Conversion to Product
20	0	1	<1
20	0	5	<1
60	0	1	<1
20	2	1	11.9
20	2	2	24.0
20	2	3	28.9

Since the DAMP ligands of catalyst complex **88** are much more basic than the aryl NMe_2 groups of its ITap NHC ligand, we hypothesized that the addition of just 2 equivalents of H_3PO_4 would yield fast initiating, fast propagating complex **88a** (Scheme 28) as seen with DMAP catalyst complex **65**. Examination of the ROMP kinetic profile (Figure 46) shows that this is indeed the case, as catalyst complex **88a** displays a much

higher activity than **88** in neutral solution based on the much faster rates of initiation, and therefore higher overall activity. In fact, catalyst **88a** is slightly more active than catalyst **12**, which is extrodinary considering the unsaturated backbone of the ITap ligand, which usually provides catalysts with a significantly reduced activity compared to catalysts bearing NHC ligands with saturated backbones.[51] Surprisingly, DMAP catalyst **88** also showed higher ROMP activity than its PPh_3 ligated precursor **87** under both non-acidic and acidic conditions. Increased activity was also observed in the RCM reactions with two equivalents of H_3PO_4, with complex **88a** displaying higher rates of initiation and higher overall activity when compared to complexes **12** and non-acidified complex **83** (Figure 47). This confirms that the activity profile of catalyst **88** can be externally controlled via addition of acid. More importantly, the somewhat sluggish performance of catalyst **88** can be externally stimulated to make it comparable in performance to catalyst **12**, a catalyst considered to have excellent activity.

Scheme 28. Protonation of Catalyst **88**

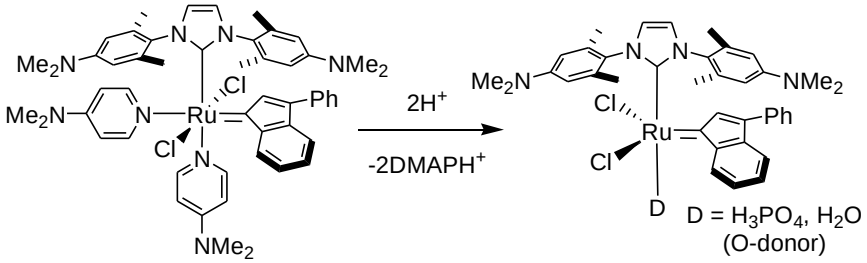

88
Slow Initiator
Fast Propagator

88a
Fast Initiator
Fast Propagator

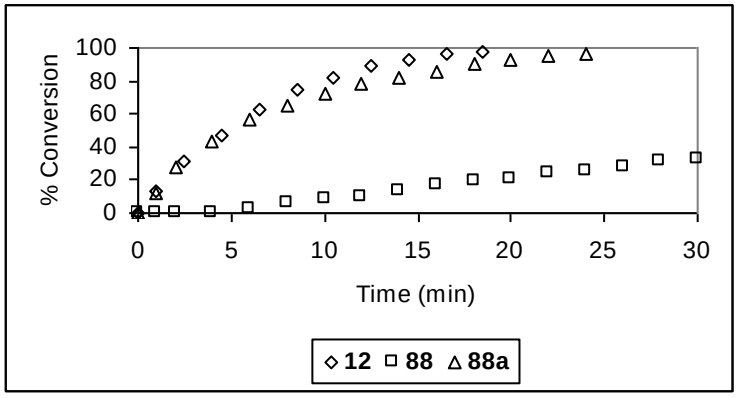

Figure 46. ROMP of COE With Complexes **12**, **88**, and **88a**
[Ru] = 0.5 mM, 0.5% Catalyst Loading, 20 ^{o}C

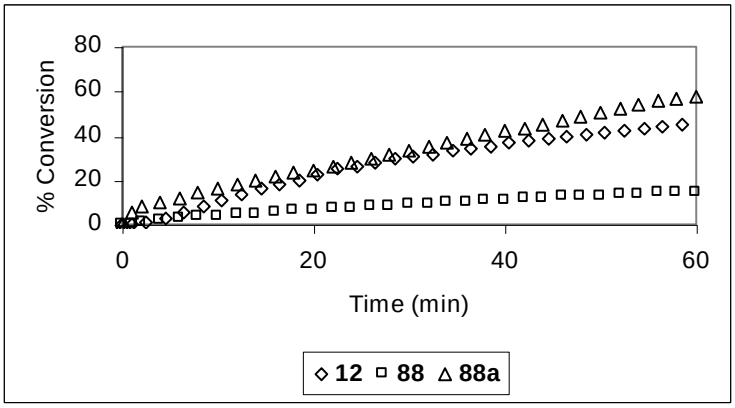

Figure 47. RCM of DEDAM With Complexes **12**, **88**, and **88a**
[Ru] = 1.0 mM; 1.0% Catalyst Loading; 20 ^{o}C

Summary

Kinetic studies were conducted in organic media to asses the metathesis activity for each of the new catalysts bearing NMe_2 modified NHC ligands. This activity was determined through a series of ROMP and RCM reactions using appropriate metathesis substrates. The kinetic profiles that were generated were then compared to those obtained for commercially available catalysts under similar reaction conditions to asses the relative rates of activity. The general trend observed was that in the absence of acid in organic solution catalysts bearing the H_2ITap ligand were more active than their counterparts bearing other pH-responsive NHC ligands synthesized in this project, with a few even outperforming their commercially available counterparts **12** and **13**, which are

considered the standard of high metathesis activity. As expected, benzylidene carbene catalysts outperformed the phenylthiomethylidene complexes, though the performance of these catalysts was improved, for some by several orders of magnitude, at elevated temperature (60 ^{o}C). Under standard conditions, the indenylidene complexes also exhibited lower activities than their homologous benzylidene carbene catalysts though, unlike the phenyltiomethylidene complexes, no major increase in metathesis activity was observed at elevated temperature.

For several of these catalysts, additional kinetic studies were conducted in the presence of non-nucleophillic acid in order to determine the influence on the catalyst activity by the protonation of their pH-responsive groups. For those catalysts bearing the H_2ITap ligand, protonation of this ligand typically reduced catalyst activity. (H_2ITap)(PCy_3)Cl_2Ru=CH-Ph (**61**) and (H_2ITap)Cl_2Ru=CH-(C_6H_4-O-*i*Pr) (**62**) were used to conduct ROMP polymer studies and relative initiation kinetics with EVE, which, when coupled with DFT calculations for several model complexes, unambiguously confirmed that this decrease in catalyst activity was a result of a reduced rate of propagation. To the best of our knowledge, this is the only example of independent propagation control of a metathesis reaction to date.

For several of the catalysts additionally coordinated by N-donor ligands, selective protonation was used to determine the ROMP kinetic profiles afforded by protonation of specific pH-responsive groups. Upon dissociation of the N-ligands via acid addition, all catalysts exhibited faster initiation, which was expected based on previous studies by the Schanz research group.[64] For (H_2ITap)$(DMAP)_2Cl_2$Ru=CH-Ph **65**, (H_2ITap)Cl_2Ru(=CH-CH_2-CH_2-C_5H_4N) **66**, and (ITap)$(DMAP)_2Cl_2$Ru-3-phenylindenylidene **88** this resulted in an increase in overall catalyst activity. For phenylindenylidene catalyst **88**, this increase in activity was particularly dramatic, as it was converted from a very sluggish catalyst to one with comparable activity to catalyst

12 upon the addition of acid. However, (H_2ITap)(DMAP)$_2$$Cl_2$Ru=CH-SPh **81** and (ITap)(PPh_3)Cl_2Ru-3-phenylindenylidene **87** experienced fast decomposition with the addition of acid, resulting in very low conversion into metathesis products.

CHAPTER V

KINETIC STUDIES IN ACIDIC PROTIC MEDIA

Substrates and Methods for Relative Kinetic Studies in Acidic Protic Media

The main goal of this dissertation was to generate Ru-based olefin metathesis catalysts capable of performing ROMP and RCM reactions in both organic and aqueous media. To this end, several target catalysts were synthesized, each bearing an NHC ligand modified with pH-responsive NMe_2 groups. These NMe_2 groups provided the means for external control of catalyst solubility profiles via acid addition, which converts these basic NMe_2 groups into ionic ammonium groups (N^+HMe_2). Benzylidene catalyst $(H_2ITap)Cl_2Ru(=CH\text{-}CH_2\text{-}CH_2\text{-}C_5H_4N)$ **66,** phenylthiomethylidene catalysts $(H_2ITap)(PCy_3)Cl_2Ru=CH\text{-}SPh$ **79**, $(H_2ITap)(DMAP)_2Cl_2Ru=CH\text{-}SPh$ **81**, and phenylindenylidene catalysts phenyl(ITap)$(PPh_3)Cl_2$Ru-3-phenylindenylidene **87**, (ITap)$(DMAP)_2Cl_2$Ru-3-phenylindenylidene **88** all exhibited insufficient solubility in acidic aqueous media, so kinetic studies with these catalysts were not conducted. The other catalysts exhibited sufficient solubility in acidic protic media, and they were employed in homogenous ROMP and RCM reactions with water-soluble substrates.

The following metathesis reactions were conducted: ROMP of *exo*-7-oxanorbornene derivatives **95** and **96** and RCM of diallylmalonic acid **97** (Scheme 29). Acidic protic solvents selected for the metathesis reactions conducted in these studies included 1 M HCl_{aq}–2-propanol (1:9 v/v) or 0.1M HCl_{aq}. Because these substrates are solids, accurate addition to an NMR tube was not feasible. Hence, relative kinetic studies were only conducted by taking aliquots of the reaction solution in precise time intervals, quenching them with ethyl vinyl ether (EVE),[20] followed by removal of the volatiles. The samples were then dissolved in D_2O and individually analyzed via ^1H NMR spectroscopy (300 MHz, 20 ^oC) by integrating signals representing the substrate and product.

Scheme 29. ROMP and RCM Substrates for Rections in Acidic Protic / Aqueous Media

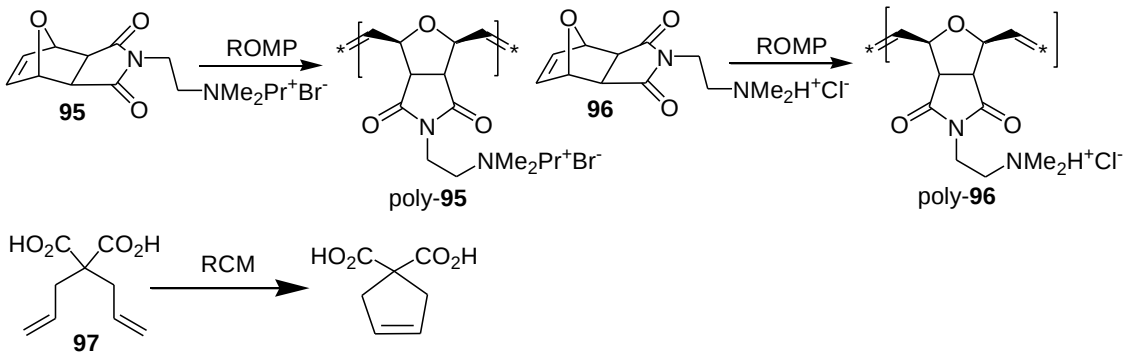

Kinetic Studies

Aqueous Metathesis Reactions for Catalysts Bearing H_2ITap and ITap Ligands

The first two catalysts examined for metathesis reactions in acidic protic and aqueous media were complexes **61**, (H_2ITap)(PCy_3)Cl_2Ru=CH-Ph, and **62**, (H_2ITap)Cl_2Ru=CH-(C_6H_4-O-*i*Pr). Both of these complexes appeared to exhibit an externally controllable solubility profile, as they both precipitated from organic solutions upon the addition of two equivalents of DCl, which made them very attractive candidates for this study. However, catalyst **61** exhibited low solubility in purely aqueous media when protonated with two equivalents of DCl. ^{1}H NMR analysis indicated this was partially due to the incomplete protonation of the NMe_2 groups of its NHC ligand. Instead, a mixture of complexes **61a**-**61d** was formed (Scheme 30), including unstable phosphine-deficient complexes plus the PCy_3D^+ cation, formed by partial protonation of the phosphine ligand, which was observed by ^{31}P NMR spectroscopy. The mixture exhibited low stability, as it decomposed within a few hours in solution.[79] Catalyst **62** was soluble in 0.1M DCl / D_2O and formed complex **62a** (Scheme 31), which exhibited very slow hydrolysis of the Ru-NHC bond (51% in 7 d).

Scheme 30. Protaonation of Catalyst **61**

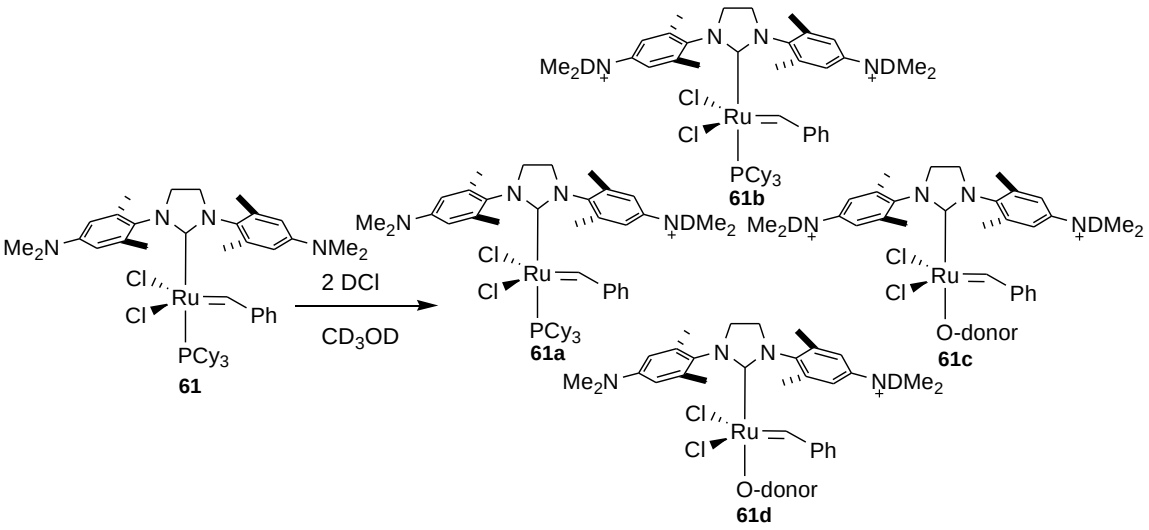

Scheme 31. Protonation of Catalyst Complex **62**

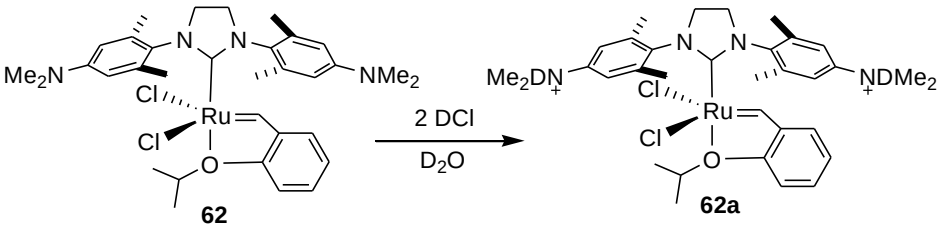

Based on these results, ROMP of cationic *exo*-7-oxanorbornene derivative **95** and RCM reactions of diallylmalonic acid **97** were carried out in acidic protic media with a 1 M HCl_{aq}–2-propanol (1:9 v/v) solution for catalyst **61** and a 0.1 M HCl_{aq} solution for catalyst **62**. The catalyst loadings were 4% in each of these experiments, with [Ru] = 2.0 mM and a reaction temperatures of 50 ^{o}C. The catalytic performance of both catalysts **61** and **62** in acidic protic media was quite disappointing, as neither complex produced any noticeable amounts of polymer during the ROMP reaction. Furthermore, the RCM of **97** reached only 56% for catalyst **61** and 44% for catalyst **62** in 30 minutes at 50 ^{o}C. Additional reaction times did not afford further conversions, likely due to catalyst decomposition. As shown in Chapter IV, converting the π-donating NMe_2 groups into σ-withdrawing NMe_2H^+ moieties had decreased catalyst activity. The fact that the ROMP

activity was almost zero must be attributed to the solvent since the deprotonated species **61** and **62** exhibit metathesis activity in organic solvents (vide supra). In our experience, reactions in water are sluggish. We believe that water may act as an inhibitor to many catalysts, including **61** and **62**.[93] Hence, as a result of slower propagation of species **62a** and **61b-d**, respectively, and additional H_2O inhibition, the tested ROMP reactions did not afford noticeable amounts of product.

The next catalyst studied was $(H_2ITap)(DMAP)_2Cl_2Ru$=CH-Ph **65**. In Chapter IV, a gradual protonation scheme (Scheme 25) was proposed in which fast initiating, slow propagating complex **65b** would be formed upon protonation with four equivalents of acid. A similar methodology was attempted, using an excess of acid to form this complex (Scheme 32). Upon protonation in 0.1M solutions of acid in water this catalyst was soluble, though small amounts of catalyst did precipitate. As with catalyst complexes **61** and **62**, no noticeable amounts of polymer were produced during the ROMP reaction of norbornene substrate **96** under similar reaction conditions. RCM reactions of substrate **97** did afford conversion, though at low levels (Table 13). The low observed activity in aqueous media was likely caused by extremely slow propagation based on the presence of the N^+HMe_2 groups. For all ROMP and RCM reactions, catalyst loadings were 4%, with [Ru] = 2.0 mM and a reaction temperatures of 50 ^oC. The higher conversion with H_3PO_4 may be a result of a lower degree of protonation by the weaker acid, which may have resulted in a faster propagating species. However, at this point, this is pure speculation.

Scheme 32. Protonation of Catalyst Complex **65** With Excess Acid

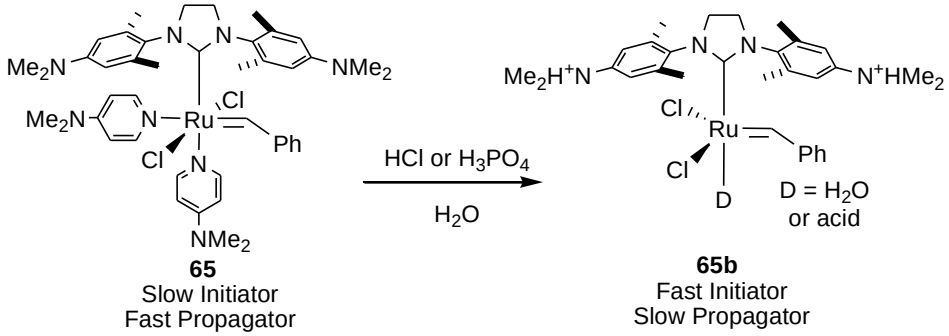

65
Slow Initiator
Fast Propagator

65b
Fast Initiator
Slow Propagator

Table 13. RCM of 97 With Catalyst 65
[Ru] = 2.0 mM, 4% Catalyst Loading, 50 ^{o}C

Acid	Time (min)	% Conversion
H_3PO_4	30	25.2
HCl	30	8.7
HCl	60	10.3

The same effect was observed for all of the complexes bearing an ITap ligand (Figure 48). For all of these reactions catalyst loadings were 4%, in 0.1M HCl_{aq}, with [Ru] = 2.0 mM, and reaction temperatures of 60 ^{o}C. For these complexes, (ITap)$(PCy_3)Cl_2Ru$=CH-Ph **67**, (ITap) (ITap)Cl_2Ru=CH-(C_6H_4-O-*i*Pr) **68**, $(DMAP)_2Cl_2Ru$=CH-Ph **69**, (ITap)$(PCy_3)Cl_2Ru$=CH-SPh **80**, and (ITap)$(DMAP)_2Cl_2Ru$=CH-SPh **82**, some precipitation of the catalyst was observed. ROMP reactions of norbornene derivative **96** afforded no ROMP activity with any these catalysts. Lower conversion rates were also observed for RCM reactions of **97** than was seen for catalysts **61** and **62** with similar reaction conditions (Table 14). The kinetic results for these ITap bearing catalysts further emphasize the strong influence that acidification of the aryl NMe_2 of the NHC ligand substituent has on the activity profile of catalysts with these types of modified NHC ligands.

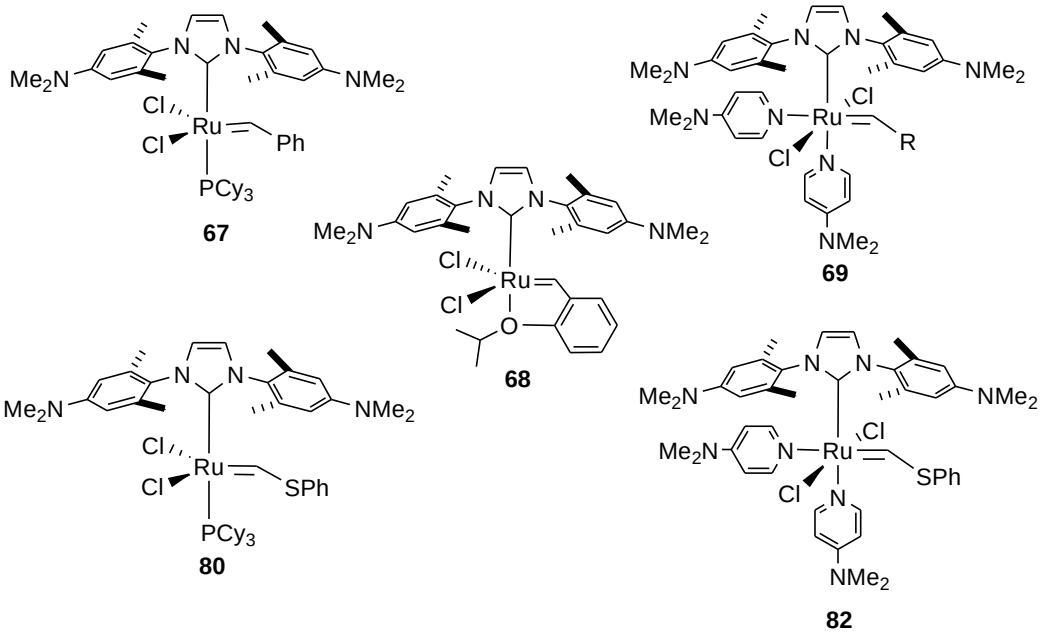

Figure 48. ITap Ligand Bearing Catalysts Used for Aqueous Kinetic Studies

Table 14. RCM of DAM With Catalysts Bearing ITap Ligands
[Ru] = 2.0 mM, 4% Catalyst Loading, 0.1M HCl_{aq}, 60 ^{o}C

Catalyst	Time (min)	% Conversion
(ITap)(PCy_3)Cl_2Ru=CH-Ph **67**	60	6.9
(ITap)Cl_2Ru=CH-(C_6H_4-O-*i*Pr) **68**	60	7.2
(ITap)(DMAP)$_2Cl_2$Ru=CH-Ph **69**	60	2.7
(ITap)(PCy_3)Cl_2Ru=CH-SPh **80**	60	1.0
(ITap)(DMAP)$_2Cl_2$Ru=CH-SPh **82**	60	0.3

Aqueous Metathesis Reactions for Catalysts Bearing NHC Ligand With Remote NMe_2 Groups

ROMP and RCM reactions for catalysts bearing NHC ligands modified with remote NMe_2 groups were also conducted in aqueous media. For these catalysts (**70**, **77**, and **78**), the NMe_2 groups were separated from the aryl substituents of the NHC ligand by an E-CH_2-CH_2 spacer, where E = O or S. For these catalysts, their activity in organic solvents was significantly lower than their H_2ITap counterparts. In aqueous media, however, it was anticipated that the formation of the NMe_2H^+ groups should not dramatically affect the electronic catalyst environment. Thus, these catalysts were expected to exhibit a faster propagation in aqueous media than the H_2ITap and ITap ligand bearing catalysts.

The first of these catalysts to be studied was ($IXyONMe_2$)(PCy_3)Cl_2Ru=CH-Ph **70** (Scheme 33). Similar to catalyst complex **61**, sufficient catalyst solubility was accomplished using 1 M HCl_{aq}–2-propanol (1:9 v/v), so this was the solvent chosen for aqueous olefin metathesis reactions with this catalyst. As before aqueous ROMP and RCM reactions for this catalyst were initially conducted with [Ru] = 2.0 mM solution with 4% catalyst loading. The results for ROMP reactions of norbornene substrate **96** with catalyst **70** were surprising (Table 15). The ROMP reaction was first conducted at 60 ^{o}C, which afforded >99% conversion to polymer within 15 minutes. This reaction was then repeated at room temperature using the same concentrations, which yielded almost the same conversion. Decreasing the catalyst loading to 2% did result in a slight decrease in the conversion, and no further conversion was observed after 15 minutes, indicating a loss of activity due to catalyst degradation. However, the conversions observed were a dramatic improvement over catalyst **61**. In fact, in these ROMP reactions catalyst **70** even outperformed Grubbs' water soluble catalyst **26** (Figure 49), which is considered to be the most active Ru-based olefin metathesis catalyst for use in homogenous aqueous olefin metathesis applications. That catalyst, by comparison, required three hours to achieve the same ROMP conversion of a similar substrate, at similar catalyst loadings, afforded by catalyst **70** within 15 minutes. Catalyst **97** was less active in the RCM reaction of DAM in acidic protic media, with only 75.1% conversion achieved after 15 minutes at 60 ^{o}C with no further conversion after this time, however, this result was comparable to those observed with catalyst **26** after several hours with other α,ω-diolefins.[6a] Based on these results, catalyst **70** is definitely a highly active olefin metathesis catalyst in protic media.

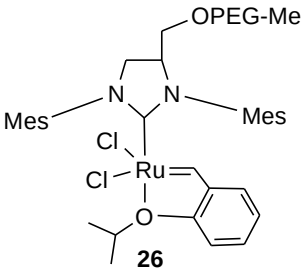

26

Figure 49. Grubbs' Water Soluble Catlyst **26**

Scheme 33. External Control of Solubility for Catalyst **70** via Protonation

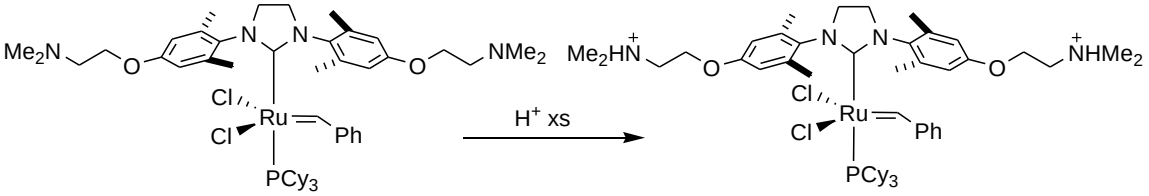

70 Soluble in Organic Media

70a Soluble in Aqueous Media

Table 15. ROMP of Norbornene Substrate 96 With Catalyst 70
[Ru] = 2.0 mM

% Catalyst Loading	Temperature (^{o}C)	Time (min)	% Conversion to Polymer
4	60	15	99.38
4	20	15	98.17
2	20	15	86.53

The last two catalysts examined via ROMP and RCM olefin metathesis reactions in aqueous media were (IDippONMe$_2$)(DMAP)Cl$_2$Ru=CH-Ph **77** and (IDippSNMe$_2$)(DMAP)$_2$Cl$_2$Ru=CH-Ph **78**. Like catalyst **70**, these two catalysts possess remote NMe$_2$ groups. These catalysts additionally bear pH-responsive DMAP ligands, resulting in higher initiation rates upon acid addition. The simultaneous protonation of the NMe$_2$ groups and the DMAP ligands of catalyst complexes **77** and **78** produced water soluble complexes **77a** and **78a** (Scheme 34). We hypothesized that these two complexes could afford an unprecedented olefin metathesis catalyst system capable of performing both ROMP and RCM reactions in aqueous media, especially considering the high activity exhibited by catalyst **70**.

Scheme 34. Protonation of Catalyst Complexes **77** and **78**

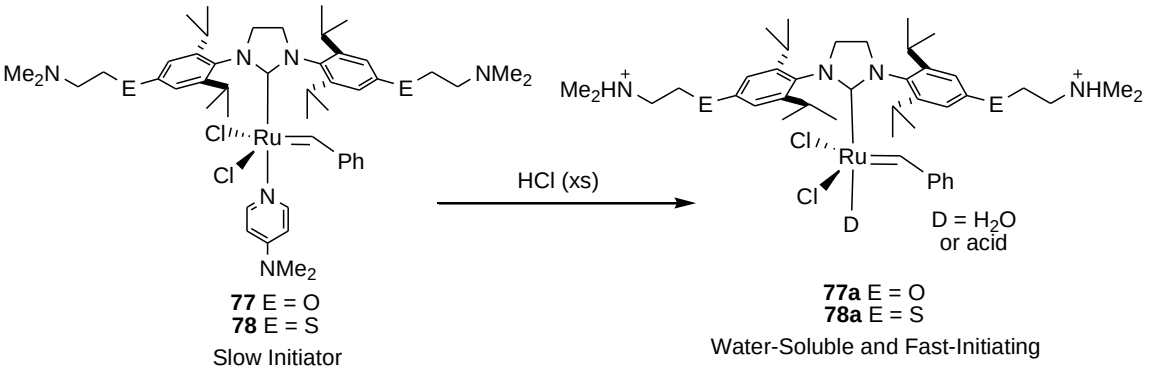

Aqueous ROMP and RCM reactions were conducted with catalysts **77** and **78** using 0.1M HCl_{aq}. The ROMP and RCM reactions proceed fast at room temperature. RCM of **97** ([Ru] = 2 mM with 4% catalyst loading) only reached 62.9% and 52.5% conversion, respectively, after 30 minutes. Again, further conversion was not observed, indicating catalyst decomposition due to the fast initiation. The ROMP reactions with substrate **96** proceeded to complete conversion at extraordinary rates, with >95% ROMP conversion achieved in each reaction within 15 min (Table 16). This extremely high activity clearly demonstrates that these two catalyst systems dramatically outperform Grubbs' water soluble catalyst **26** in aqueous media,[6a] making them the most active catalysts for aqueous olefin metathesis applications to date.

Table 16. ROMP Reactions of Norbornene Substrate 96 With Catalysts 77 and 78
[Ru] = 2.0mM

Catalyst	% Catalyst Loading	Time (min)	% Conversion to Polymer
77	4	15	>99
77	1	15	97.2
78	4	15	97.6

For catalyst **77**, >99% ROMP reaction conversion was even achieved with catalyst concentrations as low as 1.0 mM at 1.0% catalyst loading, a concentration more often applied to reactions with ROMP substrates in organic media. Very few examples can be found in the literature of Ru-based olefin metathesis catalysts for efficient ROMP in aqueous media.[6a,51] The closer examination of the kinetics of this reaction indicated

that this is, in fact, a fast initiating catalyst, as no long induction period is observed prior to the sudden onset in activity (Figure 50). This likely accounts for the increased activity displayed by these catalysts, showing that external control of catalyst solubility was afforded via protonation and subsequent dissociation of the DMAP ligand. The logarithmic plot is linear which indicates that the ROMP followed pseudo first order kinetics for much of the reaction, though some deviation is seen at high conversions and long reaction times, indicating slow catalyst decomposition (Figure 51). Catalyst **77** can be considered the most active catalyst for aqueous ROMP to date. The efficient initiation may make this catalyst suitable for controlled aqueous ROMP, however, detailed polymer analyses are needed to confirm these kinetic results.

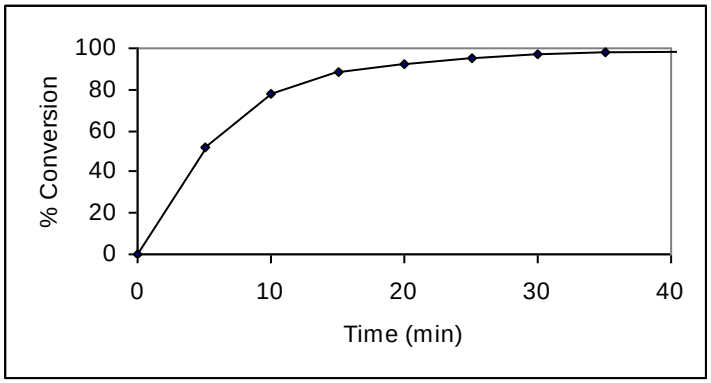

Figure 50. ROMP of Norbornene Substrate **96** With Catalyst **77**
[Ru] = 1.0 mM, 1.0% Catalyst Loading, in 0.1M HCl_{aq}, 20 ^{o}C

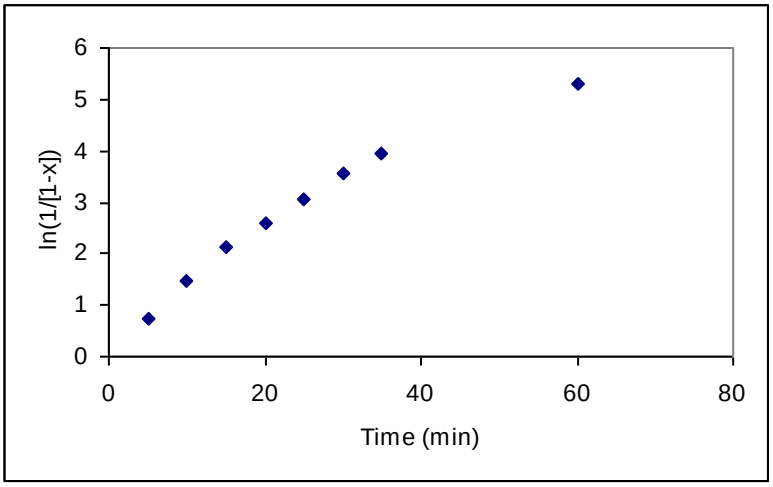

Figure 51. Logarithmic Conversion of **96** With Catalyst **77**
[Ru] = 1.0 mM, 1.0% Catalyst Loading, in 0.1M HCl_{aq}, 20 ^{o}C

Summary

ROMP and RCM reactions were conducted both acidic protic and aqueous media using catalysts bearing pH-responsive ligands. Many, but not all, catalysts exhibited solubility in acidic aqueous or aqueous/alcoholic media confirming our goal to generate a catalyst with an externally controllable solubility profile. For catalysts bearing H_2ITap or ITap ligands, a dramatic loss of activity was observed upon protonation of the aryl NMe_2 groups of their NHC ligands, which clearly showed that conversion of the their π-donating dimethylamino groups into σ-withdrawing ammonium groups significantly reduced their catalyst activity. For systems with these aryl NMe_2 groups, no noticeable ROMP activity was achieved in aqueous media, and no RCM reaction was observed accomplishing >56% substrate conversion. In most cases, complete catalyst decomposition was observed.

Much higher activities were exhibited by catalyst systems with remote NMe substituted NHC ligands in aqueous media. The ROMP reactions with these catalysts were very fast, often giving >95% within 15 minutes or less, making them the fastest ROMP catalysts for aqueous metathesis to date. Catalyst **77** (Figure 52) was

particularly impressive, achieving nearly complete conversion to ROMP polymer in aqueous media at concentrations as low as 1.0 mM with 1.0% catalyst loading in 60 minutes at room temperature. Previously published catalysts by Grubbs *et al*.[6a] did not even remotely exhibit such high activity. Closer examination of the ROMP kinetic profile for this reaction showed that this catalyst may be suitable for controlled polymerization in aqueous media due to the fast dissociation its pH-responsive DMAP ligand, however, analysis of the polymers obtained in this reaction has not yet been completed to substantiate this theory.

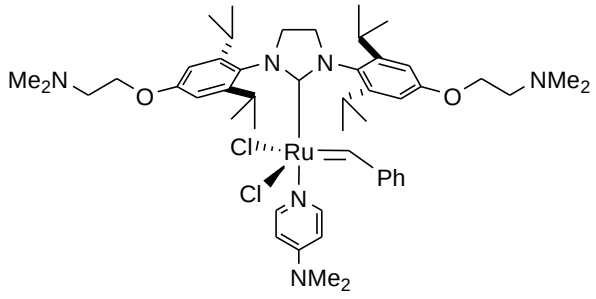

77

Figure 52. pH-Responsive Catalyst **77**

CHAPTER VI

APPLICATIONS FOR OLEFIN METATHESIS CATALYSTS WITH PH-RESPONSIVE LIGANDS

There are many practical applications available for catalysts with externally controllable solubility and activity profiles. The ability to perform homogenous olefin metathesis reactions in aqueous and acidic protic media, as explored in Chapter V, greatly expands the substrate availability for Ru-based olefin metathesis catalyst systems. Catalysts systems with reversible solubility profiles, externally controlled via acid addition, might be very economical, as these systems could be used to perform olefin metathesis reactions in both organic and aqueous media with a large variety of substrates of different solubilities. Interest has steadily grown to use olefin metathesis in aqueous and biological media.[22,51,95] This chapter describes practical applications that were or are currently being explored in our laboratories or via collaboration.

In a collaboration with Dr. Andrea Robinson (Monash University, Austrailia) we have provided (H_2ITap)Cl_2Ru=CH-(C_6H_4-O-*i*Pr) **62** to synthesize oligopeptides containing unnatural amino acids grafted on solid support. The analogous natural peptides have therapeutic value as potential drugs and antidotes to natural venoms but suffer from rapid digestion in the human body based on breaking their labile S-S bonds.[96] These S-S bonds enforce the active tertiary bicyclic structures. Thus, their replacement with HC=CH bonds is highly desirable, since they provide much elevated stability of the peptide under physiological conditions. The –CH=CH- moieties are generated via RCM. The use of aqueous media in the synthesis is much more benign to the peptides than organic solvents, thus an olefin metathesis catalyst was needed which can perform under these conditions. The project is still ongoing and we have not received any preliminary results.

The external control of the catalyst solubility afforded by the pH-responsive ligands in these catalyst systems was also proven useful when employed for the removal of the Ru-metal catalyst from olefin metathesis reactions in organic media. The effective removal of Ru-metal has become an important issue for the pharmaceutical industry, which currently uses very expensive column chromatography to remove Ru-metal contamination from their products.[6b,59] The pH-responsive catalyst systems developed for this dissertation are obviously very attractive for this process, as they have been shown to precipitate from organic reaction media upon acid addition, which would allow for easier catalyst removal.

We applied this concept by developing a protocol for catalyst **62** which reduces the Ru-metal contamination in RCM reaction mixtures (Scheme 35).[79] Catalyst **62** was selected because of its enhanced hydrolytic stability and low solubility in organic media upon protonation, a result of the formation of low-soluble dicationic Ru-species **62a** (Scheme 35). For this study, RCM reactions of diethyldiallylmalonate (DEDAM) and 3,3-diallyl-2,4-pentanedione (DAP) (Figure 53) ([Ru] = 3.3 mM, 2% catalyst loading) were carried out in either toluene or ethyl acetate at 50 ^{o}C for 30 minutes. All reaction provided >99% conversion. These reactions were then quenched through addition of ethyl vinyl ether. After 10 minutes, concentrated acid (HCl or H_2SO_4) was added via microliter syringe (approximately 10 equivalents with respect to the catalyst). This caused precipitation of the Ru-metal species within seconds of acid addition (Scheme 36). The slurry was then filtered through a plug of Na_2SO_4, followed by solvent removal under reduced pressure. The complete RCM conversion was verified via ^{1}H NMR spectroscopy before aliquots of 20–22 mg were taken and digested with concentrated HNO_3 for analysis by Inductively Coupled Plasma Mass Spectrometry (ICP-MS). The residual product that remained after the aliquots were taken was then extracted with *t*-BuOMe and washed with water. The solvent was once again removed under reduced

pressure and additional aliquots of 20–22 mg were once again taken and digested with concentrated HNO_3 for ICP-MS analysis.

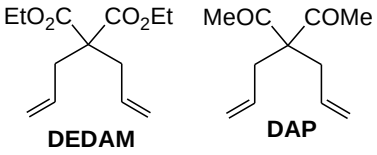

Figure 53. Substrates for Catalyst Removal Studies

Scheme 35. Precipitation of Catalyst **62** via Acid Addition

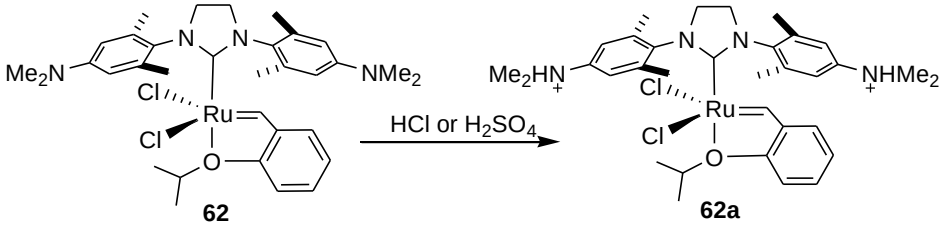

Scheme 36. Catalyst Removal Method

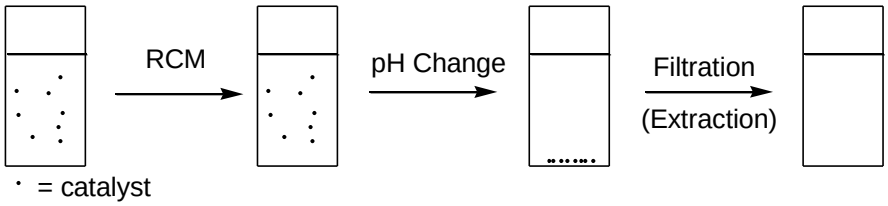

The results showed that products obtained from substrate DEDAM contained significantly lower amounts ruthenium than the products obtained from substrate DAP (Table 17). The results also showed that products obtained via filtration with subsequent extraction in water exhibit improved Ru-removal when compared to filtration alone, but significant amounts of the RCM product are also lost through this extra step. The conditions with lowest residual Ru-metal content in the RCM products were observed when the removal protocols were applied to a reaction solution with DEDAM as substrate**,** in toluene, and H_2SO_4 as acid. The residual Ru levels under these conditions of 24 ppm (after filtration only) and 11 ppm (after filtration and subsequent wash) are very close to the pharmaceutical standard of ≤ 10 ppm. This represents the most

effective, single-step Ru-removal protocol for homogenous metathesis reactions to date, including column chromatography and all scavenging methods.[60,61] Hence, this method could be a very attractive alternative to column chromatography in the pharmaceutical industry based on its effectiveness and economic feasibility. It should be noted that attempts to reuse the precipitated catalyst after deprotonation with NEt_3 were not successful.

Table 17. Results for Studies of Ru-Metal Removal After RCM Reactions
[Ru] = 3.3 mM, 2% Catalyst Loading, 50 ^{o}C

Substrate	Acid	Solvent	Method[a]	Yield (%)[b]	ppm Ru
DEDAM	HCl	Toluene	F	86.5	82
DEDAM	HCl	Toluene	W	58.8	48
DEDAM	**H_2SO_4**	**Toluene**	**F**	**72**	**24**
DEDAM	**H_2SO_4**	**Toluene**	**W**	**60.3**	**11**
DEDAM	HCl	AcOEt	F	76.9	34
DEDAM	HCl	AcOEt	W	52.9	45
DEDAM	H_2SO_4	AcOEt	F	85.7	140
DEDAM	H_2SO_4	AcOEt	W	45.7	48
DAP	HCl	Toluene	F	43.2	498
DAP	HCl	Toluene	W	68.9	160
DAP	H_2SO_4	Toluene	F	79.1	213
DAP	H_2SO_4	Toluene	W	44.5	80
DAP	HCl	AcOEt	F	78.2	335
DAP	HCl	AcOEt	W	63.3	144
DAP	H_2SO_4	AcOEt	F	68.1	149
DAP	H_2SO_4	AcOEt	W	44.3	90

[a] F = filtration alone, W = filtration with subsequent extraction; [b] Isolated yields for W were based on the extraction step alone

In collaboration with Dr. Kevin Müller of BASF (Ludwigshafen, Germany), several catalysts produced for this dissertation were investigated for emulsion ROMP,[97] which has little precedence in literature.[2c,98] The scope of studies with water-soluble catalysts was limited to highly strained norbornene,[7a] since less reactive monomers did not result in high conversions. Also, the catalyst loadings were high (3.3%). The current studies by BASF demonstrated that catalysts (H_2)ITapRu=CH-Ph, and **79**-**82** were capable of polymerizing cyclooctene (COE) and dicyclopentadiene (DCPD) in emulsion under acidic conditions to afford complete polymerization with loadings as low as 180 ppm. Stable latexes were successfully generated for not only COE and DCPD, but also for

copolymers from mixtures of these two monomers. For the first time, other, less-reactive monomers than norbornene (the most active ROMP monomer known) were successfully polymerized with this technique. Also, the catalyst loading could be lowered by two orders of magnitude than in previous examples.[98] A patent application for this process has been submitted and no detailed results have been released by our partner.[97]

Additionally, the effect of acid addition to pH-responsive catalysts **65** and **79**-**82** (Figure 54) on gelation times of ROMP substrates was also investigated by BASF.[97] The gelation times for DCPD (in hexadecane) and COE was monitored with these catalysts (66 mg per 5.35g of substrate, or 0.16-0.17% catalyst loading for DCPD and 0.14% catalyst loading for COE) at room temperature. The same experiments were then conducted in the presence of excess toluenesulfonic acid (TsOH) (0.2g). The results show that gelation times responded differently to the acid addition, depending on the nature of the catalyst and the substrate. It was observed that gelation times for DCPD are faster in the presence of acid with all catalysts tested. With COE, gelation times for catalysts bearing H_2ITap ligands were also faster in the presence of acid, particularly for Ru=CH-SPh catalysts **79** and **82**. For catalysts bearing ITap ligands (catalysts **90** and **91**), gelation times were longer in the presence of acid, which was in stark contrast to what was observed with DCPD. Most contradictory are the results for catalyst **82**. With this catalyst, the increase in gelation time was for COE was dramatic, which took two hours in the presence of acid versus 0.5 min observed without acid.

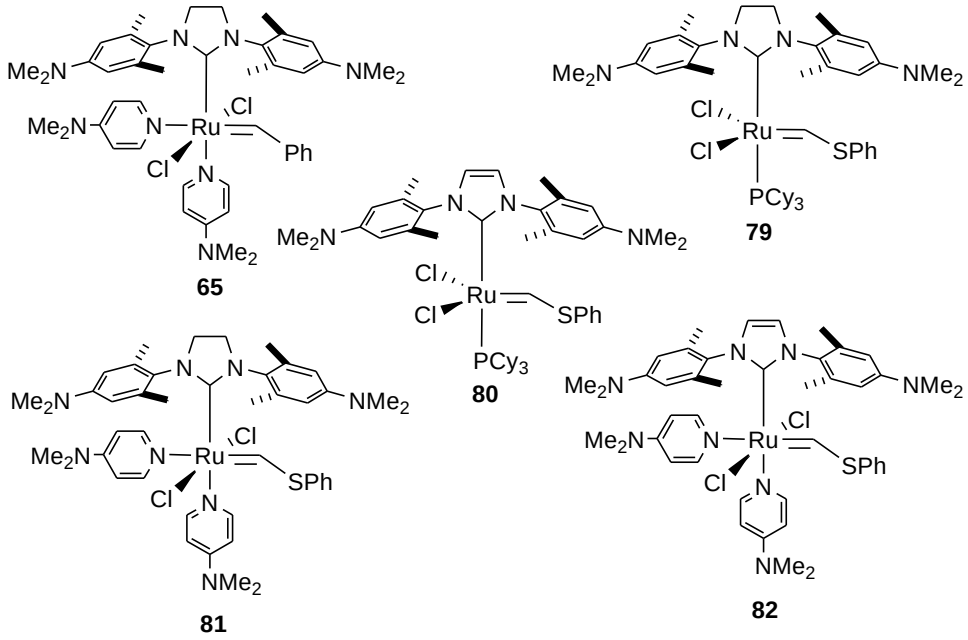

Figure 54. Catalysts Used in Gelation Studies of DCPD and COE

Table 18. Gelation Studies[a] of DCPD and COE

	DCPD[b]		COE	
	No Acid	TsOH[c]	No Acid	TsOH[c]
Catalyst	Time (min)	Time (min)	Time (min)	Time (min)
65	0.03	0.03	1.1	0.03
79	0.8	0.03	46.0	0.7
80	10.6	0.8	2.2	3.9
81	1.1	0.3	120	3.3
82	5.0	1.5	1.5	120

[a] 66 mg catalyst / 5.35 g substrate at room temperature (0.16-0.17% catalyst loading for DCPD, 0.14% catalyst loading for COE); [b] in hexadecane; [c] 0.2 g TsOH

The data from these gelation studies provides some interesting implications for ROMP reactions conducted with these catalysts bearing pH-responsive ligands. As with previous kinetic studies, this data shows that the rate of ROMP reactions, and therefore overall catalyst activity profiles, may be altered through protonation of these catalysts with pH-responsive ligands in different directions for different monomers. Because different activity trends were observed for catalysts **80** and **82** with COE and DCPD, acid addition may additionally change the catalyst affinity for one substrate over another. This implies the degree of protonation may be a parameter which could be adjusted to produce truly statistical co-polymers of monomers whose reactivity with certain catalysts

change in different directions upon protonation. This, for the first time, could allow for the generation of statistical ROMP co-polymers with different compositions. Detailed studies of this phenomenon beyond the gelation studies, however, were not conducted.

CHAPTER VII

SUMMARY

For this dissertation, novel Ru-based olefin metathesis catalysts bearing pH-responsive ligands were produced. These pH responsive ligands provided the means by which the solubility and activity profiles of the catalyst could be externally controlled via acid addition. All of the catalysts generated for this dissertation contain pH-responsive, NMe_2 modified NHC ligands. Additionally, some of the catalysts produced also contained pH-responsive N-donor ligands. The overall goal of this project was to generate catalysts systems capable of performing olefin metathesis reactions in both organic and aqueous media.

To achieve this goal, a series of NMe_2 modified NHC ligand precursor salts **37**, **38**, and **55**-**58** (Figure 55) were first produced. H_2ITap·HCl **37** and ITap·HCl **38** were made by following literature procedures, with slight modifications, for similar imidazolin-2-ylidene and imidazole-2-ylidene complexes, after the dimethylamino groups were introduced to the starting aniline compound. Both of these ligand precursors bear NMe_2 groups attached directly to the aryl substituents of their NHC ligands. By contrast, IXyONMe_2·HCl **55**, IXySNMe_2·HCl **56**, IDippONMe_2·HCl **57**, and IDippSNMe_2·HCl **58** each bear NMe_2 groups that are removed from the aryl group of the NHC ligand by an E-CH_2-CH_2 spacer (E = O or S). These precursors were synthesized via a template synthesis, based on the synthesis of precursor salt **37**, which was developed in an attempt to gain fast access to a library of ligand precursors. Key to this template synthesis is the formation of diiodinated diamine intermediates which could be functionalized through Cu-mediated C-heteroatom coupling reactions,[81] enabling a straightforward access to several unique ligand precursors.

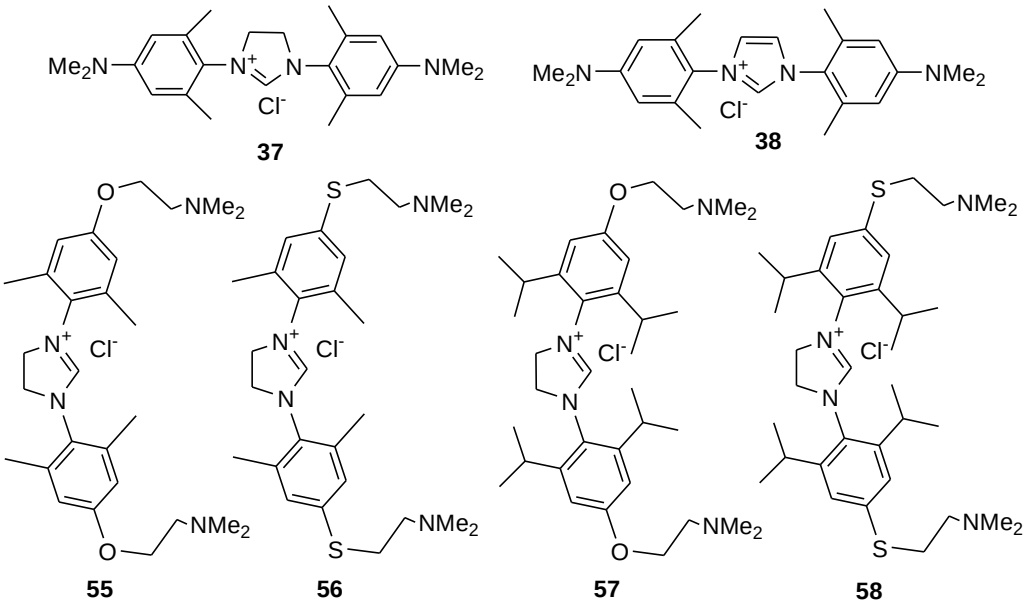

Figure 55. NMe_2 Modified NHC Ligand Precursors

After these NHC ligand precursors were synthesized, they were used to make novel Ru-based olefin metathesis catalysts. These NHC ligands were incorporated into these structures via ligand exchange reactions with phosphine-ligand bearing precatalysts. In addition, some of the product catalysts were reacted with excess N-donor ligand, which produced other derivative catalyst complexes. Most of the catalysts produced for this dissertation were benzylidene-carbene (or Grubbs-type) complexes, though phenylthiomethylidene, phenylindenylidene, and bidentate propylidene complexes were also generated.

Most of the catalysts produced for this dissertation bear either an H_2ITap or ITap ligand (Figures 56 and 57), the catalyst syntheses were straightforward in accordance with literature procedures. By contrast, complexes with remote NMe_2 groups on their NHC ligands proved much more difficult to synthesize and isolate. Alternative synthesis methods attempted with these ligand precursors, but were unsuccessful. As a result, only three of the catalysts generated for this study bear this NHC ligand motif (Figure 58). In total, 16 novel catalyst complexes were generated for this study.

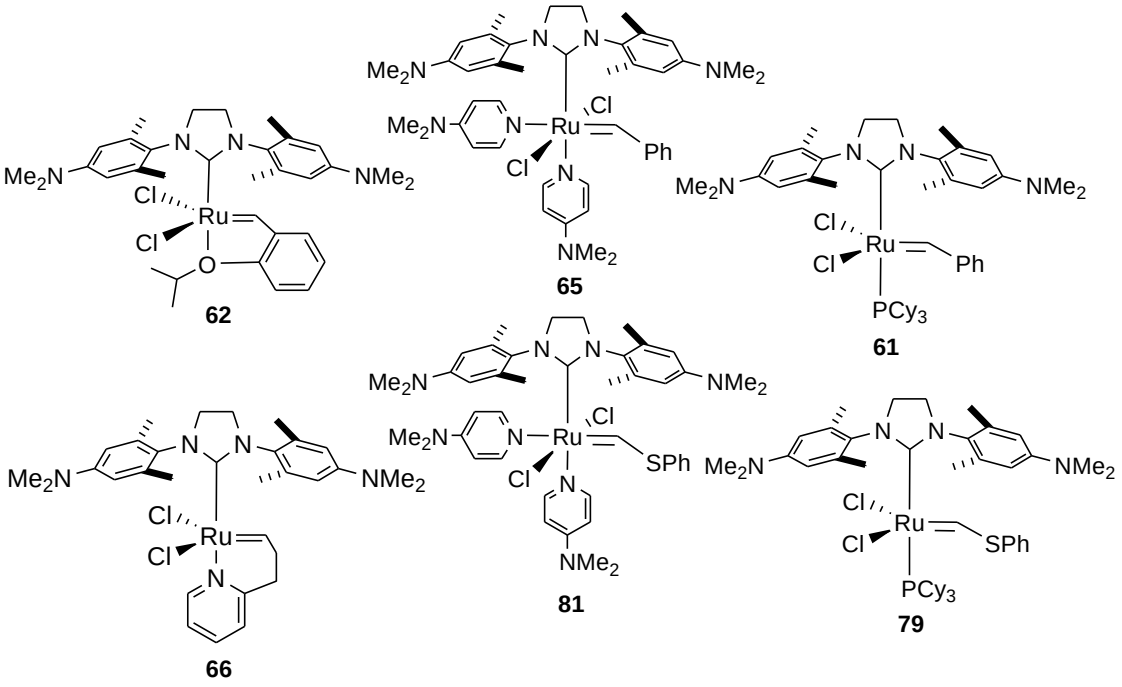

Figure 56. Catalysts Bearing an H_2ITap Ligand

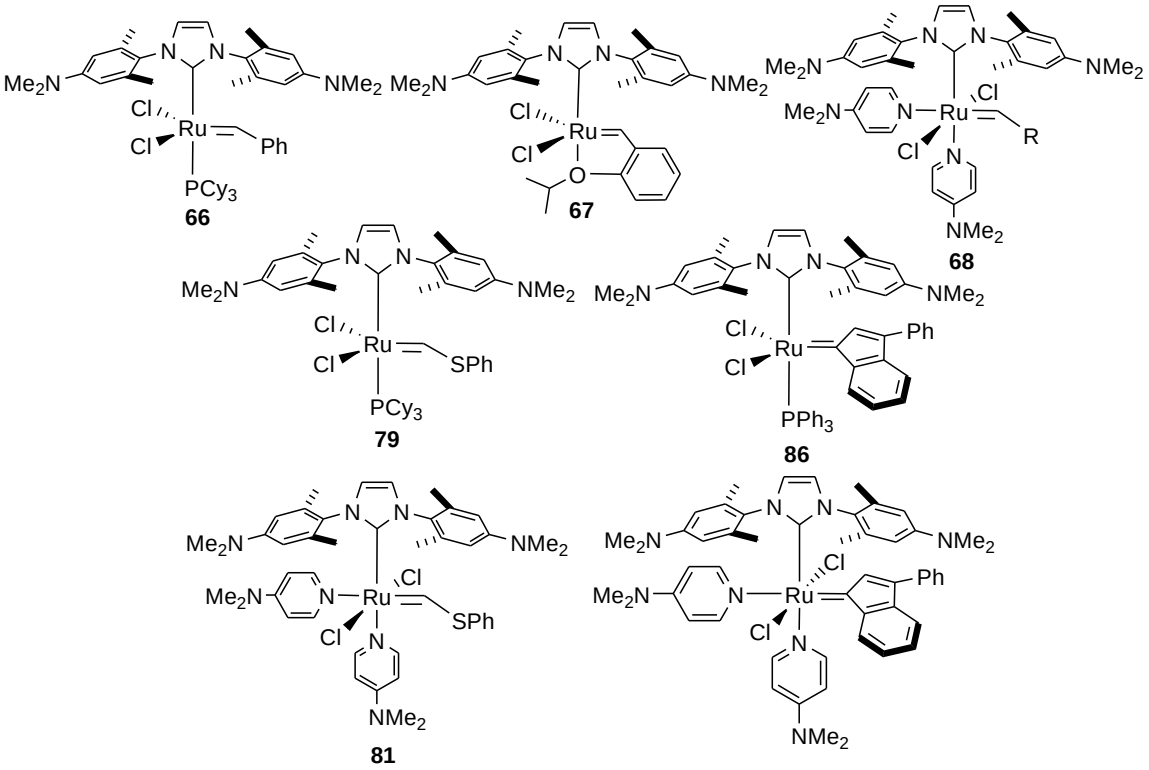

Figure 57. Catalysts Bearing an ITap Ligand

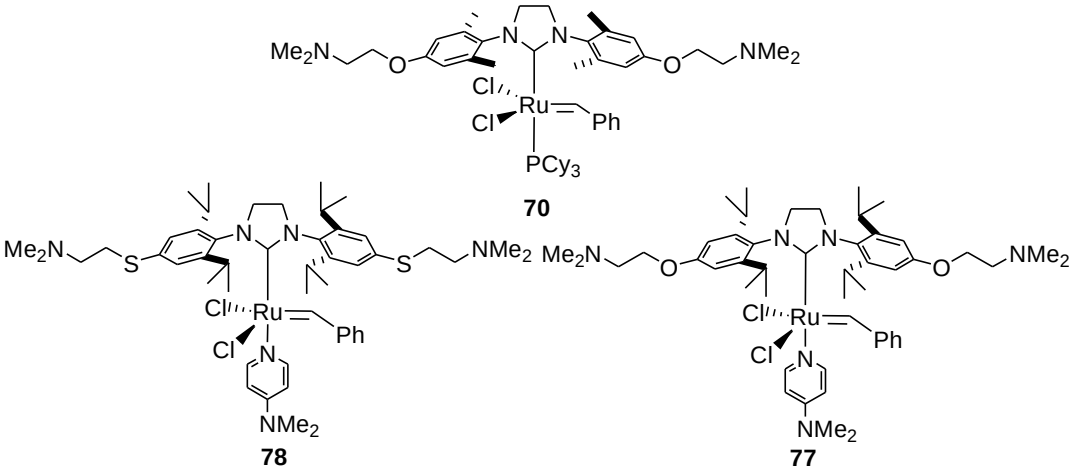

Figure 58. Catalysts Bearing NHC Liagnds With Remote NMe_2 Groups

To assess the olefin metathesis activity of these catalysts in comparison to literature catalyst complexes, ROMP and RCM reactions were conducted in organic media. The kinetic profiles that were generated were then compared to those obtained for commercially available catalysts **12** and **13** under similar reaction conditions to asses the relative activities. In the absence of acid, metathesis reactions in organic showed that H_2ITap ligand ligand bearing counterparts were more active than catalysts bearing other pH-responsive ligands synthesized in this project. As expected, benzylidene-carbene catalysts outperformed analogous phenylthiomethylidene catalysts and phenylindenylidene-carbene complexes. However, with the phenylthiomethylidene complexes, catalyst performance was dramatically improved with elevated temperature (60 ^{o}C).

For some catalysts generated in this study, kinetic studies in organic media were also conducted in the presence of non-nucleophillic to asses the change in catalyst solubility and activity profiles afforded via protonation of the pH-responsive groups. The first to be examined in the acid studies were catalysts **61** and **62**. Under standard, non-acidic conditions, these two catalysts exhibited very similar activity profiles to their commercially available counterparts, catalysts **61** and **62**. However, upon protonation of

their pH responsive NMe_2 groups with increased concentrations of TsOH, a significant decrease in activity was observed. Analysis of polymers produced in ROMP reactions under these conditions indicated that the slowing of catalyst activity was due to a decrease in the rate of propagation, since better molecular weight control was afforded with increased amounts of acid. Additional DFT calculations were used to determine the Mullikan atomic charges for similar model complexes. These indicated that the π-acceptor capability of the H_2ITap ligand was reduced upon protonation, showing that the protonation of the NMe_2 groups of the ITap ligand greatly interfered with the electronic environment of the ligand, thus causing an overall decrease in catalyst activity. Initiation kinetics conducted by reacting complexes **61** and **62** with EVE confirmed that slightly increased rates of initiation were observed when acid was added. Combined, these results unambiguously showed that the decrease of activity upon protonation of the NMe_2 groups of the H_2ITap ligand was a result of decreased rates of propagation. To our knowledge this is the first example of an external control for propagation in metathesis reactions.

Kinetic studies upon the addition of acid were also conducted with catalysts bearing pH-responsive N-donor ligands. As expected, an increase in the rate of initiation in ROMP and RCM reactions was observed when these N-donor ligands were dissociated from the metal center upon acid addition. For catalysts **65**, **66**, and **88**, dissociation of the DMAP ligand not only resulted in increased initiation efficiency, but also in an increase in overall catalyst activity. For catalyst **88** this increase was extraordinary, since this phenylindenylidene complex was converted from a slow catalyst system into one with activity similar to commercially available catalyst **12**, which is considered to have excellent metathesis activity. This was not unexpected, as these trends had previously been observed in literature for other DMAP catalyst systems.[1g,64]

Unfortunately, for catalysts **81** and **87** decreased metathesis conversions were observed, most likely due to increased catalyst decomposition in the presence of acid.

Since the main goal in this dissertation was to generate catalysts capable of performing metathesis reactions in aqueous media, the catalysts made for this project were tested in aqueous ROMP and RCM reactions. The protonation of the NMe_2 groups of the NHC ligand of these catalysts afforded complexes bearing two cationic NMe_2H^+ groups, which, for most catalysts produced in this project, provided sufficient catalyst solubility in aqueous or acidic protic media. Therefore, external control of catalyst solubility was established via protonation of the pH-responsive groups. For catalyst systems with H_2ITap and ITap ligands, the conversion of the π-donating dimethylamino groups into σ-withdrawing ammonium groups upon protonation once again resulted in a dramatic slowing of catalyst propagation. For systems with these aryl NMe_2 groups, no noticeable ROMP activity was observed in acidic aqueous media, and no RCM reaction provided more than 56% substrate conversion with a 4% catalyst loading. In most cases, significant catalyst decomposition was also observed.

Much better activity was observed with catalysts bearing NHC ligands modified with remote NMe_2 groups in acidic, protic media. These catalysts (**70**, **77**, and **78**) each completed ROMP reactions faster than Grubbs water-soluble catalyst **26**, which is considered to be the most active catalyst in aqueous olefin metathesis reactions. This catalyst has been reported to afford full ROMP conversion of norbornene substrates in a little over three hours with 3.3% catalyst loading. All three of our catalysts, by comparison, allow for the same conversion in just 15 minutes at 4% catalyst loading. Catalyst **70** was also shown to exhibit nearly complete conversion to ROMP polymer with the same norbornene substrate within 15 minutes at just 2% catalyst loading, lower than ever observed with catalyst **26**, as well as comparable RCM activity to catalyst **26**. Catalyst **77** also performs ROMP of norbornene substrate at lower concentrations, with

97.2% conversion to polymer observed with just [Ru] = 1.0 mM with 1.0% catalyst loading, which is more similar to reaction conditions applied in organic media and is significantly lower than what has ever been observed with Grubbs' catalyst **26**. This catalyst is by far the most active aqueous ROMP catalysts ever reported to date.

Many applications exist for our catalyst systems that exhibit externally controllable solubility and activity profiles. One application developed in our laboratories has enabled the removal of Ru-metal contamination after RCM reactions by way of external manipulation of catalyst solubility profile via acid addition. Another application currently being explored in collaboration with Dr. Andrea Robinson (Monash University, Austrailia) is the use of these catalysts to graft cyclic oligopeptides containing unnatural amino acids. Other collaborations with BASF have found application for use in the synthesis of stable latexes of COE, DCPD, and mixtures of the two. Other exciting results generated by our collaborators at BASF include gelation studies of these two monomers using our catalysts both in the presence and absence of TsOH. The results of this study imply that acid addition might not just afford an external control of activity and solubility, but may additionally change the catalyst affinity for one substrate over another. However, no further studies have yet been conducted to explore this phenomenon.

CHAPTER VIII

EXPERIMENTALS

General Procedures

All experiments with organometallic compounds were performed under a dry nitrogen atmosphere using standard Schlenck techniques or in an MBraun dry-box (O_2 <2 ppm). NMR spectra were recorded on a Varian Inova instrument (300.1 MHz for ^{1}H, 75.9 MHz for ^{13}C, and 121.4 MHz for ^{31}P). ^{1}H and ^{13}C NMR spectra were referenced to the residual solvent, ^{31}P NMR spectra were referenced using H_3PO_4 (δ = 0 ppm) as external standard. For sonication a Fischer Scientific Ultrasonic Cleaner FS 30 was used. The bath temperature was set to 30 ^{o}C. ICP-MS analyses were conducted by Dr. Alan M. Shiller. X-ray crystallography was conducted by Dr. Edward J. Valente. Absolute Size-Exclusion Chromatography (ASEC) of ROMP polymers was conducted by Dr. Andrew B. Lowe and Dr. Bing Yu. DFT calculations were conducted by Dr. Yong Zhang. Size exclusion chromatographic analysis was performed on a Waters system comprised of a Waters 515 HPLC pump, Waters 2487 Dual λ absorbance detector, and Waters 2410 RI detector equipped with a PolymerLabs PLgel 5μm guard column and a PolymerLabs PLgel 5μm MIXED-C column, in THF stabilized with 281 ppm BHT at a flow rate of 1.0 mL/min. The column was calibrated with a series of narrow molar mass distribution poly(methyl methacrylate) standards. The data was analyzed with Empower Pro 1154.

DFT calculations were conducted using the Gaussian 03 program.[104] All atoms in the model complexes were considered in the calculations. Geometries were optimized by using the hybrid DFT method mPW1PW91[105] together with an effective-core potential basis SDD[106] which were found to give good geometries for late transition metal complexes.[91] To compute the Mulliken charges, a hybrid DFT method B3LYP together with a large basis set was used, namely a full-electron basis DGDZVP for Ru, a 6-

311++G(2d,2p) for first coordination shell atoms, and 6-31G(d) for the rest part of the atoms. The same approach was used to calculate various electronic properties of late transition metal complexes.[91b] In case of the monoprotonated **93b**, structures of protonating the NMe2 group in both sides of the NHC ligands were considered and their Mulliken charges were found to be very similar. The average value was reported.

Materials and Methods

All solvents for manipulations under inert gas (heptane, thf, CH_2Cl_2, tBuOMe, toluene) were dried by passage through solvent purification (MBraun-Auto-SPS). Water was filtered, deionized (DI), and distilled prior to use. All NMR solvents used in combination with catalyst complexes (D_2O, DCl–D_2O, CD_2Cl_2, $CDCl_3$) were degassed prior to use. Other solvents were used as purchased. Reagents were purchased from commercial sources were degassed and stored in the dry-box when directly used in combination with organometallic complexes, and otherwise were used without further purification. 2-*i*-Propoxystyrene,[99] diethyldiallylmalonate (DEDAM) **79**,[100] diallylmalonic acid (DAM) **80**,[101] and 3,3-diallylpentane-2,4-dione (DAP) **81**[102] and monomer **77**[103] were synthesized according to literature procedures. Grubbs' catalyst **1** was purchased from Aldrich, degassed and stored in the dry-box. Phenylindenylidene catalyst precursor **21** was synthesized in accordance with literature procedure.[37b,47] BASF provided Ru=CH-SPh catalyst precursor **24.** Purity of all complexes was determined via ^{1}H NMR spectroscopy.

ICP MS Analyses

The aliquots of RCM product were digested in hot conc. HNO_3 (1 mL). The solid residue was then dissolved in 0.16 M HNO_3 containing 2 ppb In as an internal standard. The final analytical solution contained about 0.67 mg of product per mL acid. [Ru] was determined in this solution using a sector-field ICP-MS (ThermoFinnigan Element 2). Equivalent results were obtained from five different Ru isotopes (masses 99, 100, 101,

102, and 104); likewise, no difference was noted between results obtained in low resolution ($m/\Delta m$ = 300) or medium resolution ($m/\Delta m$ = 4000), suggesting a lack of interferences. Blank samples of the digested starting materials gave Ru contents of <0.1 ppm (DEDAM) and 0.6 ppm (DAP) Ru-content.

*Synthesis of N,N-3,5-Tetramethyl-1,4-phenylenediamine (**34**)*[107]

A solution of $NaNO_2$ (9.922 g, 143.8 mmol) in water (20 mL) was added slowly to a solution of *N*,*N*-3,5-tetramethylaniline **33** (20.032 g, 134.4 mmol) in conc. HCl_{aq} (50 mL) under vigorous stirring *via* a capillary which was immersed in the reaction solution at -5 ^{o}C over a period of 60 min. During the addition, a yellow precipitate (4-nitroso-*N*,*N*-3,5-tetramethylaniline·HCl) was formed. After the addition, the slurry was stirred for another 60 min at 0 ^{o}C and then filtered cold through a Buchner funnel. The yellow residue (4-nitroso-*N*,*N*-3,5-tetramethylaniline·HCl) was washed with ethanol (3 x 50 mL) and suction-dried for 60 min. Then the powdered filter residue was added in small portions to a slurry of powdered tin (7.360 g, 61.8 mmol) in conc. HCl_{aq} (50 mL) at 70^{o}C. While adding the nitrosoaniline the solution turned intensely yellow in color and reverted back to colorless within a few seconds. Once all tin was consumed, the yellow color persisted. The residual nitrosoaniline salt not used in the conversion was stored for a later transformation. It should be noted that this procedure avoids the addition of excess tin. Otherwise an insoluble precipitate is formed during the basic work-up, and this causes a significant reduction of the yield. The resulting slightly yellow solution was slowly added to ice-cold 3 M aqueous NaOH (300 mL). The aqueous phase was extracted with CH_2Cl_2 (3 x 50 mL), and the organic phases were combined and dried over $NaSO_4$. The solvent was removed to give compound **34** (9.770 g, 60.3 mmol, 45%) in over 98% purity (^{1}H NMR) as a golden-colored viscous liquid.

*Synthesis of Glyoxalbis(4-dimethylamino-2,6-dimethylphenyl)imine (**35**)*

Compound **34** (6.373 g, 39.4 mmol) was added to a solution of 40% aqueous glyoxal (3.852 g, 26.6 mmol) in methanol (100 mL) and one drop of conc. HCl_{aq} (approx. 20 mL) and stirred for 24 hrs at room temperature. During the reaction, a deep-yellow colored precipitate was formed. The slurry was filtered, the residue was washed with methanol (3 x 20 mL), dried on the filter, and then dried in the vacuum oven at 60 ^{o}C for 3 h to give compound **35** (5.874 g, 16.8 mmol, 85%) in >99% purity (^{1}H NMR) as a golden-yellow powder. ^{1}H NMR (300.1 MHz, 20 ^{o}C, $CDCl_3$): δ 8.11 (s, 2 H, N=C*H*), 6.50 (s, 4 H, C_6H_2), 2.94 (s, 12 H, $N(CH_3)_2$), 2.24 (C_6H_2–CH_3); ^{13}C NMR (75.9 MHz, 20 ^{o}C, $CDCl_3$): δ 162.5 (N=*C*H), 148.1, 140.6, 128.9, 112.8 (C_6H_2), 40.8 ($N(CH_3)_2$), 19.2 (C_6H_2–CH_3).

*Synthesis of N,N-Bis(4'-dimethylamino-2',6'-dimethylphenyl)ethylene-1,2-diamine (**36**)*

A solution of compound **35** (3.380 g, 9.66 mmol) in thf (100 mL) containing $NaBH_4$ (0.821 g, 21.6 mmol) and boric acid (1.781 g, 28.8 mmol) was stirred at 30 ^{o}C over a period of 60 min. In this time period the solution turned colorless. The solution was cooled to room temperature and water (40 mL) was added carefully and then conc. HCl_{aq} (10 mL) was added dropwise until the solution stopped developing gas. The solution was warmed to 50 ^{o}C under stirring for 10 min and then cooled to room temperature. The thf was removed under reduced pressure and the aqueous solution was neutralized with Na_2CO_3. The aqueous phase was extracted with *t*BuOMe (60 mL), and the organic layer was washed with brine (3 x 40 mL). The organic phase then was dried over Na_2SO_4 and filtered. The solvent was removed under reduced pressure with a rotary evaporator, and the residue was dried in the vacuum oven at 60 ^{o}C for 2 h to give compound **36** (3.000 g, 8.47 mmol, 88%) as a colorless, viscous liquid in >98% purity (^{1}H NMR) which solidified at room temperature over 12 h. ^{1}H NMR (300.1 MHz, 20 ^{o}C, $CDCl_3$): δ 6.51 (s, 4 H, C_6H_2), 3.11 (s, 4 H, NH–CH_2), 2.89 (s, 12 H, $N(CH_3)_2$), 2.34 (s, 12

H, C_6H_2–CH_3); ^{13}C NMR (75.9 MHz, 20 ^{o}C, $CDCl_3$): δ 146.7, 136.7, 131.5, 113.9 (C_6H_2), 49.7 (NH–CH_2), 41.3 (N(CH_3)$_2$), 18.8 (C_6H_2–CH_3).

*Synthesis of 1,3-Bis(2',6'-dimethyl-4'-dimethylaminophenyl)-4,5-dihydroimidazolium chloride, H_2ITap·HCl (**37**)*

A solution of diamine **36** (2.567 g, 7.25 mmol) and ammonium chloride (0.380 g, 7.22 mmol) in triethyl *ortho*-formate (30 mL) was heated under stirring at 130 ^{o}C for 16 h. The excess triethyl *ortho*-formate was distilled under reduced pressure (0.1 Torr) and collected to be reused. Cyclohexane (30 mL) was added to the solid residue and sonicated for 30 min at 30^{o}C. The slurry was filtered, washed with cyclohexane (3 x 20 mL), sucked dry on the filter for 10 min and dried in the vacuum oven at 60^{o}C for 3 h to give ligand precursor **37** (2.499 g, 6.31 mmol, 87%) as a slightly off-white powder in >99% purity (^{1}H NMR). ^{1}H NMR (300.1 MHz, 20 ^{o}C, d_6-DMSO): δ 8.97 (s, 1 H, N–C*H*=N), 6.55 (s,4H, C_6H_2), 4.37 (s, 4H, N–CH_2), 2.92 (s, 12 H, N(CH_3)$_2$), 2.32 (s, 12 H, aryl-CH_3); ^{13}C NMR (75.9 MHz, 20 ^{o}C, d_6-DMSO): δ 160.8 (N-*C*H=N), 150.8, 135.9, 122.2, 111.7 (C_6H_2), 51.3 (N–CH_2), 40.0 (N(CH_3)$_2$), 17.8 (C_6H_2–CH_3).

*Synthesis of 1,3-Bis(2',6'-dimethyl-4'-dimethylaminophenyl)imidazolium chloride, ITap·HCl (**38**)*

Under non-inert conditions, a solution of chlorotrimethylsilane (0.345 g, 3.20 mmol) in ethyl acetate (20 mL) was added to a solution of diimine **35** (1.086 g, 3.09 mmol) in ethyl acetate (50 mL) containing paraformaldehyde (0.139 g, 4.64 mmol) under stirring at 70 °C over a period of 5 h. After the addition, the reaction was kept under stirring at 70 °C for another 16 h. During this time, a slightly reddish-purple precipitate formed. After cooling to room temperature, the slurry was filtered, the residue was washed with ethyl acetate (2 × 10 mL) and dried in the vacuum oven at 60 °C to give ligand precursor **38** (0.998 g, 2.50 mmol, 78 %) as a slightly off white powder in >99 % purity (^{1}H NMR). ^{1}H NMR (300.1 MHz, $CDCl_3$, 20 ^{o}C): δ 10.09 (t, $^3J[^1H^1H]$ = 1.5 Hz, 1H),

7.67 (d, $^{3}J[^{1}H^{1}H]$ = 1.5 Hz, 2H, $C_3H_3N_2$), 6.46 (s, 4H, 2 × C_6H_2), 3.00 (s, 6H, $N(CH_3)_2$), 2.17 (s, 6H, 2 × $C_6H_2(CH_3)_2$); ^{13}C NMR (75.9 MHz, $CDCl_3$, 20 ^{o}C): δ 151.3, 138.9, 121.8, 111.6 (C_6H_2), 134.7, 125.3 ($C_3H_3N_2$), 40.2 ($N(CH_3)_2$), 18.2 ($C_6H_2(CH_3)_2$).

*Synthesis of 4-iodo-2,6-dimethylbenzenamine (**42**)*[108]

Iodine (22.622 g, 89.1 mmol) was added to a solution of compound 2,6-dimethylaniline (10.027 g, 82.7 mmol) and $NaHCO_3$ (8.367 g, 99.5 mmol) in 250 mL CH_2Cl_2–H_2O 1:1 v/v in air with stirring at -5 ^{o}C over a period of 60 min. After the addition was complete, the reaction was stirred for 60 min at room temperature. Sodium thiosulfate (9.000 g, 36.2 mmol) was added and the reaction was stirred an addition 10 min to reduce the residual iodine. The organic phase was separated, washed with H_2O (3 x 100 mL), and the organic phase was separated and dried over $NaSO_4$. The solvent was removed to give compound **42** (19.610 g, 79.3 mmol, 96%) in >98% purity (^{1}H NMR) as a dark-colored solid.

*Synthesis of 4-iodo-2,6-diisopropylbenzenamine (**43**)*[109]

Iodine (22.015 g, 86.7 mmol) was added to a solution of 2,6-diisopropylaniline (14.552 g, 82.1 mmol) and $NaHCO_3$ (8.308 g, 98.9 mmol) in 250 mL CH_2Cl_2 – DI H_2O 1:1 (v/v) in air with stirring at -5 ^{o}C over a period of 60 min. After the addition was complete, the reaction was stirred for 60 min at room temperature. Sodium thiosulfate was added and the reaction was stirred an addition 10 min to reduce the residual iodine. The organic phase was separated, washed with H_2O (3 x 100 mL), and the organic phase was separated and dried over $NaSO_4$. The solvent was removed to give compound **43** (19.610 g, 79.3 mmol, 96%) in >97% purity (^{1}H NMR) as a dark-colored solid.

*Synthesis of 2-iodo-4,6-dimethylbenzenamine (**44**)*[110]

Iodine (17.818 g, 70.2 mmol) was added to a solution of 2,4-dimethylaniline (7.008 g, 57.9 mmol) and $NaHCO_3$ (5.881 g, 70.0 mmol) in 120 mL CH_2Cl_2 - DI H_2O 1:1 (v/v) in air with stirring at -5 ^{o}C over a period of 60 min. After the addition was complete,

the reaction was stirred for 60 min at room temperature. Sodium thiosulfate was added and the reaction was stirred an addition 10 min to reduce the residual iodine. The organic phase was separated, washed with H_2O (3 x 100 mL), and the organic phase was separated and dried over $NaSO_4$. The solvent was removed to give compound **44** (17.070 g, 69.1 mmol, 94%) in >96% purity (^{1}H NMR) as a dark-colored solid.

*Synthesis of Glyoxalbis(4-iodo-2,6-dimethylphenyl)imine (**45**)*

Aniline **42** (9.800 g, 32.9 mmol) was added to a solution of 40% aqueous glyoxal (3.982 g, 27.5 mmol) in methanol (100 mL) and one drop of conc. HCl_{aq} and stirred for 24 hrs at room temperature. During the reaction, a deep-yellow colored precipitate was formed. The slurry was filtered, the residue was washed with methanol (3 x 20 mL), sucked dry and the dried in the vacuum oven at 60 ^{o}C for 3 h to give compound **45** (5.562 g, 10.8 mmol, 54%) in >98% purity (^{1}H NMR) as a yellow powder. ^{1}H NMR (300.1 MHz, 20 ^{o}C, $CDCl_3$): δ 8.06 (s, 2H, N=C*H*), 7.44 (s, 4H, C_6H_2), 1.57 (s, 12H, C_6H_2–CH_3); ^{13}C NMR (75.9MHz, 20 ^{o}C, $CDCl_3$): δ 163.4 (N=*C*H), 149.7, 137.2, 129.1, 89.3 (C_6H_2), 18.1 (CH_3).

*Synthesis of Glyoxalbis(4-iodo-2,6-diisopropylphenyl)imine (**46**)*

Aniline **43** (4.323 g, 14.2 mmol) was added to a solution of 40% aqueous glyoxal (2.059 g, 14.3 mmol) in methanol (50 mL) and one drop of conc. HCl_{aq} and stirred for 24 hrs at room temperature. During the reaction, a deep-yellow colored precipitate was formed. The slurry was filtered, the residue was washed with methanol (3 x 20 mL), sucked dry and the dried in the vacuum oven at 60^{o}C for 3 h to give compound **46** (5.432 g, 5.61 mmol, 79%) in >98% purity (^{1}H NMR) as a golden-yellow powder. ^{1}H NMR (300.1 MHz, 20 ^{o}C, $CDCl_3$): δ 8.03 (s, 2H, N=C*H*), 7.44 (s, 4H, C_6H_2), 2.84 (m, 4H, iPr-C*H*), 1.18 (d, $^3J[^1H^1H]$ = 6.9 Hz, 24H, iPr–CH_3); ^{13}C NMR (75.9MHz, 20 ^{o}C, $CDCl_3$): δ 160.4 (N=*C*), 147.8, 139.5, 132.7, 90.5 (C_6H_2), 28.5 (iPr–*C*H), 23.4 (iPr-*C*H_3).

*Synthesis of Glyoxalbis(2-iodo-4,6-dimethylphenyl)imine (**47**)*

Aniline **44** (12.454 g, 41.9 mmol) was added to a solution of 40% aqueous glyoxal (6.096 g, 42.1 mmol) in methanol (100 mL) and one drop of conc. HCl_{aq} and stirred for 24 hrs at room temperature. During the reaction, a deep-yellow colored precipitate was formed. The slurry was filtered, the residue was washed with methanol (3 x 20 mL), sucked dry and the dried in the vacuum oven at 60 ^{o}C for 3 h to give compound **47** (5.562 g, 10.8 mmol, 54%) in >96% purity (^{1}H NMR) as a yellow powder. ^{1}H NMR (300.1 MHz, 20 ^{o}C, $CDCl_3$): δ 8.14 (s, 2H, N=C*H*), 7.57 (s, 2H, C_6H_2), 7.03 (s, 2H, C_6H_2), 2.29 (s, 6H, C_6H_2–CH_3), 2.21 (s, 6H, C_6H_2–CH_3); ^{13}C NMR (75.9MHz, 20 ^{o}C, $CDCl_3$): δ 165.3 (N=*C*), 156.7, 138.3, 137.9, 130.4, 133.2, 84.6 (C_6H_2), 24.1 (CH_3), 15.3 (CH_3).

*Synthesis of N,N'-Bis(4'-iodo-2',6'-dimethylphenyl)amino-1,2-ethane (**48**)*

A solution of compound **45** (4.822 g, 9.31 mmol) in thf (100 mL) containing $NaBH_4$ (0.932 g, 24.6 mmol) and boric acid (1.568 g, 25.3 mmol) was stirred at 30 ^{o}C over a period of 90 min. In this time period the solution turned colorless. The solution was cooled to room temperature and water (40 mL) was added carefully and then conc. HCl_{aq} (16 mL) was added dropwise until the solution stopped developing gas. The solution was warmed to 50 ^{o}C under stirring for 10 min and then cooled to room temperature. The thf was removed under reduced pressure and the aqueous solution was neutralized with Na_2CO_3. The aqueous phase was extracted with *t*BuOMe (60 mL), and the organic layer was washed with brine (3 x 50 mL). The organic phase then was dried over Na_2SO_4 and filtered. The solvent was removed under reduced pressure with a rotary evaporator, and the residue was dried in the vacuum oven at 60 ^{o}C for 2 h to give compound **48** (4.500 g, 8.71 mmol, 94%) as an off-white solid in >98% purity. ^{1}H NMR (300.1 MHz, 20 ^{o}C, $CDCl_3$): δ 7.33 (s, 4H, C_6H_2), 3.31 (br, 2H, N*H*) 3.17 (s, 4H, NH–CH_2), 2.25 (s, 12H, C_6H_2–CH_3); ^{13}C NMR (75.9MHz, 20 ^{o}C, $CDCl_3$): δ 145.9, 137.6, 132.1, 85.4 (C_6H_2), 48.8 (NH-CH_2), 18.6 (CH_3).

*Synthesis of N,N'-Bis(4'-iodo-2',6'-diisopropylphenyl)amino-1,2-ethane (**49**)*

A solution of compound **46** (5.003 g, 8.02 mmol) in thf (100 mL) containing $NaBH_4$ (1.587 g, 15.9 mmol) and boric acid (1.3300 g, 21.1 mmol) was stirred at 30 ^oC over a period of 90 min. In this time period the solution turned colorless. The solution was cooled to room temperature and water (40 mL) was added carefully and then conc. HCl_{aq} (17 mL) was added dropwise until the solution stopped developing gas. The solution was warmed to 50 ^oC under stirring for 10 min and then cooled to room temperature. The thf was removed under reduced pressure and the aqueous solution was neutralized with Na_2CO_3. The aqueous phase was extracted with *t*BuOMe (60 mL), and the organic layer was washed with brine (3 x 50 mL). The organic phase then was dried over Na_2SO_4 and filtered. The solvent was removed under reduced pressure with a rotary evaporator, and the residue was dried in the vacuum oven at 60 ^oC for 2 h to give compound **49** (4.661 g, 7.41 mmol, 93%) as an opaque solid in >98% purity (^1H NMR). ^1H NMR (300.1 MHz, 20 ^oC, $CDCl_3$): δ 7.39 (s, 4H, C_6H_2), 3.26 (br., 2H, N*H*), 3.20 (m, 4H, iPr-C*H*), 3.10 (s, 4H, NH–CH_2), 1.22 (d, $^3J[^1H^1H]$ = 7.2 Hz, 24H, iPr-CH_3); ^{13}C NMR (75.9MHz, 20 ^oC, $CDCl_3$): δ 145.3, 143.3, 133.1, 88.9 (C_6H_2), 52.2 (NH-CH_2), 28.0 (iPr–*C*H), 24.3 (iPr-CH_3).

*Synthesis of N,N'-Bis(2'-iodo-4',6'-dimethylphenyl)amino-1,2-ethane (**50**)*

A solution of compound **47** (5.174 g, 10.0 mmol) in thf (100 mL) containing $NaBH_4$ (2.0670 g, 54.7 mmol) and boric acid (1.695 g, 27.4 mmol) was stirred at 30 ^oC over a period of 90 min. In this time period the solution turned colorless. The solution was cooled to room temperature and water (40 mL) was added carefully and then conc. HCl_{aq} (16 mL) was added dropwise until the solution stopped developing gas. The solution was warmed to 50 ^oC under stirring for 10 min and then cooled to room temperature. The thf was removed under reduced pressure and the aqueous solution was neutralized with Na_2CO_3. The aqueous phase was extracted with *t*BuOMe (60 mL),

and the organic layer was washed with brine (3 x 50 mL). The organic phase then was dried over Na_2SO_4 and filtered. The solvent was removed under reduced pressure with a rotary evaporator, and the residue was dried in the vacuum oven at 60^{o}C for overnight to give compound **50** (3.928 g, 7.51 mmol, 75%) as an off-white solid in >98% purity (^{1}H NMR). ^{1}H NMR (300.1 MHz, 20 ^{o}C, $CDCl_3$): δ 7.43 (s, 2H, C_6H_2), 6.91 (s, 2H, C_6H_2), 3.49 (br, 2H, N*H*) 3.15 (s, 4H, NH–CH_2), 2.34 (s, 6H, C_6H_2–CH_3), 2.20 (s, 6H, C_6H_2–CH_3); ^{13}C NMR (75.9MHz, 20 ^{o}C, $CDCl_3$): δ 151.6, 137.6, 130.8, 128.4, 126.6, 81.2 (C_6H_2), 49.1 (NH-CH_2), 23.9 (CH_3), 15.0 (CH_3).

*Synthesis of N,N'-Bis(4'-[2''-dimethylaminoethoxy]-2',6'-dimethylphenyl)amino-1,2-ethane (**51**)*

Diamine **48** (2.105 g, 4.00 mmol) was added to a solution of KO*t*Bu (1.820 g, 16.2 mmol) in N,N-Dimethylethanolamine (30 mL) and stirred under inert gas conditions at 60 ^{o}C for 60 min. After 60 min, CuCl (1.01, 10.2 mmol) was added under N_2 gas. Then vacuum was applied and the reaction was stirred at 130 ^{o}C overnight. *t*BuOMe (100 mL) and aqueous ammonia (1.5M, 100 mL) was added and the solution was stirred in air at room temperature for 60 min. The yellow-colored organic phase was separated, washed with brine (6 x 100 mL), then dried over Na_2SO_4 and filtered. The solvent was removed from the filtrate under reduced pressure with a rotary evaporator, and the residue was dried in the vacuum oven at 60 ^{o}C for 3 h to give compound **51** (1.438 g, 3.23 mmol, 80%) as a dark-colored solid in >98% purity (^{1}H NMR). ^{1}H NMR (300.1 MHz, 20 ^{o}C, $CDCl_3$): δ 6.61 (s, 4H, C_6H_2), 4.01 (t, $^3J[^1H^1H]$ = 5.7 Hz, 4H, O-CH_2), 3.49 (br, 2H, N-*H*), 3.08 (s, 4H, NH-CH_2), 2.70 (t, $^3J[^1H^1H]$ = 5.7 Hz, 4H, CH_2-NMe_2), 2.32 (s, 12H, C_6H_2-CH_3), 2.29 (s, 12H, N(CH_3)$_2$); ^{13}C NMR (75.9MHz, 20 ^{o}C, $CDCl_3$): δ 146.3, 137.8, 127.6, 112.2 (C_6H_2), 65.3 (O-CH_2), 59.6 (CH_2-NMe2), 52.6 (NH-CH_2), 46.2 (N(CH_3)$_2$), 16.2 (CH_3).

*Synthesis of N,N'-Bis(4'-[2''-dimethylaminoethanethio]-2',6'-dimethylphenyl)amino-1,2-ethane (**52**)*

Diamine **48** (2.005 g, 3.90 mmol) was added to a solution of 2-(Dimethylamino) ethanethiol hydrochloride (1.643 g, 12.0 mmol) and KO*t*Bu (3.479 g, 31.0 mmol) in 1-methyl-2-pyrrolidinone (60 mL) and stirred under inert gas conditions at 60 ^{o}C for 60 min. After 60 min, CuCl (1.187 g, 12.0 mmol) was added under inert gas atmosphere. Vacuum was applied for 10 sec and the flask was sealed off. The reaction was stirred under vacuum at 110 ^{o}C for 16 h. *t*BuOMe (100 mL), aqueous ammonia (100 mL) and 0.1 M NaOH (4 mL) was added and the solution was stirred in air at room temperature for 2 hrs. The organic phase was separated, washed with 0.1 M NaOH (3 x 80 mL) and brine (5 x 80 mL), and then dried over Na_2SO_4. The solvent was removed under reduced pressure with a rotary evaporator, and the residue was dried in the vacuum oven at 60 ^{o}C for overnight to give compound **52** (1.409 g, 3.01 mmol, 77%) as a light yellow powder with >96% purity (^{1}H NMR) . ^{1}H NMR (300.1 MHz, 20 ^{o}C, $CDCl_3$): δ 8.80 (s, 4H, C_6H_2), 3.39 (br, 2H, N-*H*), 3.18 (s, 4H, NH-CH_2), 2.96 (t, $^{3}J[^{1}H^{1}H]$ = 8.1 Hz, 4H, S-CH_2), 2.52 (t, $^{3}J[^{1}H^{1}H]$ = 8.1 Hz, 4H, CH_2-NMe_2), 2.30 (s, 12H, N(CH_3)$_2$), 2.26 (s, 12H, C_6H_2-CH_3); ^{13}C NMR (75.9MHz, 20 ^{o}C, $CDCl_3$): δ 145.1, 131.5, 130.4, 127.9 (C_6H_2), 59.1 (CH_2-NMe2), 48.9 (S-CH_2), 45.6 (NH-CH_2), 33.1 (N(CH_3)$_2$), 18.8 (CH_3).

*Synthesis of N,N'-Bis(4'-[2''-dimethylaminoethoxy]-2',6'-diisopropylphenyl)amino-1,2-ethane (**53**)*

Diamine **49** (4.007 g, 6.32 mmol) was added to a solution of KO*t*Bu (1.493 g, 13.3 mmol) in N,N-dimethylethanolamine (25 mL) and stirred under inert gas conditions at 60 ^{o}C for 60 min. After 60 min, CuCl (1.318, 13.3 mmol) was added under N_2 gas. Then vacuum was applied and the reaction was stirred at 120 ^{o}C for 16 h. *t*BuOMe (100 mL) and aqueous ammonia (1.5M, 100 mL) was added and the solution was stirred in air at room temperature for 60 min. The organic phase was separated, washed with brine (8

x 100 mL), then dried over Na_2SO_4 and filtered. The solvent was removed from the filtrate under reduced pressure and the filtrate residue was dried in the vacuum oven at 60^{o}C for 3 h to give compound **53** (2.792 g, 5.04 mmol, 79%) as a viscous brown liquid in >95% purity (^{1}H NMR). ^{1}H NMR (300.1 MHz, 20 ^{o}C, $CDCl_3$): δ 6.70 (s, 4H, C_6H_2), 4.06 (t, $^3J[^1H^1H]$ = 6.0 Hz, 4H, O-CH_2), 3.37 (sept, $^3J[^1H^1H]$ = 6.9 Hz, 4H, iPr-C*H*), 3.06 (s, 4H, NH-CH_2), 2.73 (t, $^3J[^1H^1H]$ = 6.0 Hz, 4H, NMe_2-CH_2), 2.35 (s, 12H, N(CH_3)$_2$), 1.67 (br, 2H, N-*H*), 1.24 (d, $^3J[^1H^1H]$ = 6.0 Hz, 24H, iPr-CH_3); ^{13}C NMR (75.9MHz, 20 ^{o}C, $CDCl_3$): δ 155.7, 144.7, 136.7, 109.8 (C_6H_2), 65.9 (O-CH_2), 58.7 (N-CH_2), 52.8 (NH-CH_2), 46.2 (N(CH_3)$_2$), 28.2 (iPr–*C*H), 24.5 (iPr-CH_3).

*Synthesis of N,N'-Bis(4'-[2''-dimethylaminoethanethio]-2',6'-diisopropylphenyl)amino-1,2-ethane (**54**)*

Diamine **49** (3.041 g, 4.82 mmol) was added to a solution of 2-(Dimethylamino)ethanethiol hydrochloride (14.921 g, 14.8 mmol) and KO*t*Bu (3.358 g, 29.9 mmol) in 1-methyl-2-pyrrolidinone (80 mL) and stirred under inert gas conditions at 60 ^{o}C for 60 min. After 60 min, CuCl (1.500, 15.2 mmol) was added under inert gas atmosphere. The reaction was stirred under vacuum at 110 ^{o}C 16 h. *t*BuOMe (100 mL), aqueous ammonia (1.5M, 100 mL) and 0.1 M NaOH (4 mL) was added and the solution was stirred in air at room temperature for 2 hrs. The organic phase was separated, washed with 0.1 M NaOH (3 x 80 mL) and brine (4 x 80 mL), and then dried over Na_2SO_4. The solvent was removed under reduced pressure with a rotary evaporator, and the residue was dried in the vacuum oven at 60 ^{o}C for 3 h to give compound **54** (2.091 g, 3.63 mmol, 74%) as a dark-colored oil which slowly solidified at room temperature to give the desired compound with >98% purity (^{1}H NMR). ^{1}H NMR (300.1 MHz, 20 ^{o}C, $CDCl_3$): δ 7.13 (s, 4H, C_6H_2), 3.31 (sept, $^3J[^1H^1H]$ = 7.2 Hz, 4H, iPr-C*H*), 3.21 (s, 2H, N-*H*), 3.14 (s, 4H, NH-CH_2), 3.02 (t, $^3J[^1H^1H]$ = 6.9 Hz, 4H, S-CH_2), 2.57 (t, $^3J[^1H^1H]$ = 6.9 Hz, 4H, CH_2-NMe_2) 2.24 (s, 12H, N(CH_3)$_2$), 1.24 (d, $^3J[^1H^1H]$ = 6.6 Hz,

24H, iPr-C*H*$_3$); ^{13}C NMR (75.9MHz, 20 ^{o}C, $CDCl_3$): δ 143.6, 135.4, 126.2, 114.3 (C_6H_2), 59.4 (N-*C*H$_2$), 55.6 (NH-*C*H$_2$), 46.1 (N(*C*H$_3$)$_2$), 31.6 (S-*C*H$_2$), 28.9 (iPr–*C*H), 24.2 (iPr-*C*H$_3$).

*Synthesis of Ligand Precursor Salt **55** (IXyONMe$_2$·HCl)*

Diamine **51** (1.200 g, 2.70 mmol) and ammonium chloride (0.183 g, 3.42 mmol) was heated in a mixture of triethyl *ortho*-formate (13 mL) and ethanol (5 mL) under reflux at 110 ^{o}C for 16 h. Then the solvent was distilled off under reduced pressure (0.1 Torr), and the unreacted triethyl-*ortho*-formate was collected to be reused. CH_2Cl_2 (5 mL) was added to dissolve the solid residue. Ethyl acetate (30 mL) was added, and the CH_2Cl_2 was removed under reduced pressure. The resulting slurry was sonicated for 30 min at 30 ^{o}C then filtered, washed with ethyl acetate (3 x 20 mL), sucked dry on the filter for 10 min and dried in the vacuum oven at 60 ^{o}C for 3 h to give NHC ligand precursor **55** (1.000 g, 2.04 mmol, 75%) as a white solid with >98 % purity (^{1}H NMR). ^{1}H NMR (300.1 MHz, 20 ^{o}C, $CDCl_3$): δ 9.18 (s, 1H, N–C*H*=N), 6.68 (s, 4H, C_6H_2), 4.58 (s, 4H, N-C*H*$_2$), 4.04 (t, $^3J[^1H^1H]$ = 5.7 Hz, 4H, O–C*H*$_2$), 2.72 (t, $^3J[^1H^1H]$ = 5.7 Hz, 4H, NMe$_2$-C*H*$_2$), 2.41 (s, 12H, C_6H_2-C*H*$_3$), 2.33 (s, 4H, N(C*H*$_3$)$_2$); ^{13}C NMR (75.9MHz, 20 ^{o}C, $CDCl_3$): δ 160.4 (N-*C*H=N), 159.7, 137.0, 125.8, 115.2 (C_6H_2), 66.2 (O-*C*H$_2$), 58.4 (*C*H$_2$-NMe$_2$), 52.3 (=N-*C*H$_2$), 46.1 (N(*C*H$_3$)$_2$), 18.5 (C_6H_2-*C*H$_3$).

*Synthesis of Ligand Precursor Salt **56** (IXySNMe$_2$·HCl)*

Diamine **52** (1.297 g, 2.73 mmol) and triethyl ammonium chloride (0.571 g, 4.16 mmol) was heated in a mixture of triethyl *ortho*-formate (13 mL) and ethanol (5 mL) under reflux at 100 ^{o}C for 16 h. Then the solvent was distilled off under reduced pressure (0.1 Torr), and the unreacted triethyl-*ortho*-formate was collected to be reused. CH_2Cl_2 (5 mL) was added to dissolve the solid residue. Ethyl acetate (30 mL) was added, and the CH_2Cl_2 was removed under reduced pressure. The resulting slurry was sonicated for 30 min at 30 ^{o}C then filtered, washed with ethyl acetate (3 x 20 mL), sucked dry on

the filter for 10 min and dried in the vacuum oven at 60 ^{o}C for 3 h to give NHC ligand precursor **56** (1.025 g, 1.97 mmol, 72%) as a white solid with >95 % purity (^{1}H NMR). ^{1}H NMR (300.1 MHz, 20 ^{o}C, $CDCl_3$): δ 10.21 (s, 1H, N–C*H*=N), 7.19 (s, 4H, C_6H_2), 4.50 (s, 4H, N-CH_2), 3.23 (t, $^{3}J[^{1}H^{1}H]$ = 7.8 Hz, 4H, S–CH_2), 2.91 (t, $^{3}J[^{1}H^{1}H]$ = 6.0 Hz, 4H, NMe_2-CH_2), 2.59 (s, 12H, C_6H_2-CH_3), 2.43 (s, 4H, N(CH_3)$_2$); ^{13}C NMR (75.9MHz, 20 ^{o}C, $CDCl_3$): δ 160.7 (N-*C*H=N), 140.3, 136.2, 130.3, 128.3 (C_6H_2), 58.1 (S-*C*H_2), 52.0 (*C*H_2-NMe_2), 45.3 (=N-*C*H_2), 30.6 (N(*C*H_3)$_2$), 18.5 (C_6H_2-*C*H_3).

*Synthesis of Ligand Precursor Salt **57** (IDippONMe$_2$·HCl)*

Diamine **53** (2.604, 4.70 mmol) and ammonium chloride (0.306 g, 5.72 mmol) was heated in a mixture of triethyl *ortho*-formate (13 mL) and ethanol (5 mL) was heated under reflux at 110 ^{o}C for 16 h. Then the solvent was distilled off under reduced pressure (0.1 Torr), and the unreacted triethyl-*ortho*-formate was collected to be reused. CH_2Cl_2 (5 mL) was added to dissolve the solid residue. Ethyl acetate (30 mL) was added, and the CH_2Cl_2 was removed under reduced pressure. The slurry was sonicated for 30 min at 30 ^{o}C then filtered, washed with ethyl acetate (3 x 20 mL), sucked dry on the filter for 10 min and dried in the vacuum oven at 60 ^{o}C for 3 h to give ligand precursor **57** (0.952 g, 1.51 mmol, 31%) as a white powder with >98 % purity (^{1}H NMR). ^{1}H NMR (300.1 MHz, 20 ^{o}C, $CDCl_3$): δ 8.09 (s, 1H, N–C*H*=N), 6.78 (s, 4H, C_6H_2), 4.80 (t, $^{3}J[^{1}H^{1}H]$ = 11.4 Hz, 4H, N-CH_2) 4.08 (t, $^{3}J[^{1}H^{1}H]$ = 5.7 Hz, 4H, O–CH_2), 3.00 (sept, $^{3}J[^{1}H^{1}H]$ = 10.4 Hz, 4H, iPr-C*H*), 2.75 (t, $^{3}J[^{1}H^{1}H]$ = 5.7 Hz, 4H, NMe_2-CH_2), 2.36 (s, 12H, N(CH_3)$_2$), 1.22 (d, $^{3}J[^{1}H^{1}H]$ = 6.6 Hz, 12H, iPr-CH_3), 1.37 (d, $^{3}J[^{1}H^{1}H]$ = 6.9 Hz, 12H, iPr-CH_3); ^{13}C NMR (75.9MHz, 20 ^{o}C, $CDCl_3$): δ 161.0 (N-*C*H=N), 158.9, 147.9, 122.2, 111.0 (C_6H_2), 66.1 (O-*C*H_2), 58.4 (N-*C*H_2), 55.7 (=N-*C*H_2), 46.1 (N(*C*H_3)$_2$), 29.6 (iPr-*C*H), 25.6, 23.9 (i-Pr-*C*H_3).

*Synthesis of Ligand Precursor Salt **58** (IDippSNMe$_2$·HCl)*

Diamine **54** (2.091, 3.61 mmol) and ammonium chloride (0.235 g, 4.40 mmol) in a mixture of triethyl *ortho*-formate (13 mL) and ethanol (5 mL) was heated under reflux at

110 ^{o}C for 16 h. Then the solvent was distilled off under reduced pressure (0.1 Torr), and the unreacted triethyl-*ortho*-formate was collected to be reused. CH_2Cl_2 (5 mL) was added to dissolve the solid residue. Ethyl acetate (30 mL) was added, and the CH_2Cl_2 was removed under reduced pressure. The slurry was sonicated for 30 min at 30 ^{o}C then filtered, washed with ethyl acetate (3 x 20 mL), sucked dry on the filter for 10 min and dried in the vacuum oven at 60 ^{o}C for 3 h to give ligand precursor **58** (1.112 g, 1.91 mmol, 52%) as a white powder with >97 % purity (^{1}H NMR). ^{1}H NMR (300.1 MHz, 20 ^{o}C, $CDCl_3$): δ 8.96 (s, 1H, N–C*H*=N), 7.09 (s, 4H, C_6H_2), 4.64 (s, 4H, N-CH_2), 3.04 (t, $^{3}J[^{1}H^{1}H]$ = 6.6 Hz, 4H, S–CH_2), 2.89 (sept, $^{3}J[^{1}H^{1}H]$ = 6.9 Hz, 4H, C$H(CH_3)_2$), 2.59 (t, $^{3}J[^{1}H^{1}H]$ = 6.6 Hz, 4H, Me_2N-CH_2), 2.26 (s, 12H, N(C$H_3)_2$), 1.30 (d, $^{3}J[^{1}H^{1}H]$ = 6.9 Hz, 12H), 1.19 (d, $^{3}J[^{1}H^{1}H]$ = 6.9 Hz, 12H, CH(C$H_3)_2$); ^{13}C NMR (75.9MHz, 20 ^{o}C, $CDCl_3$): δ 159.2 (N-*C*H=N), 146.3, 141.2, 126.6, 123.6 (C_6H_2), 58.0 (=N-*C*H_2), 55.0 (Me_2N-*C*H_2), 45.3 (N($CH_3)_2$), 30.6 (S-*C*H_2), 29.1 (*C*H$(CH_3)_2$), 25.2, 23.4 (CH(*C*$H_3)_2$).

*Synthesis of N,N'-Bis(2'-[2''-dimethylaminoethoxy]-4',6'-dimethylphenyl)amino-1,2-ethane (**59**)*

Diamine **50** (1.650 g, 3.23 mmol) was added to a solution of KO*t*Bu (1.067 g, 9.51 mmol) in N,N-dimethylethanolamine (25 mL) and stirred under inert gas conditions at 60 ^{o}C for 60 min. After 60 min, CuCl (0.944, 9.52 mmol) was added under inert gas atmosphere. Then vacuum was applied and the reaction was stirred at 120 ^{o}C for 16 h. *t*BuOMe (100 mL) and aqueous ammonia (1.5M, 100 mL) was added and the solution was stirred in air at room temperature for 60 min. The organic phase was separated, washed with brine (8 x 100 mL), then dried over Na_2SO_4 and filtered. The solvent was removed under reduced from the filtrate pressure and the residue was dried in the vacuum oven at 60^{o}C for 3 h to give compound **59** (0.854 g, 1.79 mmol, 56%) as a viscous brown liquid in >93% purity. ^{1}H NMR (300.1 MHz, 20 ^{o}C, $CDCl_3$): δ 7.10 (s, 2H, C_6H_2), 6.86 (s, 2H, C_6H_2), 4.42 (br, 2H, N-*H*), 3.19 (s, 4H, NH-CH_2), 2.87 (t, $^{3}J[^{1}H^{1}H]$ =

7.8 Hz, 4H, O-CH_2), 2.48 (t, $^3J[^1H^1H]$ = 6.6 Hz, 4H, CH_2-NMe_2), 2.30 (s, 6H, C_6H_2-CH_3), 2.30 (s, 6H, C_6H_2-CH_3), 2.27 (s, 6H, C_6H_2-CH_3), 2.23 (s, 12H, N(CH_3)$_2$). ^{13}C NMR data was not determined for this compound.

*Synthesis of N,N'-Bis(2'-[2''-dimethylaminoethanethio]-4',6'-dimethylphenyl) amino-1,2-ethane (**60**)*

Diamine **50** (1.529 g, 2.92 mmol) was added to a solution of 2-(Dimethylamino)ethanethiol hydrochloride (1.275 g, 9.00 mmol) and KO*t*Bu (2.603 g, 23.2 mmol) in 1-methyl-2-pyrrolidinone (35 mL) and stirred under inert gas conditions at 60 ^{o}C for 60 min. After 60 min, CuCl (0.891 g, 9.04 mmol) was added under inert gas atmosphere. Vacuum was applied for 10 sec and the flask was sealed. The reaction was stirred under vacuum at 110 ^{o}C 16 h. *t*BuOMe (60 mL), aqueous ammonia (1.5M, 60 mL) and 0.1 M NaOH (3 mL) was added and the solution was stirred in air at room temperature for 2 hrs. The organic phase was separated, washed with 0.1 M NaOH (4x 60 mL) and brine (3 x 60 mL), and then dried over Na_2SO_4. The Na_2SO_4 was removed via filtration. The solvent was removed from the filtrate under reduced pressure with a rotary evaporator, and the residue was dried in the vacuum oven at 60 ^{o}C for 16 h to give compound **60** (0.902 g, 1.90 mmol, 66%) as a viscous brown liquid in >90% purity (^{1}H NMR). ^{1}H NMR (300.1 MHz, 20 ^{o}C, $CDCl_3$): δ 6.60 (s, 2H, C_6H_2), 6.41 (s, 2H, C_6H_2), 4.46 (br, 2H, N-*H*), 3.31 (s, 4H, NH-CH_2), 2.91 (m, 4H, O-CH_2), 2.68 (m, 4H, CH_2-NMe_2), 2.38 (s, 6H, C_6H_2-CH_3), 2.34 (s, 6H, C_6H_2-CH_3), 2.21 (s, 6H, C_6H_2-CH_3), 2.23 (s, 12H, N(CH_3)$_2$). ^{13}C NMR data was not determined for this compound.

*Synthesis of (H_2ITap)(PCy_3)Cl_2Ru=CH-Ph (**61**)*

Ligand precursor **37** (0.637 g, 1.61 mmol) and KO*t*Bu (0.178 g, 1.60 mmol) were heated under stirring to 60 ^{o}C in n-heptane for 60 min under inert gas conditions. After cooling to room temperature, Grubbs' first generation catalyst **9** (1.003 g, 1.22 mmol) was added and the slurry was heated to 65 ^{o}C for 24 h also under inert gas conditions.

In this time period an orange-brownish precipitate was formed. The solution then was cooled to room temperature, the solvent was removed under reduced pressure and methanol was added under non-inert conditions. The resulting slurry was sonicated for 30 min in air and then filtered. The filter residue was washed with water (10 mL) and methanol (3 x 10 mL). The resulting light brown powder was dried in the vacuum oven at 60^{o}C for 60 min to give catalyst **61** (0.794 g, 0.86 mmol, 70%) in >98% purity (^{1}H and ^{31}P NMR spectroscopy). ^{1}H NMR (300.1 MHz, 20 ^{o}C, CD_2Cl_2): δ 19.02 (s, 1 H, Ru=C*H*), 8.95 (br, 2 H), 7.07 (br, 3 H,C_6H_5), 6.49 (s, 4 H,C_6H_2), 3.91 (br, 4H,N–CH_2), 2.96 (s, 12H,N(CH_3)$_2$), 2.72 (s, 12H,C_6H_2–CH_3), 2.42–2.60 (br m, 3H), 2.12–2.37 (br m, 3 H), 1.92–2.05 (br m, 3 H), 1.29–1.55 (br m,12 H), 0.92–1.12 (br m, 12 H, PCy_3); ^{13}C NMR (75.9MHz, 20 ^{o}C, CD_2Cl_2): δ 294.1 (br, Ru=*C*), 221.4 (d, $^{2}J[^{31}P^{13}C]$ = 80.1 Hz, NHC*C*),164.4, 129.7, 128.0, 127.5 (s, =CH–C_6H_5), 152.1, 150.5, 150.1, 140.0 (br), 137.6 (br), 128.3, 112.3, 111.7 (s, NHC-Ph-*C*H), 53.1 (d, $^{4}J[^{31}P^{13}C]$ = 3.3 Hz), 52.1 (s, N–CH_2), 40.5, 40.4 (s, N(*C*H_3)$_2$), 20.9 (s), 19.3 (br, C_6H_2), 31.7 (d, $^{1}J[^{31}P^{13}C]$ = 16.5 Hz), 29.6 (br), 28.3 (d, $^{3}J[^{31}P^{13}C]$ = 10.2 Hz), 26.8 (s, PCy_3-*C*); ^{31}P NMR (121.4 MHz, 20 ^{o}C, CD_2Cl_2): δ 30.2 (s).

*Synthesis of (H_2ITap)Cl_2Ru=CH-(C_6H_4-O-iPr) (**62**)*

Catalyst **61** (0.303 g, 0.33 mmol) in CH_2Cl_2 (15 mL) was stirred at room temperature under inert gas conditions with CuCl (0.036 g, 0.40 mmol) and 2-*i*-propoxystyrene (0.054 g, 0.33 mmol) for 2 h. The solution turned from brown to green in this time period. Then the solvent was removed under reduced pressure and the residue was taken up in 10 mL of a mixture of CH_2Cl_2–heptane 1:1 v/v in air. The solution was filtered, and then was loaded onto a flash column with silica gel. The column was washed with a mixture of CH_2Cl_2–ethanol 95:5 v/v until all green color was removed from the stationary phase. The solvent was removed under reduced pressure and the residue was taken up in CH_2Cl_2 (10mL). Heptane (30 mL) was added and the residual CH_2Cl_2

was removed under reduced pressure. The product precipitated and the slurry was filtered. The filter residue was washed with n-heptane (3 x 10 mL), sucked dry for 5 min and dried in the vacuum oven at 60°C for 60 min to give catalyst **62** (0.162 g, 0.23 mmol, 70%) as a green powder in >98% purity (^{1}H NMR). ^{1}H NMR (300.1 MHz, 20 °C, $CDCl_3$): *δ* 16.80 (s, 1 H, Ru=C*H*), 7.47(m, 1H), 7.01 (m, 1H), 6.85(m, 1H), 6.78 (m, 1H, C_6H_4), 6.58 (s, 4 H, NHC-C_6H_2), 4.15 (s, 4 H,N–CH_2), 3.00 (s, 12 H, N(CH_3)$_2$), 2.44 (br, 12 H, C_6H_2–CH_3), 4.89 (sept., $^3J[^1H^1H]$ = 6.0 Hz, 1H, C*H*(CH$_3$)$_2$), 1.28 (d, $^3J[^1H^1H]$ = 6.0 Hz, 6 H, CH(CH_3)$_2$); ^{13}C NMR (75.9 MHz, 20 °C, $CDCl_3$): *δ* 299.0 (Ru=*C*), 211.7 (N=*C*–N), 161.0, 150.8, 122.8, 122.2, 112.9, 112.2 (s, =CH–C_6H_4), 152.2, 145.5, 129.3, 112.2 (s, C_6H_2), 74.8 (*C*H(CH$_3$)$_2$), 26.9 (CH(*C*H$_3$)$_2$), 40.8 (s, N(*C*H$_3$)$_2$), 21.1 (C_6H_2–*C*H$_3$).

*Crystal Structure Determination of Catalysts **61** and **62***

Deep brown crystals of **61** are triclinic, *a* = 9.6949(5) Å, *b* = 13.969(2) Å, *c* = 17.5080(7) Å, α = 99.287(7)°, β = 99.451(4)°, γ = 90.001(7)°, volume = 2307.4(4)Å^3, two molecules per cell in space group P-1 (#2); very small green crystals of **62** are monoclinic, *a* = 19.6502(11) Å, *b* = 10.9433(5) Å, *c* = 33.440(2) Å, β = 104.928(7)°, volume = 6948.2(7)Å^3, eight molecules per cell in space group P2(1)/a (#14). Data was collected with MoKα radiation (λ = 0.71073Å) at 295(2)K, and an analytical absorption correction was applied. Structures were solved with SHELXS-86;[81] non-H atoms were modeled with anisotropic vibrational parameters, H-atoms were located in difference electron density maps but placed in idealized positions with isotropic vibrational parameters 20% larger than the equivalent isotropic vibrational factor of the adjacent carbon atom. In each structure, aryl methyl H's are disordered over alternate trigonal positions; these were modeled by refining occupancy factors. Structural models were refined to convergence by full-matrix least-squares using SHELXL-97.[82] Final R for **61**

was 0.040 for 9628 reflections with $I > 2\sigma_I$, 513 parameters, goodness-of-fit 1.04; for **62**, final R was 0.086 for 5128 reflections with $I > 2\sigma_I$, 774 parameters, goodness-of-fit 0.99.

*Synthesis of (H_2ITap)(DMAP)$_2$$Cl_2$Ru=CH-Ph (**65**)*

4-Dimethylaminopyridine (DMAP, 0.488 g, 4.00 mmol) was added to a slurry of catalyst **61** (1.232 g, 1.36 mmol) in *t*-butyl methyl ether (50 mL) and the solution was stirred for 16 h. In this time, a bright green precipitate formed and the supernatant solution turned colorless from a previous light brown. The precipitate is filtered in air and washed once with a 1 mM solution of DMAP in *t*-butyl methyl ether (20 mL) and the residue was dried in the vacuum oven at 60 ^{o}C for 2 h to give compound **65** (1.065 g, 1.22 mmol, 90 %) in > 99 % purity (^{1}H NMR). ^{1}H NMR (300.1 MHz, C_6D_6, 20 ^{o}C): δ 19.81 (s, Ru=*CH*), 8.57 (d, $^3J[^1H^1H]$ = 7.2 Hz, 2H), 7.23 (t, $^3J[^1H^1H]$ = 8.4 Hz, 1H), 7.01 (m, 2H, =CH-C_6H_5), 8.29 (d, $^3J[^1H^1H]$ = 7.5 Hz, 2H), 8.18 (d, $^3J[^1H^1H]$ = 6.3 Hz, 2H), 6.08 (d, $^3J[^1H^1H]$ = 7.5 Hz, 2H), 5.43 (d, $^3J[^1H^1H]$ = 6.3 Hz, 2H, 2 × C_5NH_4), 6.59 (s, 2H), 6.34 (s, 2H, 2 × C_6H_2), 3.57 (m, 2H), 3.48 (m, 2H, CH_2-CH_2), 3.01 (s, 6H), 2.61 (s, 6H), 2.58 (s, 6H), 2.54 (s, 6H, 4 × N(CH_3)$_2$), 2.20 (s, 6H), 1.80 (s, 6H, 2 × C_6H_2(CH_3)$_2$). ^{13}C NMR (75.9 MHz, 20^{o}C, C_6D_6): δ 309.8 (Ru=*C*H), 221.2 (N-*C*-N), 153.7, 153.5, 152.5 (2 signals), 152.1, 150.5 (2 signals), 150.4, 140.8, 138.7, 130.9, 130.6, 128.9, 128.6, 113.1, 112.6, 106.7, 106.2 (aryl-*C*), 51.9, 51.1 (N-*C*H_2-*C*H_2-N), 40.5, 40.3, 38.2, 37.8 (N-*C*H_3), 21.7, 19.6 (C_6H_2(*C*H_3)$_2$).

*Synthesis of (H_2ITap)Cl_2Ru(=CH-CH_2-CH_2-C_5H_4N) (**66**)*

Complex **61** (0.100 g, 0.110 mmol) and 2-but-3'-enylpyridine (0.022 g, 0.17 mmol) were stirred in *t*BuOMe (20 mL) for 16 h at room temperature. After this time, the resulting greenish slurry was filtered in air, and the residue washed with *t*BuOMe (2 × 10 mL) and dried in the vacuum oven (60 °C, 4 h) to give complex **66** (0.064 g, 0.097 mmol, 88%) as a gray-green powder in >96% purity (^{1}H NMR). ^{1}HNMR (300.1 MHz, 20 ^{o}C,

C_6D_6): δ 18.99 (t, $^3J[^1H^1H]$ = 2.5 Hz, 1H, Ru=C*H*), 8.26 (m, 1H), 6.56 (m, 1H), 6.27 (m, 1H), 6.16 (m, 1H, C_5H_4N), 6.59 (s, 4H, C_6H_2), 3.53 (s, 4H, N-CH_2-CH_2-N), 3.41 (t, $^3J[^1H^1H]$ = 6.0 Hz, 2H), 2.84 (m, 2H, CH_2-CH_2), 2.77 (br, 12 H, $C_6H_2(CH_3)_2$), 2.61 (s, 12H, $N(CH_3)_2$). ^{13}C NMR (75.9 MHz, 20^{o}C, C_6D_6): δ 334.4 (Ru=*C*H), 217.8 (N-*C*-N),162.2, 150.5, 150.2, 140.1, 138.6, 135.5, 123.3, 120.8, 112.4 (aryl-*C*), 53.9 (CH_2), 51.7 (CH_2), 40.2 ($N(CH_3)_2$), 34.0 (CH_2), 22.3 (CH_3), 19.6 (CH_3).

*Synthesis of (ITap)(PCy$_3$)Cl$_2$Ru=CH-Ph (**67**)*

ITap ligand precursor **38** (0.303 g, 0.76 mmol) and Potassium bis(trimethylsilyl)amide (0.158 g, 0.79 mmol) were heated under stirring to 60 ^{o}C in n-heptane for 60 min under inert gas conditions. After cooling to room temperature, Grubbs' 1st Generation catalyst **9** (0.400 g, 0.49 mmol) was added and the slurry was heated to 60^{o}C for 24 h also under inert gas conditions. In this time period the solution turned brown. The solvent was removed under reduced pressure. A mixture of 2-propanol and water 1:1 v/v (50 mL) was added under non-inert conditions. The resulting slurry was sonicated for 30 min in air and then filtered. The filter residue was washed with water (3 x 10 mL) and methanol (2 x 10 mL). The resulting light orange-brown powder was dried in the vacuum oven at 60^{o}C for 16 h to give catalyst **67** (0.379 g, 0.42 mmol, 95%) in >97% purity (^{1}H NMR and ^{31}P NMR spectroscopy). ^{1}HNMR (300.1 MHz, 20 ^{o}C, C_6D_6): δ 20.01 (s, Ru=*CH*), 7.19 (br. m, 1H), 7.12 (br. m, 2H, =CH-C_6H_5), 7.02 (br. m, 2H), 6.53 (br. s, 4H, C_6H_2), 6.35 (m, 1H), 6.30 (m, 1H, N-C*H*=C*H*-N), 2.68 (s, 12H, 2 × $N(CH_3)_2$), 2.47 (s, 12H, 2 × $C_6H_2(CH_3)_2$), 2.60 (m, 3 H) 1.73 (br. m, 6H), 1.55 (br. m, 9H), 1.12 (br. m, 15H, PCy_3); ^{13}C NMR (75.9 MHz, CD_2Cl_2, 20 ^{o}C): δ 294.7 (br., Ru=*C*H), 190.4 (d, $^2J[^{31}P^{13}C]$ = 84.8 Hz, N-*C*-N), 152.1, 150.6, 150.2, 138.8, 137.4, 137.3, 128.9, 128.0, 127.7, 125.3 (2 signals), 124.9, 111.3, 110.7 (aryl-*C* + N-*C*H=*C*H-N), 40.1(2 signals, N-CH_3), 20.2, 18.8 ($C_6H_2(CH_3)_2$), 31.5 (d, $^1J[^{31}P^{13}C]$ = 17.2 Hz), 29.4 (br. s), 28.0 (d, $^2J[^{31}P^{13}C]$ = 9.6 Hz), 26.5 (s, PCy_3); ^{31}P NMR (121.4 MHz, C_6D_6, 20 ^{o}C): δ 32.4 (s).

*Synthesis of (ITap)Cl_2Ru=CH-(C_6H_4-O-iPr) (**68**)*

Complex **67** (0.301 g, 0.33 mmol) was stirred at room temperature under inert gas conditions with 2-*i*-propoxystyrene (0.190 g, 1.17 mmol) and CuCl (0.042 g, 0.43 mmol) for 16 h. Then the solvent was removed under reduced pressure and the residue was taken up in 3 mL of CH_2Cl_2 in air. The solution was filtered, and then loaded onto a flash column with silica gel. The column was washed cyclohexane (30 mL). This filtrate was discarded. The column was then washed with a mixture of ethyl acetate–cyclohexane 90:10 v/v until all of a thick brown band was removed from the stationary phase. The solvent was removed under reduced pressure and the residue was taken up in CH_2Cl_2 (10mL). Heptane (30 mL) was added and the residual CH_2Cl_2 was removed under reduced pressure. The product precipitated and the slurry was filtered. The filter residue was washed with n-heptane (3 x 10 mL), sucked dry for 5 min and dried in the vacuum oven at 60^{o}C overnight to give catalyst **68** (0.152 g, 0.22 mmol, 67%) as a green powder in > 96% purity (^{1}H NMR). ^{1}H NMR (300.1 MHz, 20 ^{o}C, C_6D_6): δ 17.01 (s, 1H, Ru=C*H*), 7.34 (m, 1H), 7.10 (m,1H), 6.67 (m,1H), 6.31 (m, 1H, C_6H_4), 6.58 (s, 4H, C_6H_2), 6.38 (s, 2H, N-C*H*=C*H*-N), 4.49 (sept., $^3J[^1H^1H]$ = 6.0 Hz, 1H, iPr-C*H*), 2.63 (s, 12 H, N(CH_3)$_2$), 2.51 (s, 12H, C_6H_2(CH_3)$_2$), 1.43 (d, $^3J[^1H^1H]$ = 6.0 Hz, 6H, CH(CH_3)$_2$). ^{13}C NMR (75.9 MHz, 20 ^{o}C, C_6D_6): δ 287.7 (Ru=*C*), 177.7 (N=*C*–N), 152.7, 151.4, 146.1, 139.0, 135.2, 124.8, 122.1, 122.0, 113.1, 112.1, (aryl-*C*), 111.8 (N-*C*=*C*-N), 75.0 (*C*H(CH_3)$_2$), 40.3 (N(CH_3)$_2$), 21.4 (CH(CH_3)$_2$), 20.1 (*C*H_3), 18.3 (*C*H_3).

*Synthesis of (ITap)(DMAP)$_2$$Cl_2$Ru=CH-Ph (**69**)*

4-Dimethylaminopyridine (DMAP, 0.165 g, 1.36 mmol) was added to a slurry of complex **67**(0.300 g, 0.33 mmol) in *t*-butyl methyl ether (80 mL) and the solution was sonicated at 30 ^{o}C for 2 h and then stirred at room temperature for another 16 h. The grayish-green precipitate was filtered in air, washed once with a 1 mM solution of DMAP in *t*-butyl methyl ether (20 mL) and the residue was dried in the vacuum oven at 60°C for

2 h to give compound **69** (0.251 g, 0.28 mmol, 84 %) in a purity of >99 % pure. ^{1}H NMR (300.1 MHz, 20 ^{o}C, C_6D_6): *δ* 20.18 (s, 1H, Ru=C*H*), 8.82 (br., 2H), 7.26 (m, 1H), 7.04 (m, 2H, =CH-C_6H_5), 8.36 (d, $^{3}J[^{1}H^{1}H]$ = 7.5 Hz, 2H), 8.18 (d, $^{3}J[^{1}H^{1}H]$ = 7.2 Hz, 2H), 6.00 (d, $^{3}J[^{1}H^{1}H]$ = 7.5 Hz, 2H), 5.43 (d, $^{3}J[^{1}H^{1}H]$ = 6.3 Hz, 2H, 2 × C_5NH_4), 6.50 (s, 2H, N-C*H*=C*H*-N), 6.45 (br., 2H), 6.38 (br., 2H, 2 × C_6H_2), 2.87 (br. s, 6H), 2.58 (s, 12H), 2.51 (br. s, 6H, 4 × $N(CH_3)_2$), 2.12 (s, 6H), 1.76 (s, 6H, 2 × $C_6H_2(CH_3)_2$). ^{13}C NMR (75.9 MHz, 20^{o}C, C_6D_6): *δ* 311.8 (Ru=*C*H), 188.1 (N-*C*-N), 153.3, 153.1, 152.0, 150.7,150.5, 131.0, 128.4, 124.6, 112.1, 106.4, 105.9 (aryl-*C*), 139.4, 138.2 (N-*C*H=*C*H-N), 40.2 ($N(CH_3)_2$), 38.1 (C_6H_4-$N(CH_3)_2$), 37.7 (C_6H_4-$N(CH_3)_2$), 20.9 (CH_3), 19.6 (CH_3).

*Synthesis of (IXyONMe$_2$)(PCy$_3$)Cl$_2$Ru=CH-Ph (**70**)*

Ligand precursor salt **55** (0.260 g, 0.53 mmol) and potassium bis(trimethylsilyl)amide (0.111 g, 0.55 mmol) were heated under stirring to 60 ^{o}C in n-heptane for 60 min under inert gas conditions. After cooling to room temperature, Grubbs' 1st Generation Catalyst **9** (0.357 g, 0.43 mmol) was added and the slurry was heated to 60 ^{o}C for 48 h also under inert gas conditions. The solution was then filtered, and the filter residue was dried in a vacuum oven at 60 ^{o}C. The solvent was removed from the filtrate. The filtrate residue was sonicated in 2-propanol – DI H_2O 1:1 v/v (20 mL) for 30 min. The filter residue was washed with water (3 x 10 mL) and methanol (1 x 10 mL). The resulting light pink powder was dried in the vacuum oven at 60 ^{o}C for overnight to give catalyst **70** (0.171 g, 0.17 mmol, 40%) in >99% purity (^{1}H NMR). ^{1}H NMR (300.1 MHz, 20 ^{o}C, C_6D_6): *δ* 19.71 (s, Ru=*CH*), 7.23 (m, 3H), 7.10 (m, 2H), 6.84 (br., 4H, 2 × C_6H_2), 3.94 (t, $^{3}J[^{1}H^{1}H]$ = 5.7 Hz, 2H), 3.61 (t, $^{3}J[^{1}H^{1}H]$ = 6.0 Hz, 2H, 2 x O-CH_2), 3.30 (br., 6H), 2.75 (br., 6H, 2 × $N(CH_3)_2$), 2.62 (t, $^{3}J[^{1}H^{1}H]$ = 5.7 Hz, 2H), 2.54 (t, $^{3}J[^{1}H^{1}H]$ = 6.0 Hz, 2H, 2 x N-CH_2), 2.19 (s, 12H, 2 × $C_6H_2(CH_3)_2$), 2.55 (br., m, 3H), 1.60 (br., m, 12H), 1.15 (br. m, 18H, PCy_3); ^{13}C NMR (75.9 MHz, 20 ^{o}C, d_6-benzene): *δ* 272.6 (br., Ru=*C*H), 189.5 (d, $^{2}J[^{31}P^{13}C]$ = 87.6 Hz, N-*C*-N), 150.8, 150.0, 141.9, 139.3, 138.0,

129.2, 128.7, 127.1, 125.6, 125.4, 124.9, 124.8, 112.0, 111.3 (s, aryl-*C* + N-*C*H=*C*H-N), 39.9, 39.5, (N-*C*H_3), 20.7, 19.8 ($C_6H_2(CH_3)_2$), 32.5 (d, $^1J[^{31}P^{13}C]$ = 16.1 Hz), 29.8 (s), 28.1 (d, $^2J[^{31}P^{13}C]$ = 10.2 Hz), 26.7 (s, PCy_3); ^{31}P NMR (121.4 MHz, 20 ^{o}C, C_6D_6): δ 30.4 (s).

*Synthesis of (IDippONMe$_2$)(DMAP)Cl$_2$Ru=CH-Ph (**77**)*

Ligand precursor **57** (0.332 g, 0.55 mmol) and KOtBu (0.066 g, 0.59 mmol) were stirred under vacuum at 90 ^{o}C in n-heptane for 5 h. After cooling for 5 min, Grubbs' first generation catalyst **9** (0.301 g, 0.36 mmol) was added and the slurry was stirred at 60 ^{o}C for 48 h under vacuum. The solution was then filtered under inert gas into a schlenk flask containing 4-Dimethylaminopyridine (DMAP) (0.1512 g, 1.24 mmol). The solution was then sonicated for 3 h under inert gas conditions. The resulting slurry was cooled on ice for 30 min, then filtered in air. The filter residue was washed with heptane (3 x 10 mL). The resulting green powder was dried in the vacuum oven at 60 ^{o}C for overnight to give catalyst **77** (0.215 g, 0.20 mmol, 55%) in >95% purity (^{1}H NMR). ^{1}H NMR (300.1 MHz, 20 ^{o}C, C_6D_6): δ 19.63 (s, 1 H, Ru=C*H*), 8.21 (d, $^3J[^1H^1H]$ = 6.6 Hz, 2 H, DMAP), 8.10 (d, $^3J[^1H^1H]$ = 7.5 Hz, 2 H, *o*-Ph), 7.18 (m, 2H, *m*-Ph), 7.03 (m, 1H, *p*-Ph), 6.98 (s, 4H, C_6H_2), 5.48 (d, $^3J[^1H^1H]$ = 6.6 Hz, 2 H, DMAP), 4.36 (m, 4H, CH_2), 4.02 (m, 4H, CH_2), 3.81 (m, 4H, CH_2), 2.66 (m, 4H, C*H*-CH_3), 2.21 (6H, N(CH_3)$_2$), 2.14 (6H, N(CH_3)$_2$), 1.78 (6H, N(CH_3)$_2$), 1.73 (d, $^3J[^1H^1H]$ = 5.7 Hz, 6 H, CH-CH_3), 1.36 (d, $^3J[^1H^1H]$ = 6.0 Hz, 6 H, CH-CH_3), 1.22-1.28 (m, 12H, CH-CH_3). ^{13}C NMR (75.9 MHz, 20 ^{o}C, d_6-benzene): δ 310.1 (Ru=*C*H), 224.2 (N-*C*-N), 160.3, 159.9, 153.5, 152.5, 152.1, 152.0, 149.7, 132.0, 130.1, 129.5, 111.0, 110.3, 106.2 (aryl-*C*), 66.9, 66.4 (O-*C*H_2), 58.7 (N-*C*H_2-*C*H_2-N), 54.8, 54.0 (N-*C*H_2), 46.1 (4 x N(*C*H_3)$_2$), 37.8 (N(*C*H_3)$_2$), 29.8, 28.7 (4 x *C*H), 27.5, 26.7, 26.5, 24.1 (CH-*C*H_3).

*Synthesis of (IDippSNMe$_2$)(DMAP)Cl$_2$Ru=CH-Ph (**78**)*

Ligand precursor **58** (0.256 g, 0.41 mmol) and potassium bis(trimethylsilyl)amide (0.086 g, 0.43 mmol) were heated under stirring to 60^{o}C in n-heptane for 60 min under

inert gas conditions. After cooling to room temperature, Grubbs' first generation catalyst **9** (0.262 g, 0.32 mmol) was added and the slurry was heated to 60 ^{o}C for 24 h also under inert gas conditions. The solution was then filtered under inert gas. 4-Dimethylaminopyridine (0.159 g, 1.32 mmol) was added to the filtrate and sonicated in *t*BuOMe for 60 min under inert gas conditions. In this time period, a bright green precipitate was formed. The resulting slurry was stirred at room temperature 16 h, then sonicated an additional 60 min and filtered. The filter residue was washed with a 1 mM DMAP solution in *t*BuOMe (3 x 10 mL). The resulting green powder was dried in the vacuum oven at 60^{o}C for overnight to give catalyst **78** (0.084 g, 0.10 mmol, 24%) in >95% purity (^{1}H NMR). ^{1}H NMR (300.1 MHz, 20 ^{o}C, C_6D_6): δ 19.51 (s, 1H, Ru=C*H*), 8.12 (d, $^{3}J[^{1}H^{1}H]$ = 7.2 Hz, 2H), 8.03 (d, $^{3}J[^{1}H^{1}H]$ = 7.2 Hz, 2H), 7.06 (d, $^{3}J[^{1}H^{1}H]$ = 7.2 Hz, 2H), 5.57 (d, $^{3}J[^{1}H^{1}H]$ = 7.2 Hz, 2H, 2 × C_5NH_4), 7.65 (s, 2H), 7.41 (s, 2H, 2 x C_6H_2), 7.17 (m, 2 H), 7.09 (m, 3H, =CH-C_6H_5), 4.26 (m, 2 H), 4.00 (m, 2H, N-CH_2), 3.78 (m, 4H, C*H*$(CH_3)_2$), 3.03 (m, 4H, S–CH_2), 2.61 (m, 4H, Me_2N-CH_2), 2.06 (s, 12H), 1.81 (s, 6 H), 1.19 (s, 6H, 4 x N(CH_3)$_2$), 1.65 (d, $^{3}J[^{1}H^{1}H]$ = 5.7 Hz, 12H), 1.29 (d, $^{3}J[^{1}H^{1}H]$ = 6.0 Hz, 12H, 4 x CH(CH_3)$_2$); ^{13}C NMR (75.9 MHz, 20 ^{o}C, C_6D_6): δ n.o. (Ru=*C*H), 222.4 (N-*C*-N), 158.0, 153.0, 140.0, 128.6, 127.0, 125.7, 114.2, 114.1, 106.2, 105.9 (aryl-*C*), 66.4, 65.8, 58.6, 58.5, 51.8 (N-*C*H_2-*C*H_2-N), 46.1 (N(*C*H_3)$_2$), 38.1, 37.7, 27.1, 27.0, 26.7(*C*H_3), 26.6(*C*H_3), 20.3 (*C*H_3), 20.0 (*C*H_3).

*Synthesis of (H_2ITap)(PCy_3)Cl_2Ru=CH-SPh (**79**)*

H_2ITap·HCl **37** (0.374 g, 0.93 mmol) and KO*t*Bu (0.120 g, 1.07 mmol) were heated to 80 °C in heptane (60 mL) for 30 min. After the slurry cooled to room temperature, precatalyst **24** (0.606 g, 0.77 mmol) was added and the mixture was stirred at 60°C for 6 d in a closed vacuum. In this time period, a light-pink precipitate was formed. The reaction mixture was cooled to room temperature and then filtered in air. The residue was washed with heptanes (2 x 10 mL) and then dried in the vacuum oven

at 60 °C for 4 h. A mixture of 2-propanol and 0.5 M aqueous ammonium chloride (3:1 v/v, 50 mL) was added to the dry residue under non-inert conditions and the mixture was sonicated at 30 °C for 60 min. The slurry was filtered in air, the residue was washed with methanol (2 × 10 mL) and then dried in the vacuum oven at 60°C for 2 h to give compound **79** (0.474 g, 0.50 mmol, 65 %) in >99 % purity (^{1}H NMR). ^{1}H NMR (300.1 MHz, 20^{o}C, C_6D_6): δ 17.98 (s, Ru=*CH*), 7.21 (d, $^3J[^1H^1H]$ = 7.2 Hz, 2H), 6.97 (t, $^3J[^1H^1H]$ = 8.4 Hz, 1H), 6.88 (m, 2H, =CH-C_6H_5), 6.50 (s, 2H), 6.13 (s, 2H, 2 × C_6H_2), 3.35 (m, 4H, CH_2-CH_2), 2.90 (s, 6H), 2.75 (s, 6H, 2 × N(CH_3)$_2$), 2.60 (s, 6H), 2.28 (s, 6H, 2 × C_6H_2(CH_3)$_2$), 2.57 (br., m, 3H), 1.88 (br., m, 6H), 1.65 (br., m, 6H), 1.55 (br., m, 3H), 1.45-1.02 (br., m, 18H, PCy_3). ^{13}C NMR (75.9 MHz, 20 ^{o}C, d_6-benzene): δ 272.2 (br., Ru=*C*H), 219.4 (d, $^2J[^{31}P^{13}C]$ = 81.6 Hz, N-*C*-N), 150.5, 149.5, 141.8, 140.4, 138.6, 129.3, 128.7, 126.5, 125.5, 125.4, 112.7, 111.9 (s, aryl-*C*), 52.3, 52.1 (s, N-CH_2-CH_2-N), 40.5, 40.3, 40.0, 39.6 (N-CH_3), 21.0, 20.0 (C_6H_2(CH_3)$_2$), 32.3 (d, $^1J[^{31}P^{13}C]$ = 15.6 Hz), 29.7 (s), 28.1 (d, $^2J[^{31}P^{13}C]$ = 10.2 Hz), 26.7 (s, PCy_3); ^{31}P NMR (121.4 MHz, 20 ^{o}C, C_6D_6): δ 23.4 (s).

*Synthesis of (ITap)(PCy$_3$)Cl$_2$Ru=CH-SPh (**80**)*

ITap·HCl **38** (0.599 g, 1.50 mmol) and KO*t*Bu (0.193 g, 1.72 mmol) were heated to 80°C in heptane (120 mL) for 30 min. After the slurry cooled to room temperature, precatalyst **24** (0.992 g, 1.16 mmol) was added and the mixture was stirred at 60 °C for 96 h in a closed vacuum. In this time period, a light-pink precipitate was formed. The reaction mixture was cooled to room temperature and then filtered in air. The residue was washed with heptanes (2 x 10 mL) and then dried in the vacuum oven at 60°C for 4 h. A mixture of 2-propanol and 0.5 M aqueous ammonium chloride (3:1 v/v, 50 mL) was added to the dry residue under non-inert conditions and the mixture was sonicated at 30 °C for 60 min. The slurry was filtered in air, the residue was washed with methanol (2 × 10 mL) and then dried in the vacuum oven at 60°C for 2 h to give compound **80** (0.820 g,

0.91 mmol, 78 %) in >99 % purity (^{1}H NMR). ^{1}H NMR (300.1 MHz, 20 ^{o}C, C_6D_6): δ 18.21 (s, Ru=*CH*), 7.25 (d, $^3J[^1H^1H]$ = 7.5 Hz, 2H), 6.99 (t, $^3J[^1H^1H]$ = 7.5 Hz, 2H), 6.89 (t, $^3J[^1H^1H]$ = 7.5 Hz, 1H, =CH-C_6H_5), 6.48 (s, 2H), 6.11 (s, 2H, 2 × C_6H_2), 6.29 (m, 1H), 6.27 (m, 1H, N-C*H*=C*H*-N), 2.73 (s, 3H), 2.60 (s, 3H), 2.57 (s, 3H), 2.28 (s, 3H , 2 × $N(CH_3)_2$ + 2 × $C_6H_2(CH_3)_2$), 2.61 (br., m, 3H), 1.93 (br., m, 6H), 1.64 (br., m, 6H), 1.52 (br., m, 3H), 1.45-1.08 (br., m, 18H, PCy_3). ^{13}C NMR (75.9 MHz, 20 ^{o}C d_6-benzene): δ 272.6 (br., Ru=*C*H), 189.5 (d, $^2J[^{31}P^{13}C]$ = 87.6 Hz, N-*C*-N), 150.8, 150.0, 141.9, 139.3, 138.0, 129.2, 128.7, 127.1, 125.6, 125.4, 124.9, 124.8, 112.0, 111.3 (s, aryl-*C* + N-*C*H=*C*H-N), 39.9, 39.5, (N-CH_3), 20.7, 19.8 ($C_6H_2(CH_3)_2$), 32.5 (d, $^1J[^{31}P^{13}C]$ = 16.1 Hz), 29.8 (s), 28.1 (d, $^2J[^{31}P^{13}C]$ = 10.2 Hz), 26.7 (s, PCy_3); ^{31}P NMR (121.4 MHz, 20^{o}C, C_6D_6): δ 26.0 (s).

*Synthesis of (H_2ITap)(DMAP)$_2$$Cl_2$Ru=CH-SPh (**81**)*

4-Dimethylaminopyridine (DMAP, 0.412 g, 3.38 mmol) was added to a slurry of catalyst **79** (1.237 g, 1.32 mmol) in *t*-butyl methyl ether (80 mL) and the solution was sonicated at 30°C for 2 h and then stirred at room temperature for another 16 h. The grayish-green precipitate was filtered in air, washed once with a 1 mM solution of DMAP in *t*-butyl methyl ether (20 mL) and the residue was dried in the vacuum oven at 60°C for 2 h to give compound **81** (1.110 g, 1.23 mmol, 93 %) in >98 % purity (^{1}H NMR). ^{1}H NMR (300.1 MHz, 20 ^{o}C, $CDCl_3$): δ 17.33 (s, Ru=*CH*), 8.26 (br., 2H), 7.16 (br., 2H), 6.49 (br., 2H), 6.22 (br., 2H, 2 × C_5NH_4), 6.47 (s, 2H), 6.15 (s, 2H, 2 × C_6H_2), 7.13 (m, 5H, S-C_6H_5), 4.11 (m, 2H), 3.98 (m, 2H, CH_2-CH_2), 3.00 (s, 6H), 2.96 (s, 6H), 2.90 (s, 6H), 2.69 (s, 6H, 4 × $N(CH_3)_2$), 2.60 (s, 6H), 2.40 (s, 6H, 2 × $C_6H_2(CH_3)_2$). ^{13}C NMR (75.9 MHz, 20 ^{o}C, $CDCl_3$): The compound was not sufficiently soluble in C_6D_6. Thus, the spectra were recorded in $CDCl_3$. The compound suffered from partial degradation during the recording time (approx. 20% in 16 h). This was observed for all bis-DMAP Ru-carbene complexes in chlorinated solvents thus far. However, several signals for the compound

were observed. 220.9 (n-C-N), 154.2, 152.6, 150.3, 149.3, 138.7, 129.2, 128.4,127.8, 127.2, 126.7, 112.2, 111.4, 106.5 (s, s, aryl-*C*), 52.3 (DMAP-*C*H_3), 40.7, 40.1, 39.8, 39.2 (N-(*C*H_3)$_2$), 20.9, 19.6 (C_6H_2(*C*H_3)$_2$).

*Crystal Structure Determination of Catalyst **81***

Dark red or brown crystals of **81** are triclinic, *a* = 10.2523(5) Å, *b* = 12.3752(6) Å, *c* = 18.3356(6) Å, α = 86.269(4)^o, β = 88.750(4)^o, γ = 78.653(4)^o, volume = 2275.91(19)Å^3, space group P-1 (#2). Data was collected with MoKα radiation (λ = 0.71073Å) at 300(2)K, and an analytical absorption correction was applied. Structures were solved with SHELXS-86[111] and refinements were done using SHELXL-97;[112] non-H atoms were modeled with anisotropic librational factors, H-atoms were located in difference electron density maps but placed in idealized positions with isotropic displacement parameters of 120% of the U (eq) of the attached atom.[82] Final R for **81** was 0.0555 for 4827 reflections with I > 2σ_I, 520 parameters, goodness-of-fit 1.009.

*Synthesis of (ITap)(DMAP)$_2$Cl$_2$Ru=CH-SPh (**82**)*

4-Dimethylaminopyridine (DMAP, 0.244 g, 2.00 mmol) was added to a slurry of catalyst **80** (0.601 mg, 0.64 mmol) in *t*-butyl methyl ether (30 mL) and the solution was sonicated at 30 °C for 2 h and then stirred at room temperature for another 16 h. The bright-green precipitate was filtered in air, washed once with a 1 mM solution of DMAP in *t*-butyl methyl ether (10 mL) and the residue was dried in the vacuum oven at 60 °C for 2 h to give compound **82** (0.498 g, 0.55 mmol, 86 %) in >99 % purity (^{1}H NMR). ^{1}H NMR (300.1 MHz, 20 ^{o}C, $CDCl_3$): δ 17.68 (s, 1H, Ru=*CH*), 7.17 (m, 5H, S-C_6H_5), 6.85 (br., 2H, N-C*H*=C*H*-N), 8.61 (br., 2H), 8.03 (br., 2H), 6.09 (br., 8H, 2 × C_5NH_4 + 2 × C_6H_2), 2.93 (br., 12H), 2.77 (br., 6H), 2.65 (br., 6H, 4 × N(CH_3)$_2$), 2.27 (br., 12H, 2 × C_6H_2(CH_3)$_2$). ^{13}C NMR (75.9 MHz, 20 ^{o}C, $CDCl_3$): The compound was not sufficiently soluble in C_6D_6. Thus, the spectra were recorded in $CDCl_3$. The compound suffered from partial

degradation during the recording time (approx. 20% in 16 h). This was observed for all bis-DMAP Ru-carbene complexes in chlorinated solvents thus far. However, several signals for the compound were observed. δ 288.0 (br., Ru=*C*H), 187.5 (N-*C*-N), 151.3, 149.1, 130.1, 128.1, 124.5, 111.8, 106.6 (s, aryl-*C* + N-*C*H=*C*H-N), 40.1(2 x N-CH_3), 39.1 (4 x N(CH_3)$_2$), 26.9 (C_6H_2-CH_3), 19.6 (C_6H_2-CH_3).

*Synthesis of (ITap)(PPh$_3$)Cl$_2$Ru-3-phenylindenylidene (**87**)*

ITap·HCl ligand precursor **38** (0.678 g, 1.67 mmol) and KO*t*Bu (0.220 g, 1.96 mmol) were heated under stirring to 60 ^{o}C in toluene (50 mL) for 60 min under inert gas conditions which resulted in the formation of a relatively clear solution with small salt crystals settling quickly. After cooling to room temperature, catalyst **21** (1.154 g, 1.30 mmol) was added and the slurry was heated to 60 ^{o}C for 24 h also under inert gas conditions. The solvent was then removed under reduced pressure. A mixture of 2-propanol and water 1:1 v/v (50 mL) was added under inert conditions. The resulting slurry was sonicated for 60 min and then filtered. The filter residue was washed with methanol (4 x 10 mL). The resulting light deep purple powder was dried in the vacuum oven at 60 ^{o}C overnight to give catalyst **87** (0.811 g, 0.82 mmol, 63%) in >97% purity (^{1}H NMR). ^{1}H NMR (300.1 MHz, 20 ^{o}C, $CDCl_3$): δ 7.80 (d, $^{3}J[^{1}H^{1}H]$ = 7.5 Hz, 1H), 7.62 (m, 2H), 7.51 (m, 1H), 7.34 (m, 2H) 7.20 (m, 9H), 7.06 (m, 6H), 6.90 (m, 1H), 6.86 (t, $^{3}J[^{1}H^{1}H]$ = 7.5 Hz, 1H), 6.66 (2 × s, 2 × 1H), 6.65 (s, 1H), 6.64 (s, 1H), 6.46 (s, 1H), 5.94 (m, 1H), 5.61 (m, 1H), 3.61 (s, 6H), 2.67 (s, 6H, 2 × N(CH_3)$_2$), 2.53 (s, 3 H) 2.47 (s, 3H), 2.01 (s, 3H), 1.73 (s, 3H, aryl-CH_3); ^{13}C NMR (75.9 MHz, 20 ^{o}C, $CDCl_3$, significant signals): δ 300.7 (d, $^{2}J[^{31}P^{13}C]$ = 12.9 Hz, Ru=*C*), 185.1 (d, $^{2}J[^{31}P^{13}C]$ = 96.0 Hz, N-*C*-N), 40.4, 39.9 (N-CH_3), 20.6, 19.0 (C_6H_2(CH_3)$_2$); ^{31}P NMR (121.4 MHz, 20 ^{o}C,C_6D_6): δ 28.8 (s).

*Synthesis of (ITap)(DMAP)$_2$Cl$_2$Ru-3-phenylindenylidene (**88**)*

4-Dimethylaminopyridine (DMAP, 0.209 g, 1.71 mmol) was added to a slurry of complex **87** (0.414 g, 0.42 mmol) in *t*-butyl methyl ether (50 mL) and the solution was stirred at 50 °C for 24 h. The reddish-purple precipitate was filtered in air, washed once with a 1 mM solution of DMAP in *t*-butyl methyl ether (20 mL) and the residue was dried in the vacuum oven at 60 °C for 2 h to give compound **88** (0.355 g, 0.37 mmol, 87 %) in >96% purity (^{1}H NMR). ^{1}H NMR (300.1 MHz, 20 ^{o}C, C_6D_6): 10.08 (1H), δ 9.37 (m, 2H), 9.19 (m, 2H), 8.44 (m, 1H), 8.07 (m, 4H) 7.72 (m, 2H), 7.18 (m, 2H), 7.12 (m, 2H), 6.80-7.07 (m, 5H), 6.58 (m, 1H), 6.53 (m, 1H), 6.33 (m, 1H), 6.26 (m, 1H), 5.96 (m, 2H), 5.73 (m, 2H), 5.64 (m, 1H), 2.79 (s, 3H), 2.70 (s, 3H) 2.70 (s, 6H), 2.35 (s, 6H), 2.26 (s, 3H), 1.99 (s, 3H, 4 × N(CH_3)$_2$), 2.07 (s, 3 H) 2.06 (s, 9H, aryl-CH_3); ^{13}C NMR (75.9 MHz, 20^{o}C, $CDCl_3$, significant signals): δ 301.0 (s, Ru=*C*), 185.7 (s, N-*C*-N), 40.4, 40.1, 38.5 (2 signals, N-*C*H$_3$), 21.6 (2 signals), 19.7, 19.6 (C_6H_2(*C*H$_3$)$_2$).

General Procedure for ROMP of COE

COE (7.8 mL, 60 mmol) was added to the catalyst solution (0.60 mL, 0.50 mM, 0.30 mmol, organic solvent) under inert conditions *via* a microlitre syringe and the monomer conversion was monitored *via* ^{1}H NMR spectroscopy (300.1MHz, 20 ^{o}C) by integration of the sufficiently separated multiplet signals at δ = 5.51 ppm (COE, =C*H*–) and 5.46 ppm (polymer, =C*H*-) in regular intervals over a period of 15 min to 10days.

General Procedure for RCM of DEDAM

DEDAM (14.4 mL, 60 mmol) was added to the catalyst solution (0.60 mL, 1.00 mM, 0.60 mmol, oranic solvent) under inert gas conditions *via* a microlitre syringe and the monomer conversion was monitored *via* ^{1}H NMR spectroscopy (300.1 MHz, 20 ^{o}C) by integration of the sufficiently separated multiplet signals at δ = 2.87 ppm (DEDAM, allyl-CH_2) and 3.16 ppm [**90**, ring allyl-CH_2] in regular intervals over a period of 1 h to 3 days.

*General Procedure for ROMP of **89** With Various Amounts of TsOH*

Monomer **89** (15.9 µL, 60 µmol) in CH_2Cl_2 or $CHCl_3$ was added to the catalyst solution (0.60 mL, 1.0 mM, 0.60 µmol [**61** in CH_2Cl_2; **62** in $CHCl_3$]) containing various molar equivalents of a 0.12 M solution of *p*-Toluenesulfonic acid in the same solvent (2.0 µL, 0.24 µmol, 0.4 equiv.) which were added 2 minutes prior via microliter syringe. The monomer conversion was monitored via 1H NMR spectroscopy (300.1 MHz, 20 ^{o}C) by integration of the signals δ 6.46 ppm (s, 2H, monomer **89**) and δ 5.91, 5.51 ppm (m, 2 *cis*-H and *trans*-H, poly-**89**).

*General Procedure for Synthesis of Poly-**89***

A stock solution of monomer **89** (0.10 M, 2.0 mL, 0.20 mmol) in CH_2Cl_2 or $CHCl_3$ was added to a catalyst stock solution (1.0 mM, 2.0 mL, 2.0 µmol [**61** in CH_2Cl_2; **62** in $CHCl_3$]) containing various molar equivalents of a 0.25 M solution of TsOH in 2-propanol (3.2 µL = 0.4 equivalents) which were added 2 minutes prior via microliter syringe. After appropriate time intervals (20 min – 10 h), the reactions were quenched with ethylvinyl ether and dried under vacuum. The resulting residue was dissolved in ethyl acetate (from catalyst **61**) or CH_2Cl_2 (from catalyst **62**), filtered through a short flash column of silica gel (1 cm) and additional solvent (5 ml) was used for elution. The solvent was removed from the filtrate in the vacuum oven (60 °C) and the residue was analyzed via ASEC.

*General Procedure for the Reaction of Catalysts **61** and **62** With EVE*

Ethylvinyl ether (EVE) (31 µL, 320 µmol) in CH_2Cl_2 or $CHCl_3$ was added to the catalyst solution (0.60 mL, 4.0 mM, 3.2 µmol [**61** in CD_2Cl_2; **62** in $CDCl_3$]) containing various molar equivalents of a 0.60 M solution of *p*-Toluenesulfonic acid in 2-PrOH (0.60 M, 4.0 µL = 1 equiv.) which were added 2 minutes prior via microliter syringe. The monomer conversion was monitored via ^{1}H NMR spectroscopy (300.1 MHz, 20 °C) by integration of the signals δ 19.02 ppm (s, 1H, **61**) or δ 16.25 ppm (s, 1H, **62**) and δ 13.73

ppm (s, 1H, for catalyst **61** without acid), δ 7.50 ppm (m, 1H, 2-*i*propoxybenzylidene/styrene, for catalyst **62** without acid) or δ 7.86 ppm (m, 2 H, TsOH).

*General Procedure for ROMP of Monomers **95** and **96***

The catalyst (8 mmol) and monomer **95** (67.8 mg, 0.50 mmol) or monomer **96** (40.5, 0.5 mmol) were dissolved in the protic solvent (either in 2-PrOH–1 M HCl_{aq} 9 : 1 v/v or 0.1 M HCl_{aq}, 2.0 mL) under inert gas conditions and the solution was heated to 50 ^{o}C under stirring. An aliquot (0.3 mL) was taken after 30 min, quenched with ethylvinyl ether, dried under vacuum, and the monomer conversion was monitored via ^{1}H NMR spectroscopy (300.1 MHz, 20 ^{o}C, D_2O) by integration of the signals *δ* 6.49 ppm (m, 2 H, **95**), *δ* 5.97 ppm (m, 2 *trans*-H, polymer) and *δ* 5.81 ppm (m, 2 *cis*-H, polymer) for monomer **95** and *δ* 6.46 ppm (m, 2 H, **96**), *δ* 5.99 ppm (m, 2 *trans*-H, polymer) and *δ* 5.79 ppm (m, 2 *cis*-H, polymer) for monomer **96**.

*General Procedure for RCM of **97***

The catalyst (8 mmol) and **97** (36.8 mg, 0.20 mmol) were dissolved in the protic solvent (2-PrOH–1MHCl_{aq} 9 : 1 v/v or 0.1 M HCl_{aq}, 2.0 mL) under inert gas conditions and the solution was heated to 50 ^{o}C under stirring. Aliquots (0.3 mL) were taken after 30 min and 60 min, quenched with ethylvinyl ether, dried under vacuum, and the product conversion was monitored via ^{1}H NMR spectroscopy (300.1 MHz, 20^{o}C, D_2O) by integration of the signals *δ* 2.58 (**97**-CH_2) and *δ* 2.98 ppm (cyclopentene-CH_2).

*^{1}H NMR Investigation of the Hydrolytic Stability of **61a***

Complex **61a** (2.0 mg, 3 mmol) was dissolved in 0.1 M DCl/D_2O in air and kept at room temperature in an NMR tube. ^{1}H NMR pectra were recorded in certain time intervals and the intensities were monitored for the corresponding NMR signals for complex **61** and the hydrolysis product **61a**. ^{1}H NMR (300.1 MHz, 20 ^{o}C, 0.1 M DCl/D_2O) *δ* 16.29 (s, 1 H, Ru=C*H*), 7.04 (s, 4 H, C_6H_2), 7.11 (m, 1 H), 6.49 (m, 1 H), 6.43 (m, 2 H, C_6H_4), 4.46 (m, 1H, C*H*$(CH_3)_2$), 3.64 (s, 4 H, N–CH_2), 2.81 (s, 12 H, N(CH_3)$_2$), 1.91 (s, 12

H, aryl-C*H*$_3$), 0.58 (m, 6 H, CH(C*H*$_3$)$_2$; ^{13}C NMR (75.9 MHz, 20 ^{o}C, 0.1 M DCl/D_2O) *δ* (Ru=*C*, n.o.), 207.2 (N=*C*–N), 139.2, 132.1, 122.6, 122.0, 113.7 (1 signal n.o., =CH–*C*$_6$H$_4$), 152.0, 145.0, 142.3, 120.4 (s, *C*$_6$H$_2$), 74.8 (*C*H(CH$_3$)$_2$), 26.9 (*C*H(CH$_3$)$_2$), 40.8 (s, N(*C*H$_3$)$_2$), 21.1 (C$_6$H$_2$–*C*H$_3$).

General Procedure for RCM of DEDAM / DAP With Subsequent Ru Removal

The substrate (DEDAM: 96 mg, 0.40 mmol; DAP: 108 mg, 0.60 mmol) was added to a solution of catalyst **61** (DEDAM: 5.4 mg, 8 mmol; DAP: 8.1 mg, 12 mmol) in toluene or ethyl acetate (DEDAM: 2.0 mL; DAP: 3.0 mL) under inert gas conditions and the solution was kept stirring for 60 min at 50 ^{o}C. Then the solution was cooled to room temperature and acid (4 mL, conc. HCl_{aq} or H_2SO_4 [96%]) was added under inert gas atmosphere and stirred for another 2 min causing the formation of a precipitate. The solution was filtered through Na_2SO_4, washed with the solvent (3 x 2 mL), and the solvent was removed under reduced pressure. The product was dried in the vacuum (0.1Torr) for 30 min. Isolated yields were obtained in the range of 72–87% (DEDAM) and 43–79% (DAP). ^{1}H NMR (300.1 MHz, 20 ^{o}C, D_2O) was used to determine the conversion (all >99%) by integration of distinct signals for the starting material and RCM product [(*δ* 2.86 ppm (DEDAM-C*H*$_2$) *vs. δ* 3.16 ppm (cyclopentene-C*H*$_2$); *δ* 2.65 ppm (DAP-C*H*2) *vs. δ* 2.91 ppm (cyclopentene-C*H*2)]. An aliquot of 20–22 mg was taken from each reaction for Ru analysis via ICP MS. The residual product was dissolved in *t*-butylmethyl ether (20 mL) and washed with water (3 x 20 mL), the organic phase was dried over Na_2SO_4 and the solvent was removed and the product was dried in the vacuum (0.1 Torr) for 30 min. Product recoveries after the washing steps were between 44–69%. Aliquots of 20–22 mg were taken for Ru analysis *via* ICP MS.

REFERENCES

(1) (a) Grubbs, R. H., Ed. Applications in Organic Synthesis. In *Handbook of Metathesis*; Wiley-VCH: Weinheim, 2003; Vol. 2. (b) Bieniek, M; A. Michrowska; Grela, K. *Chem.-Eur.* J. **2008**, *14*, 806-818. (c) Hoveyda, A. H.; Zhugralin, A. R. *Nature* **2007**, *450*, 243-251. (d) H. Clavier; K. Grela; Kirschning, A.; Mauduit, M.; Nolan, S. P. *Angew. Chem., Int. Ed.* **2007**, *46*, 6786-6801. (e) Ghosh, S.; Ghosh, S.; Sarkar, N. *J. Chem. Sci.* **2006**, *118*, 223-235. (f) Conrad, J. C.; Fogg, D. E. *Curr. Org. Chem.* **2006**, *10*, 185-202. (g) Chatterjee, A. K.; Choi, T. L.; Sanders, D. P., Grubbs, R. H. *J. Am. Chem. Soc.* **2003**, *125*, 11360-11370. (h) Wright, D. L. *Curr. Org. Chem.* **1999**, *3*, 211-240.

(2) (a) Grubbs, R. H., Ed. Applications in Organic Synthesis. In *Handbook of Metathesis*; Wiley-VCH: Weinheim, 2003; Vol. 3. (b) Bielawski, C. W.; Grubbs, R. H. *Prog. Polym. Sci.* **2007**, *32*, 1-29. (c) Frenzel, U.; Nuyken O. J. *J. Polym. Sci., Part A: Polym. Chem.* **2002**, *40*, 2895-2916. (d) Slugovc, C. *Macromol. Rapid Commun.* **2004**, *25*, 1283-1297. (e) Scherman, O. A.; Rutenberg, I. M.; Grubbs, R. H. *J. Am. Chem. Soc.* **2003**, *125*, 8515-8522. (f) Bielawski, C. W.; Benitez, D.; Morita, T.; Grubbs, R. H. *Macromolecules* **2001**, *34*, 8610-8618. (g) Baughman, T. W.; Wagener, K. B. *Adv. Poly. Sci.* **2005**, *176*, 1-42; (h) Trimmel, G.; Riegler, S.; Fuchs, G.; Slugovc, C.; Stelzer, F. *Adv. Polym. Sci.* **2005**, *176*, 74-87. (i) Grubbs, R. H. *Tetrahedron* **2004**, *60*, 7117-7140.

(3) (a) Chauvin, Y. *Angew. Chem., Int. Ed.* **2006**, *45*, 3740-3747. (b) Schrock, R. R. *Angew. Chem., Int. Ed.* **2006**, *45*, 3748-3759. (c) Grubbs, R. H. *Angew. Chem., Int. Ed.* **2006**, *45*, 3760-3765.

(4) Astruc, D. *New J. Chem.* **2005**, *29*, 42-56.

(5) (a) Nguyen, S. T.; Johnson, L. K.; Grubbs, R. H., Ziller, J. W. *J. Am. Chem. Soc.* **1992**, *114*, 3974-3975. (b) Schwab, P.; Grubbs, R. H.; Ziller, J. W. *Angew. Chem., Int. Ed.* **1995**, *34*, 2039-2041. (c) Fraser, C.; Grubbs, R. H. *Macromolecules* **1995**, *28*, 7248-7255. (d) Schwab, P.; Grubbs, R. H.; Ziller, J. W. *J. Am. Chem. Soc.* **1996**, *118*,

100-110. (e) Beilawski, C. W.; Grubbs, R. H. *Angew. Chem., Int. Ed.* **2000**, *39*, 2903-2906. (f) Love, J. A.; Sanford, M. S.; Day, M. W.; Grubbs, R. H. *J. Am. Chem. Soc.* **2003**, *125*, 10103-10109. (g) Colancino, E.; Martinez, J.; Lamaty, F.; *Coord. Chem. Rev.* **2007**, *251*, 726-764. (h) Wilhelm, T. E.; Belderrain, T. R.; Brown, S. N.; Grubbs, R. H. *Organometallics* **1997**, *16*, 3867-3869.

(6) (a) Hong, S. H.; Grubbs, R. H. *J. Am. Chem.Soc.* **2006**, *128*, 3508-3509. (b) Hong, S. H.; Grubbs, R. H. *Org. Lett.* **2007**, *9*, 1955-1957. (c) Jordan, J.P., Grubbs, R.H. *Angew. Chem., Int. Ed.* **2007**, *46*, 5152-5155.

(7) Muller, E.; Baryer, O.; Meerwein, H.; Ziegler, K. *Methoden der organischen Chemie. Bd. II. Analytische Methoden*, **1953**.

(8) (a) Natta, G. *Chimica e l'Industria (Milan, Italy)*, **1955**, *37*, 888-900. (b) Natta, G. *J. Polym. Sci.* **1955**, *16*, 143-154. (c) Natta, G.; Corradini, P. *Atti accad. nazl. Lincei, Rend., Classe sci. fis. mat. e nat.* **1955**, *19*, 229-23. (d) Natta, G.; Corradini, P. *Makromol. Chem*. **1955**, *16*, 77-80. (e) Natta, G.; Corradini, P. *Atti accad. nazl. Lincei, Mem. Classe sci. fis., mat. e nat. [8]* **1955**, *4*, 73-80. (f) Natta, G.; Pino, P.; Corradini, P.; Danusso, F.; Mantica, E.; Mazzanti, G.; Moraglio, G. *J. Am. Chem. Soc.* **1955**, *77*, 1708-1710.

(9) (a) Grubbs, R. H., Ed. Applications in Organic Synthesis. In *Handbook of Metathesis*; Wiley-VCH: Weinheim, 2003; Vol. 1. (b) *GB Pat.*, 896496, **1962**. (c) Banks, R. L.; Bailey G. C. *Ind. Eng. Chem. Res.* **1964**, *3*, 170-173. (d) *GB Pat.*, 921039, **1963**. (e) Heckelsberg, L. F.; Banks, R. L.; Bailey, G. C. *Ind. Eng. Chem. Res.* **1968**, *7*, 29-31. (f) *Application: IT IT Pat.*, 639147, **1962**.

(10) Rouhi, A. M. *Chem. Eng. News* **2002**, *50*, 34-38.

(11) Calderon, N.; Chen, H. Y.; Scott, K. W. *Tetrahedron Lett.* **1967**, *8*, 3327.

(12) (a) Lewandos, G. S.; Pettit, R. *J. Am. Chem. Soc*. **1971**, *93*, 7087-7088. (b) Pampus, G.; Witte, J.; Hoffmann, M. *Rev. Gen. Caoutch. Plast.* **1970**, *47*, 1343-1347. (c)

Scott, K. W.; Calderon, N.; Ofstead, E. A.; Judy, W. A.; Ward, J. P. *Adv. Chem. Ser.* **1969**, *91*, 399-418.

(13) Herisson, J. L.; Chauvin, Y. *Makromol. Chem.* **1971**, *141*, 161-176.

(14) (a) Katz, T. J.; McGinnis, J. *J. Am. Chem. Soc*. **1975**, *97*, 1592-1594. (b) Katz, T. J.; Rothchild, R. *J. Am. Chem. Soc*. **1976**, *97*, 2519-2526. (c) Katz, T. J.; Acton, N. *Tetrahedron Lett.* **1976**, *17*, 4251-4254. (d) Katz, T. J.; Lee, S. J.; Acton, N. *Tetrahedron Lett.* **1976**, *17*, 4247-4250.

(15) Grubbs, R. H.; Burk, P. L.; Carr, D. D. *J. Am. Chem. Soc*. **1975**, *97*, 3265-3267.

(16) Wengrovius, J. H.; Schrock, R. R.; Churchill, M. R.; Missert, J. R.; Youngs, W. J. *J. Am. Chem. Soc*. **1980**, *102*, 4515-4516.

(17) (a) Cumberland, R. W.; Blair, R. G.; Wallace, C. H.; Reynolds, T. K.; Kaner, R. B. *J. Phys. Chem. B* **2001**, *105*, 11922-11927. (b) Oakley, G. W.; Wagener, K. B. *Macromol. Chem. Phys.* **2005**, *206*, 15-24. (c) Schrodi, Y.; Pederson, R. L. *Aldrichimica Acta* **2007**, *40*, 45-52.

(18) Grubbs, R. H.; Trnka, T. M. Ruthenium-Catalyzed Olefin Metathesis. In *Ruthenium in Organic Synthesis*; Murahashi, S. I., Ed; Wiley-VCH: Weinheim, 2004, 153-177.

(19) Farina, V.; Shu, C.; Zeng, X.; Wei X.; Han, Z.; Yee, N. K.; Senanayake, C. H. *Org. Process Res. Dev.* **2008**, *13*, 250-254. (b) Kanada, R. M.; Itoh, D.; Nagai, M.; Niijima, J.; Asai, N.; Mizui, Y.; Abe, S.; Kotake, Y. *Angew. Chem., Int. Ed.* **2007**, *46*, 4350-4355.

(20) Ulman, M.; Grubbs, R. H. *J. Org. Chem.* **1999**, *64*, 7202-7207.

(21) (a) Al-Badri, Z. M.; Tew, G. N. *Macromolecules* **2008**, *41*, 4173-4179. (b) Burtscher, D.; Lexer, C.; Mereiter, K.; Winde, R.; Karch, R.; Slugovc, C. *J. Polym. Sci., Part A: Polym. Chem.* **2008**, *46*, 4630-4635. (c) Castle, T. C.; Khosravi, E.; Hutchings, L.

R. *Macromolecules* **2004**, *37*, 2035-2040. (d) Endo, K. *Nippon Gomu Kyokaishi* **2008**, *81*, 121-127.

(22) Deshmukh, P. H.; Blechert, S. *Dalton Trans.* **2007**, 2479-2491.

(23) *Novel Metathesis Chemistry: Well-defined Initiator Systems for Specialty Chemical Synthesis, Tailored Polymers, and Advanced Material Applications*; Imamoglu, Y., Bencze, L., Eds; Kluwer Academic Publishers: Boston, 2003.

(24) Heins, E.; Hinck, H.; Kaminsky, W.; Oppermann, G.; Raulinat, P.; Sinn, H. *Makromol. Chem.* **1970**, *134*, 1-22.

(25) Tebbe, F. N.; Parshall, G. W; Reddy, G. S. *J. Am. Chem. Soc*. **1978**, *100*, 3611-3613.

(26) (a) Grubbs, R. H.; Miyashita, A. *J. Am. Chem. Soc*. **1978**, *100*, 7418-7420. (b) Klabunde, U.; Tebbe, F. N.; Parshall, G. W.; Harlow, L. *J. Mol. Catal.* **1980**, *8*, 37-51.

(27) (a) Schaverien, C. J.; Dewan, J. C.; Schrock, R. R. *J. Am. Chem. Soc.* **1986**, *108*, 2771-2773. (b) Schrock, R. R.; DePue, T.; Feldman, J.; Schaverien, C. J.; Dewan, J. C.; Liu, H. *J. Am. Chem. Soc.* **1988**, *110*, 1423-1435.

(28) (a) Murdek, J. S.; Schrock, R. R. *Organometallics* **1987**, *6*, 1373-1374. (b) Schrock, R. R.; Krouse, S. A.; Knoll, K.; Feldman, J.; Murdzek, J. S.; Yang, D. C. *J. Mol. Catal.* **1988**, *46*, 243-253. (c) Oskam, J. H.; Fox, H. H.; Yap, K. B.; McConville, D. H.; O'Dell, R.; Lichtenstein, B. J.; Schrock, R. R. *J. Organomet. Chem.* **1993**, *459*, 185-198.

(29) Schrock, R. R.; Murdzek, J. S.; Bazan, C.; Robbins, J.; DiMare, M.; O'Regan, M. *J. Am. Chem. Soc.* **1990**, *112*, 3875-3886.

(30) Michael, R. B. In *Late Transition Metal Polymerization Catalysis*; Rieger, B.; Baugh, S., Kacker, S., Streigler, S., Eds; Wiley-VCH: Weinheim, 2003, 155-191.

(31) Novak, B. M.; Grubbs, R. H. *J. Am. Chem. Soc.* **1988**, *110*, 960-961.

(32) Nguyen, S. T.; Grubbs, R. H.; Ziller, J. W. *J. Am. Chem. Soc.* **1993**, *115*, 9858.

(33) (a) Fürstner, A.; Picquet, M.; Bruneau, C.; Dixneuf, P. H. *Chem. Commun.* **1998**, *12*, 1315-1316. (b) Picquet, M; Bruneau, C.; Dixneuf, P. H. *Chem. Comm.* **1998**, *20*, 2249-2250.

(34) Arduengo, A. J.; Harlow, R. L.; Kline, M. *J. Am. Chem. Soc*. **1991**, *113*, 361-363.

(35) Trnka, T. M.; Day, M. W.; Grubbs, R. H. *Organometallics* **2001**, *20*, 3845-3847.

36) Weskamp, T.; Schattenmann, W. C.; Spiegler, M.; Herrmann, W. A. *Angew. Chem., Int. Ed.* **1998**, *37*, 2490-2493.

(37) (a) Huang, J.; Stevens, E. D.; Nolan, P.; Petersen, J. L. *J. Am. Chem. Soc*. **1999**, *121*, 2674-2678. (b) Jafarpour, L.; Schanz, H. J.; Stevens, E. D.; Nolan, S. P. *Organometallics* **1999**, *18*, 5416-5419. (c) Schanz, H. J.; Jafarpour, L.; Stevens, E. D.; Nolan S. P. *Organometallics* **1999**, *18*, 5187-5190.

(38) (a) Louie, J.; Grubbs, R. H. *Organometallics* **2002**, *21*, 2153-2164. (b) Love, J. A.; Morgan, J. P.; Trnka, T. M.; Grubbs, R. H. *Angew. Chem., Int. Ed.* **2002**, *41*, 4035-4037.

(39) Ackerman, L.; Fürstner, A.; Weskamp, T.; Kohl, F. J.; Herrmann, W. A. *Tetrahedron Lett.* **1999**, *40*, 4787-4790. (b) Weskamp, T.; Kohl, F. J.; Hieringer, W.; Gleich, D.; Herrmann, W. A. *Angew. Chem., Int. Ed.* **1999**, *38*, 2416-2419. (c) Weskamp, T.; Kohl, F. J.; Herrmann, W. A. *J. Organomet. Chem.* **1999**, *582*, 362-365.

(40) (a) Sanford, M. S.; Ulman, M.; Grubbs, R. H. *J. Am. Chem. Soc*. **2001**, *123*, 749-750. (b) Sanford, M. S.; Love, J. A.; Grubbs, R. H. *J. Am. Chem. Soc*. **2001**, *123*, 6543-6554. (c) Hong, S. H.; Wenzel, A. G.; Salguero, T. T.; Day, M. W.; Grubbs, R. H. *J. Am. Chem. Soc*. **2007**, *129*, 7961-7968.

(41) Trnka, T. M.; Morgan, J. P.; Sanford, M. S.; Wilhelm, T. E.; Sing, S.; Day, M. W.; Grubbs, R. H. *J. Am. Chem. Soc*. **2003**, *125*, 2546-2558.

(42) Aeilts, S. L.; Cefalo, D. R.; Bonitatebus, P. J.; Houser, J. H.; Hoveyda, A. H.; Schrock, R. R. *Angew. Chem., Int. Ed.* **2001**, *40*, 1452-1456.

(43) Harrity, J. P. A.; Visser, M. S.; Gleason, J. D.; Hoveyda, A. H. *J. Am. Chem. Soc*. **1997**, *119*, 1488-1489.

(44) Garber, S. B.; Kingsbury, J. S.; Gray, B. L.; Hoveyda, A. H. *J. Am. Chem. Soc*. **2000**, *122*, 8168-8179.

(45) Gessler, S.; Randl, S.; Blechert, S. *Tetrahedron Lett.* **2000**, *41*, 9973-9976.

(46) (a) Veldhuizen, J. J. V.; Garber, S. B.; Kingsbury, J. S.; Hoveyda, A. H. *J. Am. Chem. Soc*. **2002**, *124*, 4954-4955. (b) Michrowska, A.; Bujok, R.; Harutyunyan, S.; Sashuk, V.; Dolgono, G.; Grela, K. *J. Am. Chem. Soc*. **2004**, *126*, 9318-9325. (b) Michrowska, A.; Gulajski, L.; Grela, K. *Chem. Commun.* **2006**, *8*, 841-843.

(47) Harlow, K. J.; Hill, A. F.; Wilton-Ely, J. D. E. T. *J. Chem. Soc., Dalton Trans.* **199**, 285-291.

(48) Boeda, F.; Clavier, H.; Nolan, S. P. *Chem. Commun*. **2008**, *24*, 2726-2740.

(49) Katayama, H.; Nagao, M.; Ozawa, F. *Organometallics* **2003**, *22*, 586-593.

(50) Brady, M.; Brady, P. *Reinf. Plast.* **2008**, *52*, 32-36.

(51) Vougioukalakis, G. C.; Grubbs, R. H. *Chem. Rev.* **2010**, *110*, 1746-1787.

(52) Funk, T. W.; Berlin, J. M.; Grubbs, R. H. *J. Am. Chem. Soc.* **2006**, *128*, 1840.

(53) Berlin, J. M.; Goldberg, J. M.; Grubbs, R. H. *Angew. Chem., Int. Ed.* **2006**, *45*, 7591.

(54) (a) Burtscher, D.; Grela, K. *Angew. Chem., Int. Ed.* **2009**, *48*, 442-454. (b) Zaman, S.; Curnow, O. J.; Abell, A. D. *Aust. J. Chem.* **2009**, *62*, 91-100.

(55) Gulajski, L.; Sledz, P.; Lupa, A.; Grela, K. *Green Chem.* **2008**, *10*, 279-282.

(56) Lynn, D. M.; Kanaoka, S.; Grubbs, R. H. *J. Am. Chem. Soc.* **1996**, *118*, 784-790.

(57) Binder, J. B.; Blank, J. J.; Raines, R. T. *Org. Lett.* **2007**, *9*, 4885-4888. (b) Lipschutz, B. H.; Aguinaldo, G. T.; Ghorai, S.; Voigtritter, K. *Org. Lett.,* **2008**, *10*, 1325-1328.

(58) (a) Gallivan, J. P.; Jordan, J. P.; Grubbs, R. H. *Tetrahedron Lett.* **2005**, *46*, 2577-2580.

(59) Rix, D.; Caijo, F.; Laurant, I.; Gulajski, L.; Grela, K.; Mauduit, M. *Chem. Commun.* **2007**, *36*, 3771-3773.

(60) (a) Maynard, H. D.; Grubbs, R. H. *Tetrahedron Lett.* **1999**, *40*, 4137-4140. (b) Parquette, L. A.; Schloss, J. D.; Efremov, I.; Fabris, F.; Gallou, M. A.; Yang, J. *Org. Lett.* **2000**, *2*, 1259-1261. (c) Ahn, Y. M.; Yang, K.; Georg, G. I. *Org. Lett.* **2001**, *3*, 1411-1413.

(61) Cho, J. H.; Kim, B. M. *Org. Lett.* **2003**, *5*, 531-533. (b) McEleney, K.; Allen, D. P.; Holliday, A. E.; Crudden, C. M. *Org. Lett.* **2006**, *8*, 2663-2666.

(62) Clavier, H.; Audic, N.; Mauduit, M.; Guillemin, J. C. *Chem. Commun.* **2004**, 2282-2283. (b) Clavier, H.; Audic, N.; Mauduit, M.; Guillemin, J. C. *J. Organomet.. Chem.* **2005**, *690*, 3585-3599.

(63) Allen, D. P.; van Wingerden, M. M.; Grubbs, R. H. *Org. Lett.* **2009**, *11*, 1261-1264.

(64) P'Pool, S. J.; Schanz, H. J. *J. Am. Chem. Soc*. **2007**, *129*, 14200-14212.

(65) Lynn, D. M.; Dias, E. L.; Grubbs, R. H.; Mohr, B.; U.S. Patent 6,486,279B2, 2001.

(66) (a) Gstrein, X.; Burtscher, D.; Szadkowska, A.; Brabasiewicz, M.; Stelzer, F.; Grela, K.; Slugovc, C. *J. Polym. Sci. Part A: Polym. Chem*. **2007**, *45*, 3494-3500. (b) Ung, T.; Hejl, A.; Grubbs, R. H.; Schrodi, Y. *Organometallics* **2004**, *23*, 5399-5401.

(67) Ben-Asuly, E.; Tzur, C. E.; Diesendruck, M.; Sigalov, I.; Goldberg, N. G. *Organometallics* **2008**, *27*, 811-813.

(68) Hafner, A.; Mühlback, A.; Schaaf, P. A.; *Angew. Chem., Int. Ed.* **1997**, *36*, 2121-2124.

(69) (a) Weng, D.; Wurst, K.; Knolle, W.; Decker, U.; Prager, L; Naumov, S.; Buchmeiser, M. R. *Angew. Chem., Int. Ed.* **2008**, *47*, 3267-3270. (b) A. Fürstner, L. Ackermann, *Chem. Commun*. **1999**, *1*, 95-96.

(70) Keitz, B. K.; Grubbs, R. H. *J. Am. Chem. Soc*. **2009**, *131*, 2038-2039.

(71) Szwarc, M. *Nature (London, U.K.)* **1956**, *178*, 1168-1169. (b) Szwarc, M.; Levy, M.; Milkovich, R. *J. Am. Chem. Soc*. **1956**, *78*, 2656-2657.

(72) Kanaoka, S.; Grubbs, R. H., *Macromolecules* **1985**, *28*, 4707-4713.

(73) Matyjaszewski, K. *Macromolecules* **1993**, *26*, 1787–1788.

(74) (a) Herrmann, W. A. *Synthetic Methods of Organometallic and Inorganic Chemistry*; Georg Thieme Verlag: Stuttgart, New York, 1995. (b) Herrmann, W. A.; Kocher, C.; Goossen, L. J.; Artus, G. R. *Chem.-Eur. J.* **1996**, *2*, 1627-1636. (c) Arduengo, A. J., III; Krafczyk, R.; Schmutzler, R.; Craig, H. A.; Goerlich, J. R.; Marshall, W. J.; Unverzagt, M. *Tetrahedron* **1999**, *55*, 14523-14534. (d) Weskamp, T.; Böhm, V. P.; Herrmann, W. A. *J. Organomet. Chem.* **2000**, *600*, 12-22. (e) Altenhoff, G.; Goddart, R.; Lehmann, C.; Glorius, F. *J. Am. Chem. Soc.* **2004**, *126*, 15195.

(75) Arduengo, A. J. *Acc. Chem. Res.* **1999**, *32*, 913-921.

(76) (a) Denk, M. K.; Rodezno, J. M.; Gupta, S.; Lough, A. J. *J. Organomet. Chem.* **2001**, *617-618*, 242-253. (b) Demk, M. K.; Rodezno, J. M.; *J. Organomet. Chem.* **2001**, *617-618*, 737-740.

(77) Huang, J.; Schanz, H. J.; Stevens E. D.; Nolan, S. P. *Organometallics* **1999**, *18*, 5375–5380.

(78) Toste, F. D.; Chatterjee, A. K.; Grubbs, R. H. *Pure Appl. Chem*. **2002**, *74*, 7-10.

(79) Balof, S. L.; P'Pool, S. J.; Berger, N. J.; Valente, E. J.; Shiller, A. M.; Schanz, H. J. *Dalton Trans.* **2008**, 5791-5799.

(80) Gawinecki, R. *Pol. J. Chem.* **1988**, *62*, 799-806.

(81) Hintermann, L. *Beilstein J. Org. Chem.* **2007**, *3*, article 22.

(82) Koser, G. F. C-Hetero Bond Forming Reactions. In *Topics In Current Chemistry*; Wirth, T., Ed; Springerlink: Verlag Berlin Heidelberg, 2003; *224*, 173-183.

(83) *Vogel's Textbook of Practical Chemistry, 5th ed.*; Furniss, B. S., Hannaford, A. J., Smith, P. W. G., Tatchell, A. R., Eds.; Longman Scientific & Technical: Essex, U.K., 1991.

(84) Leuthaeusser, S.; Schmidts, V.; Thiele, C. M.; Plenio, H. *Chem.-Eur. J.* **2008**, *14*, 5465-5481.

(85) Yun, J.; Marinez, E. R.; Grubbs, R. H. *Organometallics* **2004**, *23*, 4172-4173.

(86) Bieniek, M.; Michrowska, A.; Gulajski, L.; Grela, K. *Organometallics* **2007**, *26*, 1096-1099.

(87) Dunbar, M. A.; Balof, S. L.; LaBeaud, L. J.; Yu, B.; Lowe, A. B.; Valente, E. J.; Schanz, H. J. *Chem.-Eur.* J. **2009**, *15*, 12435-12446.

(88) Balof, S. L.; Yu, B.; Lowe, A. B.; Ling, Y.; Zhang, Y.; Schanz, H. J. *Chem.-Eur. J.* **2009**, *13*, 1717-1722.

(89) (a) Lynn, D. M.; Mohr, B.; Grubbs, R. H.; Henling, L. M.; Day, M. W. *J. Am. Chem. Soc.* **2000**, *122*, 6601-6609. (b) Lynn, D. M.; Mohr, B.; Grubbs, R. H. *J. Am. Chem. Soc.* **1998**, *120*, 1627-1628. (c) Sanford, M. S.; Henling, L. M.; Day, M. W.; Grubbs, R. H. *Angew. Chem. Int. Ed*. **2001**, *39*, 3451-3452. (d) Gulajski, L.; Michrowskaa, A.; Bujok, R.; Grela K. *J. Mol. Catal. A: Chem*. **2006**, *254*, 118-123. (e)

Gawin, R.; Makal, A.; Wozniak, K.; Mauduit, M.; Grela, K. *Angew. Chem. Int. Ed.* **2007**, *46*, 7206-7209.

(90) (a) Suessner, M.; Plenio, H. *Chem. Commun.* **2005**, 5417-5419. (b) Leuthaeusser, S.; Schwartz, D.; Plenio, H. *Chem.-Eur. J.* **2007**, *13*, 7195-7203.

(91) (a) Zhang, Y.; Guo, Z. J.; You, X. Z. *J. Am. Chem. Soc.* **2001,** *123*, 9378-9387. (b) Zhang, Y.; Lewis, J. C.; Bergman, R. G.; Ellman, J. A.; Oldfield, E. *Organometallics* **2006,** *25*, 3515-3519.

(92) Ghetty, K.; Delgado-Jaime, M. U.; Kennepohl, P. *J. Am. Chem. Soc*. **2007**, *129*, 15774-15776.

(93) (a) Borre, E.; Pieck, C. A.; Caijo, F.; Crevisy, C.; Mauduit, M. *Chem. Today* **2009**, 27, 74-78. (b) Ragone, F.; Poater, A.; Cuvallo, L. *J. Am. Chem. Soc*. **2010**, *132*, 4292-4258.

(94) Dunbar, M. A.; Balof, S. L.; Roberts, A. R.; Valente, E. J.; Schanz, H. J. *Organometallics* **2011**, *30*, 199-203.

(95) (a) Binder, J. B.; Raines, R. T. *Curr. Opin. Chem. Biol.* **2007**, *12*, 767-773. (b) Hoveyda, A. H.; Malcolmson, S. J.; Meek, S. J.; Zhugralin, A. R. Catalytic Enantioselective Olefin Metathesis and Natural Product Synthesis. In *Metesthesis in Natural Products Synthesis*; Cossy, J., Arseniyadis, S., Meyer, C., Eds; Wiley-VCH: Weinheim, 2010; pp. 343-348. (c) Samojlowicz, C.; Bieniek, M.; Zarecki, A.; Kadyriov, R.; Grela, K. *Chem. Comm.* **2008**, *47*, 6282-6284. (d) Drummond, L. J.; Sutherland, A. *Tetrahedron* **2010**, *66*, 5349-5356.

(96) Illesinghe, J.; Guo, C.X.; Garland, R.; Ahmed, A.; van Lierop, B.; Elaridi, J.; Jackson W.R.; Robinson, A. J. *Chem. Commun.*, **2009**, *3*, 295 – 297.

(97) Müller, K. BASF, Ludwigshafen, Germany. Personal communications, 2010.

(98) (a) Mohr, B.; Lynn, D. M.; Grubbs, R. H. *Organometallics* **1996**, *15*, 4317-4325. (b) Kovacic, S.; Krajnc, P.; Slugovc, C. *Chem. Commun.*, **2010**, *46*, 7504-7506.

(99) Synthesized according to a modified procedure described in referecene 5.

(100) Ornum, S. G.; Cook, J. M. *Tetrahedron Lett.* **1996**, *37*, 7185-7188.

(101) Bouhadir, K. H.; Zhou, J. L.; Shevlin, P. B.; *Synth. Commun.* **2005**, *35*, 1003-1010.

(102) Necas, D.; Tursky, M.; Tislerove, I.; Kotora, M. *New J. Chem* **2006**, *30*, 671-674.

(103) Rankin, d.; McLemore, K.; P'Pool, S. J.; Schanz, H. J.; Lowe, A. B. *J. Polym. Sci., Part A: Polym. Chem.* **2007**, *45*, 2113-2128.

(104) *Gaussian Program*, Frisch, M. J.; Trucks, G. W.;Schlegel, H. B.; Scuseria, G. E.; Robb, M. A.; Cheeseman, J.; Montgomery, J. A.; Vreven, T.; Kudin, K. N.; Burant, N.; Millam, J. M.; Iyengar, S. S.; Tomasi, J.; Barone, V.; Mennucci, B.; Cossi, M.; Scalmani, G.; Rega, N.; Petersson, G. A.; Nakatsuji, H.; Hada, M.; Ehara, M.; Toyota, K.; Fukuda, R.; Hasegawa, J.; Ishida, M.; Nakajima, T.; Honda, Y.; Kitao, O.; Nakai, H.; Klene, M.; Li, X.; Knox, J. E.; Hratchian, H. P.; Cross, J. B.; Bakken, V.; Adamo, C.; Jaramillo, J.; Gomperts, R.; Stratmann, R. E.; Yazyev, O; Austin, A. J.; Cammi, R.; Pomelli, C.; Ochterski, J. W.; Ayala, P. Y.; Morokuma, K.; Voth, G. A.; Salvador, P.; Dannenberg, J. J.; Zakrzewski, V. G.; Dapprich, S.; Daniels, A. D.; Strain, M. C.; Farkas, O.; Malick, D. K.; Rabuck, A. D.; Raghavachari, K.; Foresman, J. B.; Ortiz, J. V.; Cui, Q.; Baboul, A. G.; Clifford, S.; Cioslowski, J.; Stefanov, B. B.; Liu, G.; Liashenko, A.; Piskorz, P.; Komaromi, I.; Martin, R. L.; Fox, D. J.; Keith, T. Al-Laham, M. A.; Peng, C. Y.; Nanayakkara, A.; Challacombe, M.; Gill, P. M. W.; Johnson, B.; Chen, W.; Wong, M. W.; Gonzalez, C.; Pople, J. A. Gaussian 03, Revision D.01; Gaussian, Inc.: Wallingford CT, **2004**.

(105) Adamo, C.; Barone, V. *J. Chem. Phys.* **1998,** *108*, 664-675.

(106) Leininger, T.; Nicklass, A.; Stoll, H.; Dolg, M.; Schwerdtfeger, P. *J. Chem. Phys.* **1996,** *105*, 1052-1059.

(107) Gawinecki, R. *Polish J. Chem.* **1988**, *62*, 799-806.

(108) Goerl, C.; Alt, H. G. *J. Organomet. Chem.* **2007**, *692*, 4580-4592.

(109) Brboric, J. S.; Vladimirov, S. ; Jovanovic, M. S.; Dogovic, N *Monatshefte fuer Chemie* **2004**, *135*, 1009-1014.

(110) Kajigaeshi, S.; Kakinami, T.; Yamasaki, H.; Fujisaki, S.; Okamoto, T. *Bull. Chem. Soc. Jpn.* **1988**, *61*, 600-602.

(111) Sheldrick, G. M. In *Crystallographic Computing 3*; Sheldrick, G. M., Kruger, C., Goddard, R., Eds.; Oxford University Press, 1985; pp. 175-189.

(112) Sheldrick, G. M. In *SHELX97: Programs for Crystal Structure Analysis (Release 97-2)*; Institut für Anorganische Chemie der Universität, Tammanstrasse 4, D-3400 Göttingen, Germany, 1998.